POLYTECHNIQUE MONTRÉAL

affiliée à l'Université de Montréal

Appraisal of Surface Treatment to Steady Tumor Spheroid Formation on-Chip

NEDA AZIZIPOUR

Institut de génie biomédical

Thèse présentée en vue de l'obtention du diplôme de *Philosophiæ Doctor*

Génie biomédical

Avril 2022

POLYTECHNIQUE MONTRÉAL

affiliée à l'Université de Montréal

Cette thèse intitulée :

Appraisal of Surface Treatment to Steady Tumor Spheroid Formation on-Chip

présentée par **Neda AZIZIPOUR**

en vue de l'obtention du diplôme de *Philosophiæ Doctor*

a été dûment acceptée par le jury d'examen constitué de :

Gregory DE CRESCENZO, président
Abdellah AJJI, membre et directeur de recherche
Mohamad SAWAN, membre et codirecteur de recherche
Derek ROSENZWEIG, membre et codirecteur de recherche
Houman SAVOJI, membre
Christopher MORAES, membre externe

DEDICATION

To my better half, RAHI

My diamond, ASA

My sunshine, ARSHAN

For constant love, patience, and support

ACKNOWLEDGEMENTS

During this PhD journey, I had the opportunity to meet exceptional people that were essential to the completion of this dissertation. First, I am eternally grateful to my supportive PhD director, Prof. Abdellah Ajji, who welcomed me with open arms to have the honor to be a part of his wonderful research team. Without his continuous support, excellent supervision, and invaluable guidance, I would not have completed this dissertation. I have learned from him not only through my scientific journey, but also in my life. I also would like to express my sincere gratitude to my co-director, Prof. Mohamad Sawan, who has been always a supportive mentor for me, even from overseas. His encouragement, invaluable advice, and constant support were crucial to the success of this work. I am honored to have been within his amazing research team at Polytechnique. I am deeply grateful to Prof. Derek H. Rosenzweig, my co-director, who granted me the honor to join to his dynamic research team. His insightful suggestions, brainstorming scientific discussions, constant support, and guidance enabled me to complete this multidisciplinary research project.

I am sincerely grateful to my dissertation committee members: Prof. Gregory De Crescenzo, Prof. Houman Savoji, and Prof. Christopher Moraes for accepting to evaluate this dissertation. It is an undeniable fact that their valuable feedback and constructive suggestions have enriched the presented materials in this dissertation.

I would like to express my deep gratitude to Prof. Thomas Gervais for his generous support, insightful guidance, and invaluable advice during my Pre-Doctoral exam. I am sincerely grateful to Dr. Roberto J.Diaz for his valuable support before and during my Pre-Doctoral exam. I am sincerely grateful to Prof. Michael R. Wertheimer, and Prof. Marc Lavertu for generously giving me the opportunity to have access to their laboratories to complete some parts of this work.

I would like to deeply acknowledge my wonderful friend, Amal Bennani, for always being there for constant support, and encouragement. I am sincerely grateful to my amazing colleagues at Polytechique Montréal who accompanied me along this journey, offering me valuable technical supports specially: Laurent Mouden, Jean-Paul Levesque, Claire Cerclé, Matthieu Gauthier, Richard Silverwood, Marie-Yannick Laplante, Réjean Lepage, Patricia Moraille, Sean Watson, Amélie St-Georges-Robillard, Anik Chevrier, Sylvie Taillon, Dong Wang and Arina Soare. I am truly grateful to my amazing friends at Polytechique for valuable practical supports and warm

friendships specially: Dina Dorigiv, Bahareh Samadi, Mansoureh Mohseni, Bentolhoda Heli, Pierre-Alexandre Goyette, Samuel Castonguay, and to my wonderfull colleagues and friends at McGill University specially: Ateeque Siddique, Li Li, Megan Cooke, Hyeree Park, Eleane Hamburger, Audrey Pitaru, , Matthew Mannarino, Rita Lo, Ka Yee, Hamid Sad Abaadi, Ahmad Sohrabi, and many more whose names I might have forgotten to mention.

I do not even know how to appreciate my beloved parents, Fereshteh Soleimani, and Nematollah Azizipour. Their unwavering love, support and always belief in me helped me remain positive and strong! They have taught me to work hard for the things that I aspire to achieve! I am grateful to my lovely sister, Naghmeh, for her unconditional love. I am deeply grateful to my amazing brother, Mohamad, for always being there for constant and unconditional support. I can not express how much I am grateful for having my very special friends: Shadi Rahimi, Solmaz Rashvand, and Amitis Olfatpour. Thank you for making ordinary moments extraordinary in the past decades! Moreover, for keeping me mentally sane through the thicks and thins of life!

Very special thanks to my pillar of strength, my wonderful husband, and my life's two treasures! There are not enough words to express how indebted I am to them! This work definitely would not have been possible to complete without their extraordinary patience, and constant support! My daughter, Asa! Thank you for making my life brilliant and for your beautiful smile, inspiring words, and extreme patience during the challenges of my life! Remember: “If you have a dream, fight for it!” My son, Arshan! Thank you for making my life colourful and for being extremely patient with me, taking care of me, and giving me big hugs and chocolates on hard days! Remember: “Where there is a will, there is a way!”

Finally, and above all, I can not begin to express my unfailing gratitude to my wonderful life partner, Rahi Avazpour, who I also consider my PhD co-director unofficially. His invaluable scientific suggestions, insightful guidance, encouragement and constantly challenging me to pass my comfort zoom and be a better researcher helped me to grow into who I have become! My love, Rahi! Having you by my side always reassures me, and I am truly blessed to have you as a constant source of love, strength, and motivation during the past 20 years! Thanks for never letting me give up! Moreover, for saving our dinners from fully burning while I was writing this dissertation!

RÉSUMÉ

Le cancer est l'une des principales causes de décès dans le monde. Malgré les progrès des thérapies anticancéreuses au cours des dernières années, la survie médiane des patients atteints d'un cancer de haut grade est encore très faible en raison du diagnostic tardif, des métastases, de la résistance aux médicaments au traitement standard, etc. L'incapacité à développer de nouveaux candidats médicaments et des thérapies personnalisées pour traiter le cancer et augmenter le taux de survie a plusieurs raisons, mais l'une des principales raisons est la fiabilité des modèles précliniques utilisés dans le pipeline de développement de médicaments et le traitement du cancer pour évaluer les réponses aux médicaments et leurs effets secondaires chez l' humain, ce qui explique en partie pourquoi les candidats médicaments anticancéreux échouent plus qu'ils ne réussissent à obtenir une approbation clinique. Divers modèles *in vitro* ont été développés pour étudier les traitements contre le cancer.

La culture en monocouches bi-dimensionnelles (2D) utilisant des lignées cellulaires établies sont les méthodes *in vitro* les plus courantes et traditionnellement utilisées dans la recherche sur le cancer et la découverte de médicaments. Cependant, les modèles 2D manquent du microenvironnement cellulaire natif et *in vivo*, car les cellules adhèrent à la surface de la culture cellulaire (par exemple, boîtes de Pétri, flacons) et se développent à plat dans une monocouche dans des conditions irréalistes et perdent donc certaines de leurs caractéristiques fonctionnelles naturelles. La manière naturelle dont les tumeurs se développent *in vivo* est en trois dimensions (3D). Par conséquent, le modèle le plus réaliste utilise des cellules tumorales de patients qui se développent en 3D pour imiter le microenvironnement tumoral complexe et physiologiquement pertinent en raison de la capacité des cellules à former des interactions cellule-cellule et cellule-microenvironnement dans des structures 3D.

Les sphéroïdes sont des agrégats de cellules sphériques auto-assemblées qui sont actuellement les modèles 3D *in vitro* les plus utilisés dans la recherche préclinique sur le cancer visant à pallier le pouvoir prédictif insuffisant associé aux modèles 2D traditionnels. Les sphéroïdes sont connus pour imiter certaines des caractéristiques tumorales naturelles importantes qui offrent un modèle *in vitro* plus fiable et sont des prédicteurs plus fiables des réponses thérapeutiques chez l'humain par rapport aux monocouches 2D. Compte tenu de l'importance cruciale de la

prédiction précise des réponses tumorales aux agents thérapeutiques pour développer de nouvelles thérapies anticancéreuses et personnaliser les molécules thérapeutiques existantes, le manque de contrôlabilité de la taille, de la forme et de la densité dans les méthodes de culture sphéroïdales conventionnelles est difficile en réduisant la précision et fiabilité des résultats des tests de dépistage de drogue dans les sphéroïdes.

Au cours des dernières années, les plates-formes des puces microfluidiques ont reçu une attention croissante pour produire des sphéroïdes uniformes dans des conditions plus physiologiques significatives parmi diverses techniques de production de sphéroïdes. La plupart des recherches en microfluidique se concentrent sur la conception de la plateforme, cependant le matériau des puces microfluidiques et ses propriétés de surface (par exemple, la mouillabilité, la chimie, la charge et la rugosité) sont aussi importants que la conception pour influencer l'adsorption des protéines sur la surface et par conséquent réguler l'adhésion cellulaire à la surface qui peut affecter la formation de sphéroïdes sur la puce.

Dans cette thèse, j'ai conçu et fabriqué des puces microfluidiques optimisées pour produire un modèle sphéroïde sur puce uniforme et homogène vers des tests de médicaments *in vitro* fiables.

Ici, j'ai évalué l'impact de la modification de surface sur la qualité et la quantité de formation de sphéroïdes uniformes sur des puces microfluidiques en PDMS. L'optimisation de surface pour la lignée cellulaire de cancer du sein MDA-MB-231 a été présentée dans l'article 1 du chapitre 4. Dans ce travail, j'ai évalué expérimentalement comment la mouillabilité et la microstructure de la surface peuvent affecter des sphéroïdes de taille et de forme uniformes sur la même conception microfluidique. La surface optimisée peut supprimer efficacement l'adhésion cellulaire à la surface du PDMS et moduler en conséquence le nombre et les caractéristiques des sphéroïdes.

Dans l'article 2 présenté au chapitre 5 par modification du design microfluidique, j'ai évalué l'impact du design avec un traitement de surface optimisé sur la formation de sphéroïdes. Dans ce travail, j'ai pu former avec succès des formes reproductibles, compactes, sphériques et des sphéroïdes de taille uniforme à partir de diverses lignées de cellules cancéreuses et d'un modèle de co-culture de cellules tumorales et de cellules stromales.

Dans l'article 3 présenté au chapitre 6, le modèle sphéroïde sur puce développé sur la conception et la surface optimisées à l'aide de cellules de métastases vertébrales secondaires à des cellules de

patients atteints de tumeur pulmonaire, de la lignée cellulaire établie A549 de tumeur pulmonaire et d'un modèle de co-culture de tumeur pulmonaire les cellules A549 et les cellules stromales les ostéoblastes Qth212. Des sphéroïdes homogènes et uniformes se sont formés sur cette plateforme de biopuces. Les résultats reproductibles des tests de dépistage de drogue confirment que ce dispositif microfluidique optimisé a le potentiel de servir d'outil *in vitro* fiable pour le dépistage de drogue.

En résumé, ce travail met en évidence l'importance de la conception de puces microfluidiques et des propriétés de la surface en tant que deux paramètres cruciaux dans la production de sphéroïdes uniformes et homogènes pour des tests de médicaments reproductibles et répétables pour de nouvelles thérapies anticancéreuses et la médecine personnalisée.

ABSTRACT

Cancer is among the leading causes of death worldwide. Notwithstanding advancement in cancer therapies over the past years, median survival of patients with high-grade cancer is still very low due to late diagnosis, metastasis, drug resistance to standard treatments, etc. Failure to develop new drug candidates and personalized therapies to treat cancer and enhance patients survival rates has multiple reasons. However, one of the main reasons is the reliability of pre-clinical models used in drug development pipeline and cancer therapy to assess drug responses and their side effects in humans, which explains in part why anticancer drug candidates fail to carry out clinical approval more than they succeed.

Various *in vitro* models have been developed to investigate cancer treatments. Two dimensions (2D) models using established cell lines are the most common and traditionally used *in vitro* methods in cancer research and drug discovery. However, 2D models lack the native and *in vivo* like cellular microenvironment as cells adhere to the cell culture surface (e.g. petri dishes, flasks) and grow flat in a monolayer under unrealistic conditions and therefore lose some of their natural functional characteristics. The natural manner in which tumors grow *in vivo* is three-dimensional (3D). Therefore, the most realistic model is using patient tumor cells growing in 3D to mimic the complex and physiologically relevant tumor microenvironment due to the ability of the cells to form cell-cell and cell-microenvironment interactions in 3D structures. Spheroids are spherical self-assembled cells aggregates, which are currently the most widely used 3D *in vitro* models in pre-clinical cancer researches aiming to overcome the insufficient predictive power associated with traditional 2D models. Spheroids are known for mimicking some of the important natural tumor characteristics, which offer a more reliable *in vitro* model to predict therapeutic responses in humans compared to 2D monolayers. Considering the crucial importance of accurate prediction of tumor responses to therapeutic agents for developing new anti-cancer therapies and personalize of existing therapeutic molecules, the lack of controllability of the size, shape and dense in conventional spheroid culture methods is challenging by reducing the precision and reliability of drug test results in spheroids.

In recent years, microfluidic biochip platforms have received increasing attention to produce uniform spheroids under more physiologically meaningful conditions among various techniques

to produce spheroids. Most of the researches in microfluidic are focused on the platform's design. However, the biochip materials and its surface properties (e.g. wettability, chemistry, charge, and roughness) are as important as design to influence protein adsorption on the surface and consequently regulate cell adhesion to the surface, which can affect spheroid formation on-chip.

In this dissertation, I have designed and fabricated an optimized microfluidic biochip to produce uniform and homogenous spheroid-on-a-chip models toward reliable *in vitro* drug testing.

Here, I have evaluated the impact of surface modification on the quality and quantity of uniform spheroid formation on the PDMS microfluidic biochip. Surface optimization for MDA-MB-231 (a breast cancer cell line) has been presented in the article 1 in Chapter 4. In this work, I have experimentally assessed how surface wettability and microstructure can adjust uniformly sized and shaped spheroids on-chip. The optimized surface can effectively suppress cell adhesion to the PDMS surface and accordingly modulate the numbers and characteristics of the spheroids.

In the article 2 presented in Chapter 5 by modification of the microfluidic design, I have assessed the impact of the design with optimized surface treatment on spheroid formation. In this work, I have successfully produced reproducible, compact, spherical forms and uniform-sized spheroids from various cancer cell lines and co-culture models of tumor cells and stromal cells.

In the article 3 presented in Chapter 6 the spheroid-on-a-chip model developed on the optimized design and surface using cells from spine metastasis secondary to lung tumor patient cells, Lung tumor established cell line A549 and co-culture model of lung tumor cells A549 and stromal cells osteoblasts. Homogenous and uniform spheroids formed on this biochip platform. The reproducible drug test results confirm that this optimized microfluidic device has the potential to serve as a reliable *in vitro* tool for drug screening.

In summary, this work highlights the importance of the design and surface properties of microfluidic biochip platforms as the two crucial parameters in producing uniform and homogenous spheroids for reproducible and repeatable drug tests for novel anti-cancer therapies and personalized medicine.

TABLE OF CONTENTS

LIST OF TABLES

LIST OF FIGURES

LIST OF SYMBOLS AND ABBREVIATIONS

AFM	Atomic force microscopy
BBB	Blood-Brain-Barrier
BioMEMS	Biomedical Micro-Electro-Mechanical Systems
BRL	Brightness level ratio
BSA	Bovine serum albumin
CE	Capillary Electrophoresis
CMs	Cardiomyocytes
CROs	Contract research organizations
DMEM	Dulbecco's Modified Eagle's Medium
ECM	Extracellular Matrix
EOF	Electro osmotic flow
EthD-1	Ethidium homodimer-1
FBS	Fetal bovine serum
GC	Gas Cromatography
GFP	Green fluorescent protein
GPC	Gas-phase chromatography
HBSS	Hank's balanced salt solution
hCG	human Chorionic Gonadortropin
HPLC	High-Pressure Liquid Chromatography
hPSCs	human Pluripotent Stem Cells
iPSCs	Induced-pluripotent stem cells
IC	Integrated Circuits
IL	Interleukin

LOC	Lab-on-a-chip
LOT	Liquid overlay technique
MCTS	Multi cellular tumor spheroid
MCTSs	Multi cellular tumor spheroids
MEMS	Micro-Electro-Mechanical Systems
OOC	Organ-on-a-chip
PBPK	Pharmacokinetics
PBS	Phosphate buffered saline
PD	Pharmacodynamics
PDMS	Polydimethylsiloxane
PEO	Polyethylene oxide
POC	Point-of-Care
PS	Penicilline/Streptomycin
PTFE	Polytetrafluoroethylene
PVA	Polyvinyl alcohol
Ra	Average roughness
R&D	Research and development
RH	Relative humidity
SD	Standard deviation
SE	Standard error
SLA	Stereolithography apparatus
3D	three dimensions
2D	two dimensions
UV	Ultraviolet

μTAS	Micro-Total Analysis Systems
WCA	Water contact angle

LIST OF APPENDICES

CHAPTER 1 INTRODUCTION

1.1 Motivation and overview

Cancer is a highly complex disease, which is the second cause of mortality around the world (around 10 million deaths yearly) [1]. The number of new cancer cases and cancer-related deaths will project to increase every year due to population growth and aging [2]. Accordingly, cancer will likely expect to be the first cause of death worldwide in 2060 (~18.63 million deaths) [1, 2].

Although various progress has been made in the prevention and treatment of some of the major cancers including lung, breast and prostate, these types of cancer are still the most commonly diagnosed cancers and the leading cause of cancer death [1]. Moreover, continuous increment in cancer incidence and mortality in every country in the world highlights the crucial need to advance reliable techniques for early detection and improvement of therapeutic outcomes [1, 3].

Persistent cancer cells are the major cause of non-effective cancer therapies. This subset of tumor cells survives cancer treatments and will cause the disease recur [4]. Understanding the mechanisms of persistent cells is critical for developing novel therapeutics for cancer treatments [4]. The lack of progress in finding effective cancer treatments despite all efforts has complex reasons, but reflects the reliability and predictive power of preclinical models, which cannot accurately mimic the biological responses that occur in cancer patients [3]. This can explain in part why the majority of successful therapeutic candidates in preclinical stages fail when they reach clinical trials [3, 5].

Conventional two-dimension (2D) cell culture models are the most popular *in vitro* models which have provided most of our current understanding about the biological mechanisms in cancer research [3]. However, the tumor microenvironment is composed of various cell types, extra cellular matrix (ECM), physicochemical and mechanical cues that are all interacting in a dynamic three-dimension (3D) environment [3, 6]. Therefore, 2D cultures lack structural architecture dynamic interactions in the tumor microenvironment and cannot adequately take into account the *in vivo* like natural tumor characteristics in which cancer develops and progress [7, 8]. Accordingly, data obtained by 2D culture models cannot be predictive enough for *in vivo* responses [9]. For this reason, 3D culture models have been developed with the hope of more relevantly representing of natural microenvironment of tumors [3, 7].

Among various types of 3D culture models, spheroids which are spherical and compact self-assembled 3D agglomerates [10, 11] of cells by recapitulating some of the important complexities of *in vivo* tumors [11], have been popular for studies involving cancer development and drug testing. However, controlling the size, shape and compactness level of spheroids, which is critical to maintain their functions and behaviours [12, 13], is challenging in conventional spheroid culture methods and this can reduce the precision and reproducibility of their responses to therapeutics[13]. Advances in microfabrication technologies lead to develop microfluidic biochip platforms to facilitate production and culture of spheroids [14, 15]. Spheroid-on-a-chip models offer apparent advantages over traditional spheroid culture techniques (e.g. hanging drop methods) as they allow for production, maintenance, testing and in situ analysis of spheroids within the same device under more physiologically relevant condition[14, 16].

Various microfluidic platforms have been developed over the past years for spheroid formation and culture[14, 16-18]. However, due to the importance of homogeneity of spheroids in their responses to drug tests, producing uniform and homogenous spheroids still need to be addressed in microfluidic platforms. [18]. Most of the research groups relied on developing microfluidic designs to enhance uniform spheroid production [18-21]. However, surface characteristics (e.g. wettability, chemistry, roughness etc.) have been shown to play a crucial role in affecting cellular behaviour [22, 23].

The aim of this dissertation work was to enhance uniformity of spheroids on-chip in a repeatable manner toward reliable drug testing. In this regard, we have implemented a series of surface modifications to optimize PDMS surface to elevate the quantity and quality of homogenous multi cellular tumor spheroids. Following, to validate our finding, we have assessed the reputability of uniform spheroid production from several cancer cell lines and co-culture models on the optimized surface in a modified design. To reach the main objective, in the last stage of this work, we have developed spheroids from patient derived cells obtained from biopsy and conducted drug test assays on-chip.

1.2 Problematic

Several papers have been published demonstrating the need for producing uniform spheroids [18, 19, 24]. In most of them, engineering design of microfluidic platforms have been discussed but

the role of biochip surface properties did not elucidate. On the other hand, there are many publications highlighting the importance of surface properties of the PDMS in its anti-biofouling characteristics [22, 25-28]. Nevertheless, to the best of our knowledge, none of the published works studied the impact of PDMS surface properties on the quality and quantity of spheroid production on-chip. However, we believe that surface characteristics and the design are the two main players in altering spheroid formation on-chip. Accordingly, in this dissertation we have worked on optimizing these two critical parameters (surface and design) to assess if they can alter spheroid production and to reach our main research objective.

1.3 Research hypotheses and objectives

The aim of this dissertation is to enhance uniform and homogenous spheroid production on biochips in a reproducible manner for reliable drug assays. In this context, we have studied the role of two critical factors: surface modification and design adaptation, to reach our main objective. The work presented in this dissertation has been driven by three specific research objectives that align with the enclosed articles in Chapters 4, 5 and 6.

The first objective of this work was to understand the correlation between PDMS surface properties and cell responses to the surface. In the first study, we aimed to determine how surface modification of PDMS with different materials in various concentrations and different durations of treatment could alter spheroid formation on the same device. The work conducted to meet this objective is presented in Chapter 4.

Objective 1: Optimize the PDMS surface ion microfluidic biochips in order to increase cell repellent properties and enhance cells self-aggregations to form uniform spheroids on microfluidic biochips in a reproducible manner.

Hypothesis 1: Change in concentration of surface coating materials and their incubation time with the surface may affect the PDMS surface wettability.

Hypothesis 2: Changing surface wettability of PDMS can modulate cell responses to the surface.

The second objective of this work was to assess if the optimized PDMS surface recognized in the first study from one cell line can be expandable to various cancer cell lines and co-culture of tumor and stromal cells, or it has some limitations dependent to the types of cell lines. In this work, we have also modified the design of microfluidic cell trapping chambers in order to assess the synchronous impact of design and surface of biochip in spheroid formation. This constitutes the second objective, which is addressed in Chapter 5.

Objective 2: Optimize PDMS surface and design of microfluidic device for homogenous and uniform spheroid production on biochip from various cancer cell lines and co-culture of tumor cells with stromal cells.

Hypothesis 1: Design optimization and surface modification are the two important parameters in altering the cell orientation in the microfluidic device.

Hypothesis 2: Optimized PDMS surface from the first study can be expandable as an optimal surface for various cell types and it can effectively decrease cell adhesion to the surface.

The third objective of this work was to get insights into whether the tumor cells obtained from patient biopsy can form uniform and compact spherical agglomerates on the biochip with the optimized surface and design. In this study, we aimed to assess the reproducibility of drug responses on uniform spheroids. Accordingly, a drug response study performed to determine if the anticancer drug Doxorubicin can reduce the metabolic activity of spheroids and the repeatable drug responses can be observed. In this work, we also have compared drug resistance in spheroids from patient cells, monotype cells and hetero-type multi cellular spheroids. The results were also compared with 2D culture model. This objective is addressed in Chapter 6.

Objective 3: Produce homogenous spheroids from patient cells on optimized biochips for reproducible drug testing.

Hypothesis 1: The surface and design optimized biochip can be expandable for patient derived cells to produce uniform spheroids in terms of size, compactness level and spherical shape.

Hypothesis 2: Spheroids from patient cells and co-culture models can better mimic the complexity of tumor microenvironment and drug resistance when compared with spheroids from a single tumor cell type.

Hypothesis 3: Reproducible drug responses on biochips can be a hallmark of uniformity and homogeneity of produced spheroids on biochips.

Moreover, in this work, we have compared three different types of multi cellular spheroids: patient derived cells, established cancer cell lines, co-culture of tumor, and stromal cells. We have also assessed comparison between 2D culture and spheroids on-chip in responses to anticancer agent (Doxorubicin).

1.4 Dissertation outline

This dissertation is composed of nine chapters. **Chapter 1** presents introduction, starting with the motivation and a brief description of the problematic, followed by the research objectives and hypothesis, and ending by dissertation structure. **Chapter 2** starts with a general literature review entitled "Evolution of biochip technology: A review from lab-on-a-chip to organ-on-a-chip" which is published in Micromachines journal in 2020, followed by a concise literature review focused on the subject of this dissertation. **Chapter 3** presents the core of the dissertation, and general methodology used throughout this work. **Chapters 4, 5 and 6** present the main findings as published manuscripts. These manuscripts are incorporated in the dissertation with modifications in the formatting and represent a copy of the published works. This dissertation concludes with a general discussion with respect to the reported articles presented in **Chapter 7** followed by conclusions and recommendations for future work in **Chapter 8.** The bibliography of this dissertation is listed in the references section. Appendices present a short summary of the preliminary experiments I have done in this PhD work and the results obtained to move in those research directions, followed by the extra materials presented in the published articles as articles appendices.

CHAPTER 2 LITTERATURE REVIEW

2.1 Chapter Overview

This chapter includes two main parts: The first part presents the article entitled Evolution of Biochip Technology: A Review from Lab-on-a-Chip to Organ-on-a-Chip which is published in Journal Micromachines in 2020. This work is a comprehensive and detailed review of microfluidic devices evolution. Here, I have reviewed the background of the microfluidic technology and lab-on-a-chip (LOC) platforms toward their novel applications as microengineered cell culture platforms and organ-on-a-chip (OOC) devices.

The second part presents a critical review focusing on the topic of this dissertation. In this part, a brief introduction to cancer and current cancer treatments and modeling is provided. Then, the advantages and disadvantages of conventional 2D models versus 3D models are briefly discussed. Next, I have discussed spheroids as the most popular 3D culture models in cancer research and various methods of spheroid formation briefly reviewed. Following, a brief discussion has been made on the microfluidic-based spheroid culture platforms and their advantages over conventional spheroid formation methods. Then, I have discussed the materials used in fabrication of microfluidic devices for cell culture and the importance of surface properties in cell responses to the surface. Lastly, the surface modification of PDMS, as the most popular material used in microfluidic biochip platforms discussed with more details.

2.2 Article: Evolution of biochip technology: A review from lab-on-a-chip to organ-on-a-chip

Neda Azizipour [1], Rahi Avazpour [2], Derek H. Rosenzweig [3, 4] and Mohamad Sawan [5, 6*], Abdellah Ajji [1, 7*]

[1] Institut de génie biomédical, Polytechnique Montréal, Montréal, QC H3C 3A7, Canada; neda.azizipour@polymtl.ca

[2] Department of Chemical Engineering, Polytechnique Montréal, Montréal, QC H3C 3A7, Canada; rahi.avazpour@polymtl.ca

[3] Department of Surgery, McGill University, Montréal, QC H3G 1A4, Canada; derek.rosenzweig@mcgill.ca
[4] Injury, Repair and Recovery Program, Research Institute of McGill University Health Centre, Montréal, QC H3H 2R9, Canada
[5] Polystim Neurotech Laboratory, Electrical Engineering Department, Polytechnique Montréal, QC H3T 1J4, Canada
[6] CenBRAIN Laboratory, School of Engineering, Westlake University, and Westlake Institute for Advanced Study, Hangzhou 310024, China
[7] NSERC-Industry Chair, CREPEC, Chemical Engineering Department, Polytechnique Montréal, Montréal, QC H3C 3A7, Canada
***** Correspondence: sawan@westlake.edu.cn (M.S.); abdellah.ajji@polymtl.ca (A.A.)

Received: 2 May 2020; Accepted: 16 June 2020; Published: 18 June 2020

2.2.1 Abstract

Following the advancements in microfluidics and lab-on-a-chip (LOC) technologies, a novel biomedical application for microfluidic based devices has emerged in recent years and microengineered cell culture platforms have been created. These micro-devices, known as organ-on-a-chip (OOC) platforms mimic the *in vivo* like microenvironment of living organs and offer more physiologically relevant *in vitro* models of human organs. Consequently, the concept of OOC has gained great attention from researchers in the field worldwide to offer powerful tools for biomedical researches including disease modeling, drug development, etc. This review highlights the background of biochip development. Herein, we focus on applications of LOC devices as a versatile tool for POC applications. We also review current progress in OOC platforms towards body-on-a-chip, and we provide concluding remarks and future perspectives for OOC platforms for POC applications.

Keywords: organ-on-a-chip; lab-on-a-chip; microfluidics; microengineering; BioMEMS; point-of-care; personalized medicine

2.2.2 Introduction

Soon after the development of micro-electro-mechanical systems (MEMS), the potential of these miniaturized platforms for various applications in life science has been revealed. During the past few decades, interest in biological or biomedical MEMS (BioMEMS) has been drastically increased and it has found widespread applications in a various areas of biomedical and life science including diagnostics, therapeutics, drug delivery, biosensors and tissue engineering [29]. These integrated systems are also known as lab-on-a-chip (LOC) or micro-total analysis systems (μTAS). Microfluidic based LOC devices have often been notified as a landmark in biomedical research and life science [30, 31]. However many microfluidic based devices which are currently categorized under BioMEMS do not have any electrical or mechanical components (e.g., DNA and protein arrays) [29].

In recent years, microfluidics technology with many advantages including precise control over the cellular microenvironment in very small volumes [32, 33], merged seamlessly with cell biology and tissue engineering techniques [3, 34]. This has enabled us to develop novel microengineered cell culture platforms [34, 35].

OOC platforms which are microfluidic cell culture devices to mimic tissue- and organ-level physiology [6, 36], have been developed very rapidly in the past few years. These platforms with great potential to advance our understanding about tissue and organ physiology [37], offer portable and cost-effective biomedical tools for diseases modeling [38, 39], pharmaceutical research [40, 41] and personalized medicine [3, 33]. In OOC, the word chip roots from the original fabrication techniques [34, 42] (e.g., a modified form of photolithography) which have been used in computer microchips manufacturing [43]. This allows us to control surface feature shapes and sizes on the nm to μm scale [44].

This paper focuses on development of LOC and OOC technologies from their origins. Here, we briefly describe LOC devices for POC application. We also highlight previous and recent progress in both areas of LOC and OOC and introduce some of the major pioneers in this market. Finally, by looking through specifications of LOC and OOC, we discuss future perspectives in the development of OOC platforms toward user friendly devices for drug discovery and POC applications.

2.2.3 BioMEMS

Dating back to the 1950s, new techniques in microfabrication technology developed rapidly when the planar technologies were introduced into the microelectronics [45, 46]. At the beginning of the 1980s, with major progress in microelectronic systems and taking the advantages of miniaturization and parallel manufacturing, the concept of microelectromechanical systems (MEMS) appeared as the integration of mechanical and electrical functions into a single chip with small structures for various applications (e.g., biochemical applications and chemical engineering applications) [30, 45]. Similar microfabrication techniques as those used in microelectronics to manufacture integrated circuits (IC) in the semiconductor industry, are used to fabricate MEMS microdevices [29]. Generally, by repeating particular orders of photolithography, etching techniques and thin-film deposition steps, fabrication of a micro/nano scale structure on planar substrates is being achieved. Figure 2.1 demonstrates the basics of the photolithography process. It starts with spinning a photoresist with a certain speed to spread to a desired plate thickness on the substrate. The next step is to heat up the photoresist to evaporate any solvents. The photoresist should be then irradiated with UV light while passed through a photomask. A post exposure bake may be needed to accelerate the curing of the photoresist. For the positive tone interaction, the areas which are exposed to UV radiation are removed after development. This is opposite for the negative tone. Interested readers are referred to References [47-49] for a review of microfabrication and microstructure formation technologies.

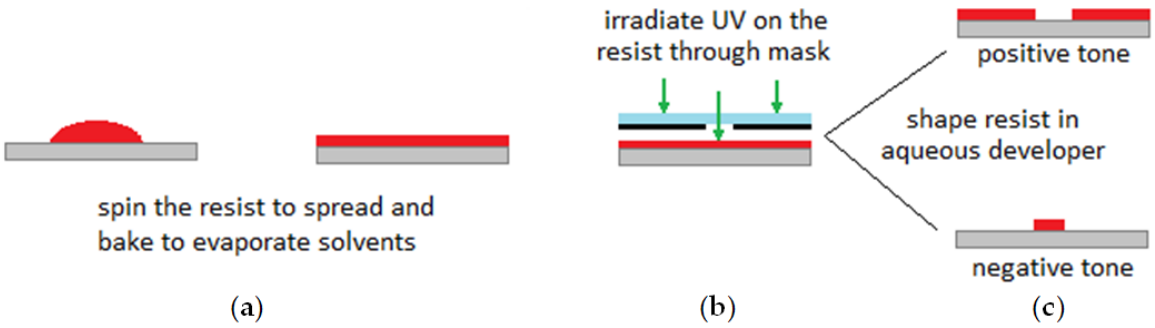

Figure 2.1 Process of photolithography
(a) Spinning a photoresist to spread and heat up to evaporate any solvents, (b) irradiating with UV light through a photomask, (c) positive/negative tone. Figure is reproduced from the Reference [31]

In the past few decades, various techniques to form micro scale structures have been developed. A brief description on the techniques which are more relevant with BioMEMS and microfluidics is provided in the following sections. During the 1980s, the total chemical analysis system concept emerged in analytical chemistry to propose the process of automation in analytical systems [30]. In the early 1990s, Manz et al. presented the concept of using planar fluidic devices to handle small volumes of liquid and established the field of miniaturized total chemical analysis system (μTAS) for this concept [50]. The high speed electrophoretic separation of fluorescent dyes [51, 52] and amino acids which are fluorescently labelled [53] are the first examples of microchip analysis, which was developed in the early 1990s. As MEMS based devices have evolved, the interest in microsystems as new research tools for biomedical applications has significantly increased and different start-ups were founded to manufacture and take advantage of these microsystems in the life science field [45]. Due to their small size, capability to work on short time scale and ability to act under physiologically relevant conditions, MEMS devices provide the unique opportunity for fabrication of analytical platforms which are particularly attractive for biological applications [54].
BioMEMS is a subset of MEMS which has the biological or biomedical applications. These miniaturized devices use manufacturing techniques inspired from microfabrication technology.

Processing, delivery, manipulation and analysis and/or construction of biological or chemical samples take place in these micro-devices [55]. Interest in BioMEMS applications such as diagnostics in DNA and protein micro-arrays, microfluidics platforms, pacemakers, biosensors, drug delivery systems etc. is increasing very rapidly [56, 57]. Stimulating neural implants, retinal implants for therapy of blind patients and microneedles for vaccination to prevent suffering from physical pain are some examples of BioMEMS applications [29]. The progress of BioMEMS technology coupled with the recent advancements in biotechnology (e.g., genomics, proteomics, tissue engineering), provide exciting opportunities for advancing the applications of BioMEMS devices. BioMEMS for detection (e.g., antibody detection, bacterial detection, viral detection), analysis (e.g., identification of bacteria and antibiotic susceptibility), diagnostics (e.g., cancer and autoimmune diseases), monitoring (blood glucose monitoring in diabetics patients), drug delivery (e.g., administration of antibiotics), cell culture (e.g., OOC platforms) are some of the practical applications achieved by the advances in microtechnologies [29, 55]. Just like the important role of microprocessors in the computer revolutions, BioMEMS devices have a significant role in the future of biomedical science. BioMEMS technology puts together the innovative talents of physicians, biological scientists, electrical, mechanical, chemical and materials engineers to develop miniaturized devices with various biomedical applications [3, 42].

Three categories of materials can be used for fabrication of MEMS based devices for biological applications. The first group includes silicon, glass and other materials that originate in the electronic industry and have been used in the early MEMS devices [29]. The second group of materials is plastic and polymers (e.g., polydimethylsiloxane known as PDMS). Polymers due to their biocompatibility, low thermal and electrical conductivities, low cost, ease of fabrication, rapid prototyping and ease of surface modification are ideally suited for fabrication of BioMEMS [58-60]. We refer the interested readers to References [61-63] for polymer-based microfabrication techniques. The third group contains biological materials such as proteins, cells and tissues which can be used in BioMEMS devices [6, 64]. However the use of biological materials is quite new. This category of materials offers many attractive opportunities in biomedical area (e.g., tissue engineering, OOC) [3, 43].

BioMEMS and μTAS are subsets of MEMS devices. Even though BioMEMS are more focused on micro-fabricated devices for biological applications, they have significant overlap with μTAS

which are basically more dedicated to the integration of the sequence of laboratory steps to accomplish chemical analysis. Such a small platform may gather the whole laboratory functions into a chip format. The idea of LOC has been developed after realizing that applications of μTAS technologies are not just limited to analytical purposes. Accordingly, LOC devices also are a subset of MEMS. LOC platforms use microfluidics, which is the science of manipulation of extremely small volumes of liquids. LOCs are integrated microfluidics platforms to perform multiple laboratory processes into a single chip. In the following section, we will review microfluidic platforms and their applications in the biomedical field.

2.2.4 Microfluidics

The annual number of new publications on the topic of microfluidics is increasing rapidly and continuously every year [65]. The investigation of fluid transport in plants is a good bio-mimicking example for studying of fluid mechanics in micro-channels, [66] on which it focuses on various specific characteristics of the dynamics of viscous flows in very small capillary tubes. However, because of the advances in microfabrication methods, the subject has received immense attention in recent decades [31, 67]. A microfluidic platform consists of micro-scale fluid handling compartments such as channels, valves, reservoirs, membranes etc. which enable integrated, automated, parallelized and miniaturized biochemical analysis in a consistent and easy manner. Microfluidics with its specific characteristics such as small size and laminar flow pattern offer new abilities in terms of spatiotemporal control of molecules [45, 68, 69], enabling biomedical devices to decrease the size and increase precise control over the platform. Laminar flow regime happens at very low fluid speed or low Reynolds-number (Re). The Re number is a critical dimensionless number in fluidic dynamics which is used to characterize the behaviour of the fluid in the system [30].The Re number is characterized by the ratio of inertial forces to viscous forces [32]. Since viscous forces tend to keep fluid steams moving very smoothly over each other without chaotic mixing, when the viscous forces are dominant (at low Re), a series of parallel fluid streams appears without mixing between them. This type of fluid flow is known as laminar flow. However, at high Re, inertial forces are dominant which results in unexpected movements and chaotic mixing between the fluid streams. This type of fluid flow is known as a turbulent flow [31, 70]. Figure 2.2 demonstrates the schema of the laminar and turbulent flow.

Fluids behave in a different way at the microscale than they do at the macroscale. One of the most important differences between macroscopic and microfluidic systems is the type of flow in microfluidic systems [71]. Generally, the flow is turbulent at the macroscale (Re > 1000), while at the microscale laminar flow is dominant. In microfluidics, fluids flow in parallel patterns without any radial, axial and tangential mixing due to the absence of turbulent vortexes and mass transfer can only happens through the interface between the molecules of the fluid layers by diffusion. This type of flow, as mentioned, is known as laminar when the viscous forces are dominant on inertia forces which are characterized by smooth flow (Re < 1) as oppose to the characteristics of turbulent flow. Thus, microfluidics provide precise and spatiotemporal control over the fluid by providing a laminar regime over the system [32].

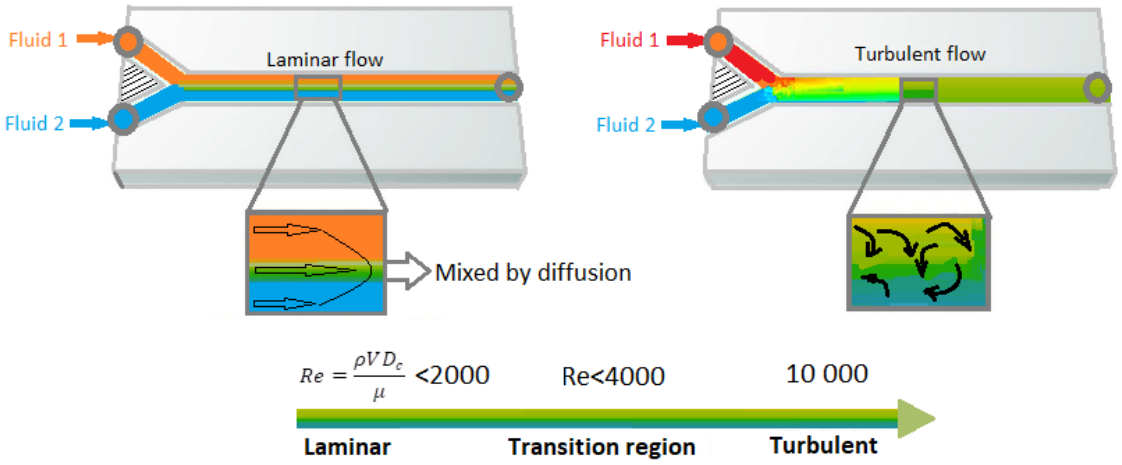

Figure 2.2 Laminar versus turbulent flow in the microfluidic channels
Figure is reproduced from Reference [70] and presenting the differences between laminar flow and turbulent flow in fluidic channels

Surface tension is another important feature in microfluidic systems. The small amount of fluids in microfluidic systems and big surface to volume ratio will result in insignificant gravitational and inertial forces and significant surface interactions such as capillary and hydration forces in these systems. Therefore, surface tension becomes dominant in such systems [71].

Culture bottles which have been in use since almost 1850 [65] and culture dishes which were introduces by Petri in 1887 [72] are some of the basic classical liquid handling tools for biological analysis and diagnostic assays. These traditional liquid handling tools have the potential of high–throughput sample processing and are easy to handle [3, 65], but lack of portability, lack of automation and high expenses to have a complex automated laboratory are some of their disadvantages [65]. Microfluidic devices have advantages to overcome these limits such as simpler automation, use of less sample volume, portability, simultaneous and parallel tests, faster analysis, lower cost per assay etc. [45, 70] and compete well against these conventional tools.

Microfabricated micro-channels have been used by many researchers in this field to accomplish capillary electrophoresis assays [73], to observe deformation of red blood cell membrane under hydrodynamic flow [74], in chemical micro-reactors [75], to transport living cells [76] and micromixers [77], among other applications.

Microfluidics have been raised from different origins of microelectronics, molecular biology, and chemical analysis [30, 78, 79]. One of the origins of microfluidics is microelectronics where microfabrication techniques such as photolithography have been shown to be very successful in microelectronics and MEMS devices. Microfluidics have been developed as a branch of MEMS devices which are specialized in liquid handling. The initial work in microfluidics has used silicon and glass as materials and microelectronic manufacturing techniques for the fabrication of micro-devices. However these materials are favorable when chemical or thermal stability is required, but neither silicon nor glass has the appropriate requirements such as gas permeability, full compatibility, and desired wettability for biological assays.

The other contribution to develop microfluidics systems has been raised from molecular biology. Genomics, Proteomics and other areas related to molecular biology (e.g., high-throughput DNA sequencing) require more sensitive and high throughput analytical methods. The ancient route of microfluidics comes from chemical and biochemical analysis. Chemical analysis techniques such as gas-phase chromatography (GPC), high-pressure liquid chromatography (HPLC) and capillary electrophoresis (CE) merged with the power of laser in optical detection to achieve sample analysis in low volume with high sensitivity. However, the number of commercialized microfluidics platforms in practical applications still is quite low and they have not been widely

used yet, but microfluidics is very well established in academia for the development of new methods and various applications in biomedical areas [3, 6].

At the beginning of the 1950s Elmqvist patented the first practical Reyleigh break-up ink-jet platform by efforts to distribute very small volume of liquids (nanoliter and picoliter)[80]. This innovation provided the basis for ink-jet techniques which are already used in printers. Later, in the year 1979, Terry et al. developed a miniaturized gas analysis platform based on the principles of gas chromatography (GC), using photolithography and chemical etching techniques on a silicon (Si) wafer [81]. Manz et al. by using Si-Pyrex technology have developed the first high-pressure liquid chromatography column device. At the beginning of the 1990s, several miniaturized microfluidics structures [82, 83] have been developed by the techniques used in the fabrication of micro-scale structures in silicon [65]. Later, simple and easy to operate microfluidic devices based on capillary liquid transport have been developed. Test strips for drug abuse [84], pregnancy tests [85], cardiac markers [86] are among the first few commercial microfluidic devices which obtained a significant market and still have high sales potential.

Following the efforts towards miniaturization to reduce the time of analysis and to have better performance, the newly emerging concept of “micro total analysis systems” (μTAS) which later expanded to “LOC” appeared [50]. In the following section, we discuss about microfluidics application to develop LOC devices.

2.2.5 Lab-on-a-Chip

Lab-on-a-Chip (LOC) based-devices integrate multiple laboratory functions on a single chip of only a few square millimeters to a few square centimeters in size. These platforms provide miniaturized, automated, integrated and parallelized chemical and/or biological analyses [87] which can offer cheaper, faster, controllable and higher performance of bio-chemical assays at a very small scale when compared with conventional laboratory tests. These microengineered devices are capable of handling extremely small fluid volumes down to less than a few picoliters. [31]. Just a few micro-droplets of whole blood, plasma, saliva, tear, urine or sweat have the potential to be tested in these miniaturized platforms for medical diagnostics [88]. This last is highly important in many clinical trials and biomedical research where usually very small

volumes of patient samples are available. In another side, automation with eliminating the human interfering parameters can increase the confidence in the analysis [89].

A clear example that demonstrates the principle of LOC is the portable blood test device which has been developed by the Biosite Company. Just a drop of patient's blood is required to displace into the reservoir of the device then the entirety of the assay takes place on a single platform and the diagnostic can be done in only a few minutes [45].

Other biomedical applications for LOC have been reported, including proteins and DNA detection [44], hormone detection [90], pathogen detection [91]. In the following section, we focus on the application of LOC platforms in POC diagnostic devices.

2.2.5.1 Lab-on-a-Chip Devices for Point-of-Care Diagnostics

Point-of-care (POC) diagnostic platforms are small medical devices which provide diagnostic results quickly in the easiest way [67]. However, these diagnostic procedures can be performed by healthcare professionals, but working with these devices does not need trained specialists and the tests can be done by the patient in a range of settings including home, laboratory, hospital or clinic. Increasingly, the need for the fast diagnostic of acute diseases such as acute myocardial infarction and for home care testing such as blood glucose monitoring in diabetic patients, has grown the interest to develop POC systems. The high surface area to volume ratio in microfluidic systems results in a significant decrease in the time of analysis in LOC for POC testing [92]. This provides the chance for rapid diagnosis and treatment at the point of care. Moreover, non-expert users can easily work and obtain the test results with these POC devices.

Lateral flow tests or capillary driven test strips which have been well known since the 1960s [87], are the major class of POC systems which use a membrane or paper strip to confirm the presence or absence of a target analyte such as host antibodies. By adding a small volume of sample, capillary action [65] is induced and the sample moves along the channel passing through the membrane where immobilized antibodies and labels have been stored. If the targeted particles are present in the sample, it will bind to the immobilized antibodies and labels and continue to move along the device. As the sample moves, the binding reagents which are located on the membrane will attach to the targeted compound at the test line. The test results can be read out qualitatively where a colored line forms, or quantitatively where the device has been combined with reader technology to provide results [92, 93].

These automated and on-site diagnostic devices provide cost-effective, easy to handle and disposable tools to detect different biomarkers including proteins, nucleic acids, cells and metabolites such as glucose, urea nitrogen, lactate, etc. [92]. Test strips for detection of infectious diseases such as pneumonia [94] and influenza [92], also for detection of sexually transmitted infections like syphilis and HIV [67], are some of the examples of lateral flow tests in POC. In developing countries, due to the little or no medical infrastructure, the mortality rate from infectious disease is quite high [95, 96]. Therefore, POC systems by fast detection of infectious diseases significantly help to increase patient survival rate [44].

The test strips for glucose-level monitoring [97] for glycemic control and the lateral-flow immunoassay [98] for home pregnancy test are some of the well-established early examples of POC systems which obtained a remarkable market. Based on the first capillary driven immunoassay system that was introduced in the later 1970s [65], the over-the-counter pregnancy test was developed and commercialized in the 1980s [99]. The device consists of a sample inlet, a sample layer, a conjugate layer, incubation and detection layer, a detection window and an absorbent layer. When the patient's sample (urine) is introduced into the sample layer through the device's inlet, it moves by capillary forces. In the conjugate layer, where the antibodies have been stored, binding between antibodies and sample's antigens (human chorionic gonadotropin or hCG) takes place. As the sample is transported into the detection layer, this binding reaction continues. Another type of antibody on the test line catches the particles which are coated with antigens. There is a third type of antibody on the control line to catch particles which did not bind to antigens. The presence or absence of hCG (pregnancy hormone) in the sample will be detected by the detection line, while the control line, which appears on every test, demonstrates that the test works properly. Within minutes, the result appears in detection window indicating whether or not hCG hormone has been detected in the sample [65, 100] (Figure 2.3).

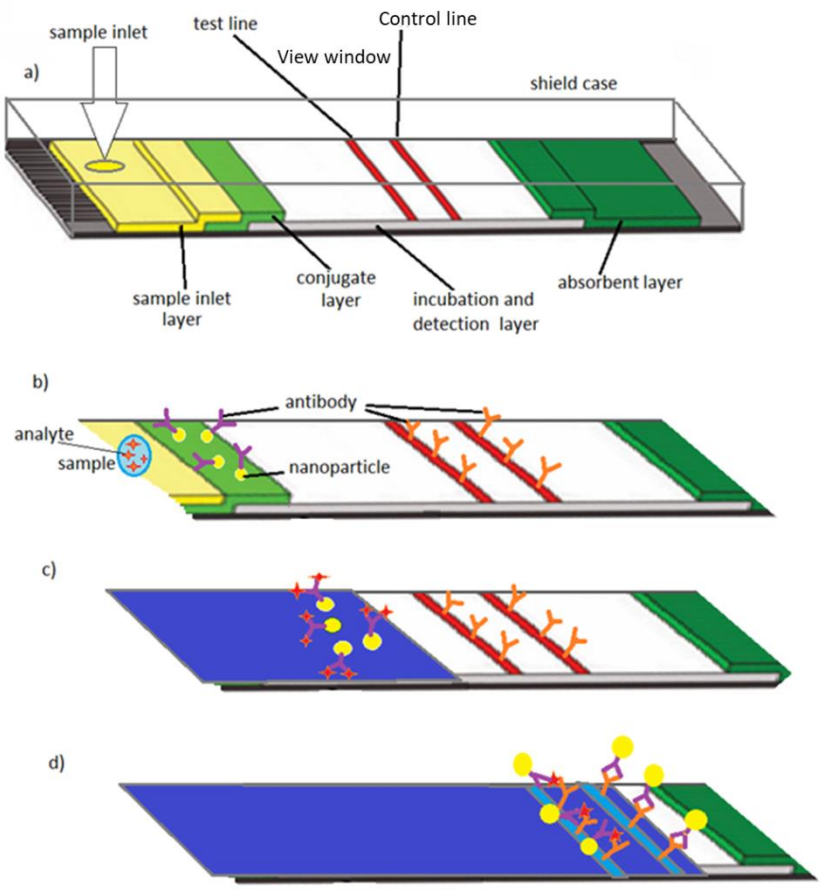

Figure 2.3 Lateral flow assay schematic design

(a) A lateral flow test strip including sample inlet, sample layer, conjugate layer (i.e., reactive agents and detection molecules), incubation, detection zone and final absorbent layers including test and control lines (i.e., analyte detection and functionality test), (b) introduction of sample into the test strip via sample inlet, (c) antibodies conjugated to labeled nanoparticles start to bind to the analyte, (d) antibodies with antigens bind to the test line and antibodies without antigens bind to the control line. Reproduced from Reference [65].

Ionic blood chemicals and metabolites can be used as biomarkers to determine various health conditions such as liver disease, diabetes etc. Glucose monitoring systems for management of diabetes, have occupied the majority of the biosensor market [101]. Blood glucose monitoring devices (Figure 2.4) that significantly improve diabetic patients' lives, also perform on membranes but its analytical method is different from lateral flow immunoassay as it use signal amplification by a redox enzyme. Reaction between glucose oxidase in the test strip and the glucose in the blood will produce an electrical current which determines the concentration of the glucose in the sample and provides numerical results for readout by the meter [67].

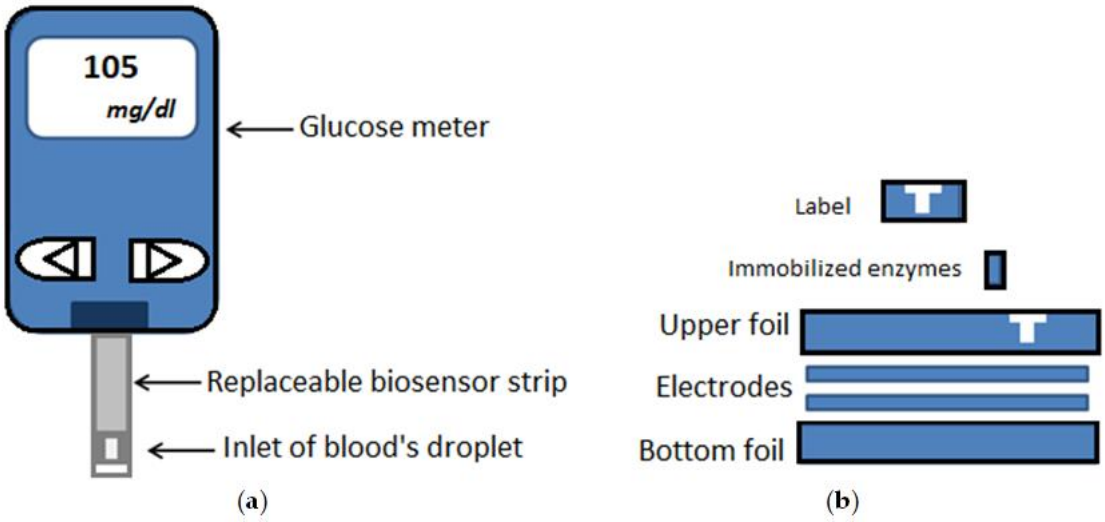

Figure 2.4 Blood glucose monitoring system
(a) Scheme of a commercial blood glucose test device, (b) different layers of a biosensor test strip. Reproduced from Reference [102]

POC diagnostic devices have significant impacts in public health of developing countries. Although, low power consumption, cost-effective analysis, fully-automated test, ability to use unprocessed specimen (e.g., whole blood), being highly user-friendly, provide interpreted results quickly and less challenges regarding to transportation and storage are some of the parameters

which should be given more attention to design of POC devices for resource-limited settings in the developing world. Table 2.1 provides a list of current microfluidics companies which provide commercialized LOC-based point of care diagnostic devices.

Table 2.1 List of selected microfluidic companies working to manufacture integrated point-of-care (POC) diagnostic devices
Adapted from Reference [67]

Company Name	Materials and Manufacturing	Analytes	Applications	Sample Types	Signal Detection	Highlights of Technology Suited for POC
Abaxis	Plastic disc	Small molecules, proteins	Blood chemistries (e.g., metaboliteselectrolytes)	Whole blood	Absorbance	Compact analyzer, injection-molded plastic discs, no pre-processing of sample
Advanced Liquid Logic	Glass, insulated electrodes	Small molecules, proteins, nucleic acids	HIV/AIDS, Iysosomal storage disease	Whole blood	Fluorescence, chemiluminescence	Sample pre-processing compact, benchtop analyzer, manipulation of nano-and micro-droplets
Alere(formerly inverness Medical)	Plastic and elastically deformable materials	Proteins, cells	HIV/AIDS, clotting time	Whole blood	Fluorescence	Disposable cartridge, portable analyzer, automated image-based immune hematology test
Biosite (Alere)	Strip with textured microstructures	Small molecules, proteins	Cardiovascular disease, drugs of abuse, waterborne parasites	Whole blood, plasma	Fluorescence	Portable reader, disposable capillary-driven microfluidic test strips
Cepheid	Disposable plastic cartridge	Nucleic acids	Respiratory infections (bacterial and viral), cancer	Whole blood, sputum	Fluorescence (with molecular beacons)	Disposable cards with benchtop analyzer , on-card sample processing (sputum)
Daktari Diagnostics	Plastic cartridge	Cells	HIV/AIDS	Whole blood	Electrochemical (impedance spectroscopy)	Handheld instrument, label-free electrochemical sensing of captured cell lysate
Diagnostic For All	Paper	Small molecules, Proteins	Liver damage from HIV/AIDS medication	Whole blood, urine	Colorimetric	Instrument-free tests based on paper, capillary-driven microfluidics, colorimetric

						readout
Epocal (Alere)	Film, epoxy laminates	Small molecules	Blood chemistries	Whole blood	Electrochemical, chemiluminescence	Self-contained cards, patterned electrodes for sensing, wireless data transmission
Focus Dx (Quest)	Plastic (polypropylene)	Nucleic acids	Flu, intestinal pathogens	Nasal and pharyngeal swabs	Fluorescence	Portable detector, discs with on-board extraction
HandyLab (BD)	Disposable cartridges	Nucleic acids	Bacterial infections and drug susceptibility testing	Vaginal, rectal, nasal swabs	Fluorescence (with molecular beacons)	Disposable cards with integrated heating, detection, sample processing in a portable instrument
i-STAT Corp (Abbott)	Plastic cartridge with silicon microchip	Small molecules	Blood chemistries, coagulation, cardiac markers	Whole blood, urine	Electrochemical (potentiometry, amperometry, conductivity)	Portable analyzer, capillary-driven microfluidics, thin-film electrodes for detection
Micronics (Sony)	Plastic, laminates, paper	Proteins, nucleic acids	Malaria, shiga toxin-producing E-coli, ABO blood typing	Whole blood, stool	Absorbance, colorimetry	Disposable cartridges composed of thin-film laminates and injection-molding
Philips	Plastic cartridge	Nucleic acids, small molecules, proteins	Cardiac damage, drugs of abuse, hormones	Whole blood, saliva	Optical (frustrated total internal reflectance)	Handheld reader with self-concentration of magnetic nanoparticles for rapid analysis
TearLab	Polycarbonate	Small molecules	Dry eye disease (tear osmolarity), ocular allergy (IgE antibodies)	Tear	Electrochemical	Portable osmolarity reader with disposable cards; capillary-driven flow, gold electrodes for detection, results in 5 s

Increasing the interests towards microfluidics and its applications in biomedical areas in the last two decades led to the emergence of novel fabrication technology using biocompatible polymers for biological applications [3, 42]. The incorporation of microfluidics with MEMS manufacturing

techniques has provided the possibility of producing delicate molds for casting microfluidic patterns by use of a biocompatible polymer such as PDMS. PDMS has unique properties including gas permeability, biocompatibility, optical transparency, elasticity, low cost and ease of microfabrication with soft lithography technique [3, 6]. These advancements in microengineering have led to innovate new generation of cell culture platforms known as OOC. In the following section, we highlight current achievements in this field.

2.2.6 Organ-on-a-Chip

As mentioned above, microfluidic cell culture platforms by providing a dynamic physiological microenvironment for cells and precise control over small amount of sample, offer unique advantages over traditional cell culture techniques (e.g., culture in Petri dishes) and static 3D cell culture models (e.g., scaffold techniques and scaffold free techniques). The majority of research relies on monoculture cell signaling and cell-cell interactions in two dimensions. However, cellular interactions in three dimensions at the tissue and organ levels have significant impacts in cellular responses to environmental cues [34, 103]. Conventional 2D cell-cultures are not able to mimic the 3D structure, mechanical properties and biochemical microenvironment that cells experience in a living organ [34, 104]. Various static 3D cell-culture models (e.g., bioreactors, spheroid and gel based cell culture techniques) were developed over 50 years ago to overcome the limitations related to 2D cell-culture [3]. Compared with conventional 2D models, 3D cell culture models better simulate the 3D microenvironment that cells normally experience *in vivo* and advanced our understanding of the cell behaviour in better bio-mimicking tissue models [38]. On the other hand, microfluidic cell culture platforms provide better mimicking of a more sophisticated manner of cell culture and analysis at the microscale [105]. As compared to static cell culture models, microfluidic cell culture platforms are able to emulate the dynamic microenvironment for the cells when macroscopic cell culture models fail to reproduce the microenvironment of the cells as it is *in vivo*. Microfluidic cell culture based platforms offer the possibility of creating biochemical gradients of metabolites, soluble factors, cytokines and other molecules in the cellular microenvironment [3]. The specific characteristics of microfluidic systems, such as the laminar flow pattern, can provide sustained biochemical gradients. For instance, Han et al. developed an in-vivo like inflammatory model in a microfluidic platform to

characterize neutrophil migration behaviour influenced by a gradient of two chemoattractants. This study showed that neutrophils demonstrate different responses to the chemoattractants [106]. With other unique benefits such as decrease in reagent consumption, smaller volume of samples, decrease the risk of contamination, and reproducibility, microfluidic based culture models offer unique *in vitro* platforms for high throughput cell culture assays [107]. Table 2.2 illustrates an overview of the significant advantages of microfluidic cell culture versus macroscopic cell culture models (e.g., 2D cell culture and static 3D cell culture models).

Table 2.2 A comparison between the advantages and disadvantages of macroscopic cell culture models and microfluidic cell culture platforms

Cell Culture Methods	**Advantages**	**Disadvantages**
2D cell culture	▪ Well established Methods ▪ Easy to work ▪ Cost effective	▪ Lack of 3D environment for cell-cell and cell-ECM interactions ▪ Uniform concentration of nutrients and drugs ▪ Fail to produce dynamic microenvironment ▪ Not enough biological relevant model
3D cell culture models	▪ Provide 3D environment for cell-cell and cell-ECM interactions ▪ Present of soluble gradient (nutrients and drugs) ▪ Provide more physiologically relevant model for drug testing	▪ Extra expenses ▪ Fail to produce dynamic microenvironment ▪ Lack of fluid flow perfusion ▪ Expensive ▪ Challenges in microscopy and measurement
Microfluidic cell culture platforms	▪ Precise control over cellular microenvironment ▪ Diffusion gradient of nutrients and drugs ▪ Ability to provide fluid flow ▪ Produce in-vivo like and dynamic environment ▪ Cost-effective(less reagents consumption) ▪ Less sample needed (advantage for personalized medicine) ▪ Provide fast test results ▪ Possibility of merging with	▪ Non-standard protocols ▪ Expenses and difficulties associated with fabrication ▪ Bubble formation in channels ▪ Channel clogging by cells ▪ Complex design and manufacturing process and challenges associated with operational control

	mechanical stimulus and sensors ▪ Real-time and on-chip analysis ▪ Custom made device

OOC platforms are new generation of 3D cell culture models that better emulate the dynamic, physicochemical, biochemical and microarchitecture properties of the microenvironment of living organs. These microfluidic cell culture platforms recapitulate the cellular microenvironment, tissue–tissue and cell–cell interface interactions, spatiotemporal, biochemical gradients and biomechanical properties of a whole living organ with the aim of mimicking the smallest functional unit of an organ.

Figure 2.5 represents the general process to fabricate a microfluidic OOC platform. The principles to manufacture OOC based platforms are almost similar. Basically, after considering various parameters to emulate the specifications of a specific organ, the desired design would be drawn with a design and drafting software (e.g., AutoCAD, CATIA). Later, an appropriate microfabrication technique (e.g., photolithography, stereolithography, soft lithography etc.) according to the aims of the device will be used to fabricate the device. Cell culture or tissue culture will be performed on the biochip in order to mimic the functionality of a specific organ and to perform biochemical or biophysical assays and drug testing.

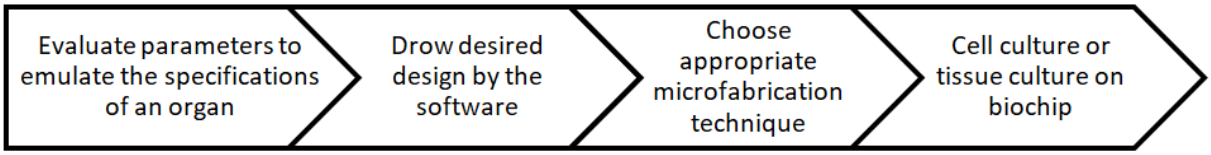

Figure 2.5 General process to fabricate a microfluidic OOC platform

Design, microfabrication, tissue culture and biological assays are the main steps to develop an OOC microfluidic platform for biological or pharmaceutical tests

In the following section, we highlight the current advancements in OOC platforms.

2.2.6.1 Current Organ-on-a-Chip Platforms

2.2.6.1.1 Lung

Gas exchange between air and blood takes place in the pulmonary system which has a complex structure. A bio-mimicking *in vitro* model of the lung is critical to model lung diseases (e.g., infectious diseases), drug development and toxicity tests. The most specific characteristic of the lung is its dynamic and periodic mechanical motion. In the pioneering work by Huh et al. [38], the first breathing lung-on-a-chip model has been introduced. In this biomimetic microdevice, the critical functional unit of the living lung (alveolar-capillary interface) has been constructed. To mimic the effect of breathing, this breathing lung-on-a-chip model used a lateral vacuum to apply cyclic stretching motion on a thin porous flexible PDMS membrane which acts as the interface between pulmonary microvascular ECs and alveolar epithelial cells (Figure 2.6). This model has been used to test immune responses to pulmonary infection and the response to nanoparticles. Interestingly, the periodic mechanical motions influenced the experimental data. This highlights the importance of physiologically relevant *in vitro* platforms to model human diseases and drug testing.

Douville et al. [108] developed an alveolar model. In this platform, alveolar epithelial cells were influenced by two different physiological conditions: the combination of solid mechanical stresses and surface-tension stresses, and exclusively cyclic stretch. The impact of fluid-filled alveolar cavities (e.g., in pneumonia) in alveolar epithelial cell death has been studied. The results demonstrated that cell detachment and cell death increased when cells experienced a combination of fluid and solid mechanical stresses.

Stucki et al. [109] presented a lung-on-a-chip model by the construction of an alveolar barrier in respiratory dynamics. A patient derived bronchial epithelial cell line demonstrated how mechanical stretch influenced epithelial barrier permeability. This model also showed that cell culture improved in the *in vivo* like dynamic model compared to a static one.

Recently, Jain et al. [110] developed a therapeutic model of microfluidic lung-on-a-chip for intravascular thrombosis in lung alveolus. Antagonist to protease-activated receptor-1 has been tested in this platform. This platform offers the potential to mimic pulmonary thrombosis pathophysiology towards antithrombotic drug development.

Benam et al. developed a small airway-on-a-chip model. This model has an air channel on top and a fluid flow channel on the bottom, between which a mucociliary bronchiolar epithelium

layer has been placed. Asthma has been mimicked *in vitro* by exposing the epithelium to interleukin-13 (IL-13). This model was able to recapitulate *in vivo* like responses to therapeutics. The global public health crisis linked to the 2019 novel Coronavirus (SARS-CoV-2 or COVID-19) pandemic and its socio-economic disaster [111] brings so much attention to the OOC community regarding the crucial importance of developing reliable models of lung-on-a-chip platforms for disease modeling and drug development purposes to tackle the continuous spreading of COVID-19 and other human respiratory viral infections. In the recent work by Si et al. [112] a human lung airway biochip was developed and lined by human lung airway epithelial cells and pulmonary microvascular endothelial cells. To investigate the potential of this lung-airway-on-a-chip to mimic lung physiology and pathophysiology, seven anti-viral therapeutics have been tested on this platform. This study demonstrated that OOC models are promising *in vitro* tools to emulate human lung responses to respiratory infections.

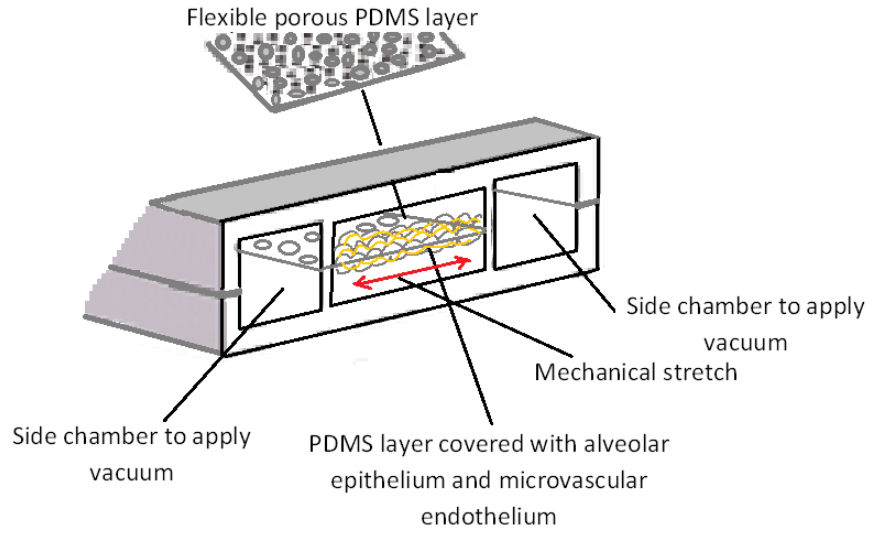

Figure 2.6 Schematic design of the microengineered lung-on-chip model

An alveolar-capillary interface constructed on a flexible and porous PDMS membrane. By applying vacuum to the side chambers, a mechanical stretch has been created on the alveolar-capillary barrier to mimic a human breathing lung. Figure is reproduced from Reference [38].

2.2.6.1.2 Cardiovascular

Multiple design factors need to be considered to mimic the cardiovascular physiological microenvironment. Cardiac muscle tissue consists of organized cardiac muscle cells (or myocardium) and fibroblasts. Blood vessels also have complex structures including smooth muscle cells, endothelial cells and blood flow which result in fluid shear and vessel deformations. Microfluidic platforms are able to apply defined shear profiles into the cells cultured in the system. In addition, microfluidic platforms can take advantages of using syringe pumps and on-chip valves [113] or Braille display devices [114] to move fluid flow over the cultured cells to create more a physiologically relevant *in vivo* like blood vessel microenvironment. Cardiovascular diseases are one of the leading causes of death worldwide [115] Therefore, new drugs and therapies to treat or prevent cardiovascular diseases are urgently needed. Moreover, many drugs to treat other diseases have adverse side effects on the cardiovascular system [115, 116] which highlights the importance of *in vitro* models of the cardiovascular system for drug testing.

Au et al. [117] developed a polystyrene cell culture chip with microgrooves. Electrical stimulation applied and mutation and elongation of neonatal rat cardiomyocytes augmented to form gap junctions. Marsano et al. [118] fabricated a three-dimensional beating cardio tissue on a microfluidic chip (Figure 2.7). Mechanical stimuli which have been applied on the platform during the culture ended up with better cell maturation and augmented the electrical and mechanical coupling. Various concentrations of isoprenaline have been tested on this device which highlights the application of this heart-on-a-chip model in drug discovery and toxicology tests.

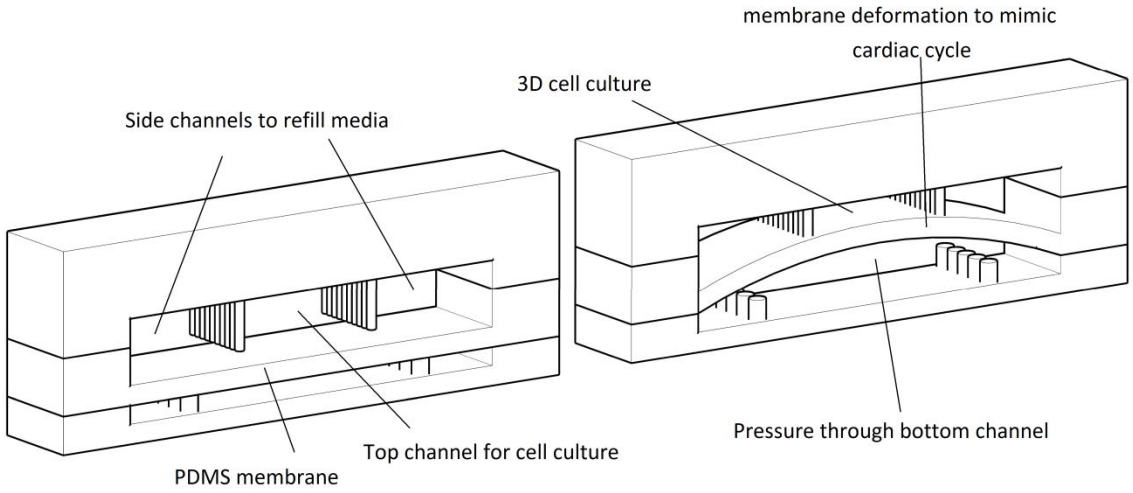

Figure 2.7 Schematic design of the heart-on-a-chip platform
This includes two microchambers which are divided by a PDMS membrane. The top chamber is subdivided into a central channel to grow 3D cell culture, and two side channels to refill culture media. The cardiac muscle's contraction and relaxation mimicked through deformation of PDMS membrane by applying pressure on the bottom channel. Figure is reproduced from Reference [118].

A mussel-inspired microfluidic chip was fabricated by Ahn et al. [119] to test cardiac contractility. Gelatins as an extracellular matrix as well as silver nanoparticles and titanium oxide have been used to fabrication of this three-dimension chip. *In vitro* contractile effects can be measured on this biomimetic analytical platform by cardiotoxicity of nanoparticles that affect calcium signal to sarcomere.

Lind et al. [120] used 3D printing to develop a cardiac tissue on a chip for drug testing applications. Xiao et al. [121] developed a microfabricated bioreactor to incorporate aspects of perfusion into the cardiac tissue model. Polytetrafluoroethylene (PTFE) tubing template, covered with neonatal rat cardiomyocytes (CMs) and human ESC derived CMs was used to create this perfusable 3D microtissue (which is called Biowire). This platform has been used for drug testing. Another cardiac model was developed by Ren et al. [122] to mimic hypoxia-induced myocardial injury. This microfluidic platform emulates the interface between cardiac tissue and blood vessels. By using the specific oxygen consumer blocking agent in the channels, hypoxic conditions were created. This resulted in morphological changes (e.g., cell shrinkage) and signs

of apoptosis. Finally, Guenther et al. [123] fabricated an artery-on-a-chip platform to study the physiological response of the small blood vessel. In this microfluidic platform, small blood vessels have been placed within the channel, and then negative pressure to specific regions applied to clamp them in place. Various concentrations of biochemical solutions can be perfused in the channel. This platform mimics the complexity of the physiological structure of the blood vessels.

2.2.6.1.3 Brain

The brain is one of the most sophisticated organs which comprises of a wide variety of cells. Human brain genetics and functions are significantly different than animals. Therefore, animal models only can give us a basic understanding of the brain functions and diseases [124]. Microfluidic brain-on-a-chip models have been developed to better mimic *in vivo* conditions including chemical, electrical and physical conditions of the human brain [3, 125]. Here, we briefly review the current developments of microfluidic brain models.

Owing to the importance of axons in neurodegenerative disease, some researchers only focused on neuronal axons. A microfluidic platform has been developed by Taylor et al. for high-resolution axonal transport. Isolation and monitoring of axonal mitochondria and axonal growth have occurred in this platform [126]. A circular microfluidic chip presented by Park et al. [127] in which the soma compartment was located in the center with sealed microgrooves divided from the axonal compartment. A straight pathway for axonal growth resulted from these microgrooves. An image processing method to quantify the axonal growth has been developed by these researchers to address the issue of invasive sampling to characterize the growth of axons. Effects of various extracellular matrix (ECM) components (e.g., matrigel, collagen, laminin and etc.) have been assessed on axons growth and soma compartments separately. Based on which parts of the neurons are exposed to these biomolecules, they have different effect on axon growth.

A multilayer microfluidic platform fabricated has been developed by Park et al. [128] to mimic *in vivo* brain microenvironement for neurodegenerative diseases and high-throughput drug testing. The pluripotent human cells were grown on a chip to incorporate the blood-brain barrier. The cellular interactions between human fetal neural progenitor cells and the mature model have been assessed in this platform. By using an osmotic micropump, the effect of flow on neurodevelopment has been investigated. Kunze et al. [129] developed a microfluidic platform

for neural cell culture to construct neural layers and 3D architecture. They described agarose–alginate mixtures which build multilayered scaffolds with layers of embedded primary cortical neurons apart from cell-free layers. To form concentration gradients, B27 supplementation has been delivered. This 3D scaffold based microdevice has the potential to be used for *in vitro* studies and drug testing.

A silicone elastomer brain-on-a-chip *in vitro* model was presented by Kilic et al. [130]. Neurospheroids were cultured on a microfluidic chip with flow control. Complex neural network and neural differentiation occurred on the platform by changing the flow. Toxic effects of amyloid-β in two different conditions (with and without flow) have been assessed in the system. The results showed that neurospheroids develop better in the dynamic conditions. Dauth et al. fabricated a multiregional brain-on-a-chip model [131]. Particular disease models can be developed on this platform. A decrease of firing activity and change in the amounts of astrocytes and particular neuronal cell types in comparison with separately cultured neurons was noticed in their research. The effects of phencyclidine (known as angel dust) which is a mind-altering drug have been investigated in this platform as well.

Magnetic hyperthermia therapy attracted researchers' attention in cancer therapy due to the generation of local heat to minimize damage to healthy cells nearby and optimize the treatment. Recently, a microfluidic based brain tumor-on-a-chip model was developed by Mimani et al. [132] to access the therapeutic effect of magnetic hyperthermia on the chip. A 3D cell culture of glioblastoma has been cultivated in the central zone of the microfluidic channel. Cell viability after exposure to magnetic hyperthermia therapy has been studied on the device. Results of fluorescence imaging have demonstrated that cell viability decreased by 100% after 30 min of exposure to magnetic hyperthermia therapy. However, tumor vasculature is absent in this model; the results of this study showed that this brain tumor OOC model has great potential to emulate the characteristics of glioblastoma brain tumor *in vitro* (Figure 2.8).

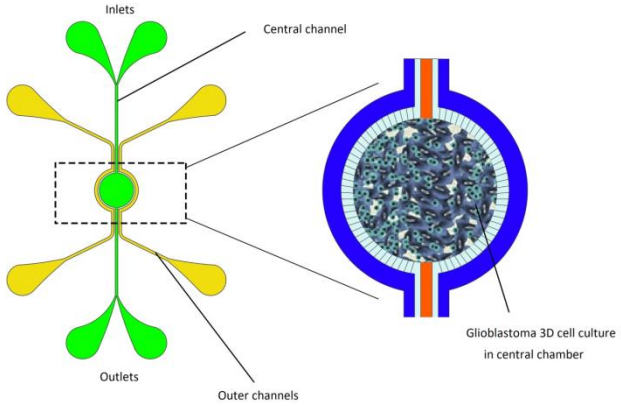

Figure 2.8 Schematic of Brain tumor-on-a-chip model

This model was developed by Mimani et al. to access magnetic hyperthermia therapy on-a-chip. This chip was formed by a central and an external compartment separated by a porous interface. Magnetic nanoparticles through the central microfluidic channel were introduced to central region of the chip which tumor cells have been cultivated in the 3D model. Then, through an alternating magnetic field, magnetic energy transforms to thermal energy and produce heat. Image reproduced from Reference [132].

2.2.6.1.4 Liver

The liver with its crucial functions such as metabolization, detoxification of blood from various metabolites and production of biomolecules for digestion, is one of the most vital organs. Since toxicity of the liver is one of the main causes of drug failure, an *in vitro* model of the liver that can mimic the *in vivo* like microarchitecture of the liver is crucial in drug development processes. Hepatic lobule (which is comprised of sinusoids and blood vessels lined with endothelial cells) is the functional unit of the liver [133]. Since the perfusion of fluid is the main characteristic of the liver, microfluidic cell culture platforms must provide perfusion conditions that better emulate liver function *in vitro* when compared to conventional cell culture models [134].

Powers et al. [135] developed a liver-on-chip model which had a silicon sheet scaffold with an array of channels which were separated by a microporous filter to provide upper and lower chambers for perfusion of the culture medium. They observed morphogenesis of 3D tissue structures under continuous flow perfusion in this platform. Lee et al. [136] presented a

microfluidic liver-on-a-chip platform to assess hepatocytes interactions and hepatic stellate cells in 3D culture model. This platform was able to provide the continuous perfusion of culture medium to the cells through an osmotic pump without the need for an external power source. They developed monoculture and co-culture of hepatocytes and hepatic stellate cells and investigated cellular interactions with or without flow.

Lee et al.[137] introduced an artificial microfluidic liver sinusoid on a chip by packing a high density of hepatocytes into a microchannel. This platform recapitulates the transport phenomena in sinusoid in which sinusoidal endothelial cells facilitate blood and plasma transport to the hepatic cords. Transport properties of the sinusoid (e.g., continuous nutrient exchange and cell–cell interactions) were maintained in this platform to give the possibility to primary rat and human hepatocytes to stay viable for a period over 7 days. By using a liver toxicant, hepatotoxicity has been assessed in this liver sinusoid on chip platform.

Bavli et al. [138] developed an integrated microfluidic liver-on-a-chip platform to monitor metabolic activities (e.g., glucose uptake, lactate production and oxygen uptake) *in vitro*. Khetani et al. [139] introduced a model in which hepatocytes and 3T3 fibroblasts were cultured on a micropatterned collagen in 24-well plates. Cho et al. [140] presented microfabrication and micropatterning techniques to create layered hepatocytes on micropatterned fibroblast feeder layers. This platform has been used to assess cellular interactions in the co-culture model of hepatocytes and 3T3-J2 fibroblasts.

In the liver-on-a-chip model presented by Delalat et al. [141], a 3D cellular microstructure was developed to mimic the hepatic sinusoid for screening the drug cytotoxicity. Furthermore, some other liver-on-a-chip platforms have been developed for *in vitro* modeling of liver injury and disease [142, 143].

Recently, Kamei et al. [144] introduced a simple 3D liver-on-a-chip model with mature hepatocyte-like cells which have been differentiated from human pluripotent stem cells (hPSCs). In this study, a microfluidic cell culture platform was used for the hepatocyte-like cells maturation. This platform can be served in drug testing and chemical-safety assays.

2.2.6.1.5 Kidney

The Kidney is one of the most sophisticated organs to mimic since it is comprised of several tissues. The kidney is known as a vital organ for its crucial functions including filtration of blood,

toxin removal and maintenance of electrolyte balance. One of the most reported adverse effects during the drug development process is the toxicity of the kidney. The first model of toxicity was a study on a kidney-on-a-chip microdevice reported by Jang et al. [145]. In this model, primary kidney proximal tubular epithelial cells have been cultured on a microfluidic device under perfusion. Fluidic flow emulates the key characteristic of the human kidney proximal tubule. Reabsorption of glucose, transport of albumin and alkaline phosphatase activity have been studied in this microfluidic kidney-on-a-chip model.

According to the importance of glomerulus which is critical in blood filtration, Musah et al. [146] developed a kidney-glomerulus-on-a-chip model. In this platform, human induced pluripotent stem cells differentiated into podocytes which are the cells that regulate selective permeability in glomerulus. Glomerular basement-membrane collagen to provide tissue–tissue interactions with glomerular endothelial cells have been generated *in vitro*. Adriamycin-induced albuminuria and podocyte injury have been emulated via this glomerulus-on-a-chip model.

A glomerulus-on-a-chip microfluidic platform developed by Zhou et al. [147] emulated the vascular and epithelial interface between podocytes and endothelial cells in the kidney glomerulus. To mimic the glomerular microenvironment *in vitro*, perfusion of fluid flow and mechanical forces have been applied in this microdevice. This study demonstrated the importance of shear stress and hydrodynamic pressure in cellular cytoskeletal rearrangement and cellular damage to emulate kidney disease such as hypertensive nephropathy.

Recently, a virus-induced kidney disease model was fabricated by Wang et al. [148] by developing a three-layer microfluidic platform. This distal tubule-on-a-chip model was presented to investigate the pathogenesis of virus induced renal dysfunction in regulation of electrolyte.

A review published by Wilmer et al. [149] focuses on development of kidney-on-a-chip technology to mimic the structural and functional properties of the human kidney for prediction of drug-induced kidney injury.

2.2.6.1.6 Gut

Human *in vitro* models of the intestine are very important in pharmacokinetics studies. Conventional *in vitro* models fail to recapitulate physiological microenvironment (e.g., cyclic peristaltic motion) of the human gut. Therefore, microfluidic platforms provide a powerful *in vitro* model of intestine to mimic *in vivo* like microenvironment for drug testing.

A microfluidic device consisting of two lumens which have been separated by a porous membrane was developed by Kimura et al. [150]. A stirring pump was integrated to the platform to control the fluid flow in the system and to create a dynamic environment for the cells. Caco-2 cells have been cultured in the system for over 30 days and Rhodamine 123 was added into the system to investigate the cells permeability.

The microfluidic gut-on-a-chip model developed by Kim et al. [151] provides *in vivo* like peristaltic movements and fluid dynamics were applied on the system to induce intestinal epithelial cells to undergo multiple intestinal cell types differentiation. The 3D structures and complex physiological functions of the human intestine can be recapitulated in this platform. An intestinal inflammation model was developed on a gut-on-a-chip platform presented by the same group. The platform can be used for the pathophysiological study of human intestinal inflammation produced by overgrowth of bacteria [152].

Recently, a gut-on-a-chip model was developed by Shin et al. [153], which provides mechanical movements and perfusion of fluid flow in the system to investigate the role of physical stimulus on intestinal morphogenesis. Human intestinal Caco-2 and primary intestinal epithelial cells have successfully been cultured in this gut-on-a-chip model. Other cell types such as mesenchymal cells can be incorporated to this system to investigate how they can contribute to intestinal morphogenesis. The 3D morphology which was observed in this model, matches perfectly with the related computational simulations.

2.2.6.1.7 Skin

The skin is considered as the largest organ with several specific functions including regulation of body temperature, prevention of dehydration and acting as the first protection shield to protect other organs against environmental stressors (biological, physical and chemical). For toxicology testing of new compounds, physiologically relevant skin models are of crucial importance for pharmaceutical, chemical and cosmetic industries to identify potential hazards on the skin [154]. In this section, we highlight the current developments on skin-on-a-chip models. One of the key features to develop biomimetic skin models is to simulate vasculature and blood circulation *in vitro*. Thus, the combination of tissue engineering with microfluidic technology by providing the possibility of media perfusion is expected to reconstitute more relevant skin models and provide valuable evaluation of drug tests [155].

Wagner et al. [156] developed a microfluidic platform integrated with a peristaltic micropump for co-cultures of human artificial liver microtissues and skin biopsies. In long-term (14 days) exposure to fluid flow, crosstalk in the co-culture has been observed. In this platform, tissue sensitivity by exposure to troglitazone, a pharmaceutical substance, has been investigated. *In vitro* skin models which consist of dermal and epidermal layers are more physiologically relevant when compared to single epidermal layer models. A skin-on-a-chip platform designed by Abaci et al. [157] had a specific capability of recirculating the media without the need for pumps or external tubing at favorable flow rates. Physiological residence time of blood in the skin tissue has been established in this platform to provide relevant concentration of drugs in the blood. This platform is used for toxicity drug testing.

The incorporation of biosensors with biochips provides in situ and real-time monitoring of skin tissue responses to the test item. A sophisticated skin-on-a-chip platform integrated with a sensor was developed by Alexander et al. [158] for monitoring the transepithelial electrical resistance of recreated human epidermis. Metabolic parameters and change of skin tissue over time have been monitored in this platform. Recently, Kwak et al. [159] fabricated a skin-on-a-chip microfluidic platform in which epidermal and dermal layers were co-cultured with human umbilical vascular endothelial cells. Immune responses such as an increase in secretion of cytokines and migration of neutrophils into the demal layer after exposure to Doxorubicin and UV irradiation have been observed.

A three-layer PDMS microfluidic skin-on-a-chip device with two porous membranes was fabricated by Wufuer et al. [160] In this model, a co-culture of human skin cells (epidermal, dermal and endothelial layers) has been developed. Separate microfluidic channels in this system provide the possibility of perfusion of various kinds of media with different flow rates. By perfusion of tumor necrosis factor alpha into the channels, skin inflammation and edema have been mimicked in this system. Drug toxicity testing by studding dexamethasone's effect on reducing inflammation and edema has been performed in this model. Although this dynamic and multilayer co-culture platform lacks the 3D microenvironment of the skin.

Lee et al. [161] developed a skin-on-a-chip model based on 3D co-culture. In their design, dermal primary fibroblasts have been embedded in hydrogel to provide a 3D dermal layer. Then, on top of the collagen-fibroblast layer, primary keratinocytes have been cultured to represent the

epidermal layer. Endothelial cell-coated microfluidic channels have maintained the growth and differentiation of skin cells in this biochip. Cell culture experiments combined with mathematical modeling have demonstrated that perfusion through a microfluidic network maintains the long-term culture of skin cells for up to two weeks. A skin-on-a-chip platform has been presented by Jusoh et al. [162] to mimic the effect of skin irritants on angiogenesis. In this model, irritated keratinocytes biochemically stimulate vascular endothelial growth factors. Autocrine and paracrine interactions between dermal fibroblasts and keratinocytes increase angiogenic sprouting in this model. The effect of the sodium lauryl sulphate (a well-known chemical irritant) and steartrimonium chloride (which is known as a non-irritant compound) has been studied in this platform.

More recently, a simplified gelatin-based skin-on-a-chip model has been developed by Jahanshahi et al. [154] for studying wound infection, skin's pro-inflammatory response and drug screening. In this platform, keratinocytes have been cultured on the microchannels which have been embedded in a gelatin matrix. After long term (6 weeks) culture, a multilayer structure of epidermis layer was formed. However this model lacked the presence of other cell types (e.g., fibroblasts). It is still a functional model to study the skin's pro-inflammatory responses to bacterial infection and drug testing.

As briefly reviewed here, in the past few years, various skin-on-a-chip models have been fabricated. However, to develop more reliable skin models to mimic the complexity of 3D architecture of human skin, the presence of vascular network and immune cells is crucial for toxicology tests and study skin diseases.

2.2.6.2 Body-on-a-Chip

Multi-OOC platforms or body-on-a-chip platforms refer to *in vitro* models which emulate interactions between two or multiple human organs within a microfluidic system. These complex microfluidic platforms can be used to emulate interactions among diverse organs for drug discovery, toxicity tests etc. [163]. There are some biological challenges such as creating a suitable media for all cell types, appropriate scaling of organs, immune responses in the system etc. that need to be considered in multi-OOC platforms. Moreover, technical challenges including avoiding bubble formation in these complex systems, maintaining long term sterility, optimizing the physiological parameters for different organs etc. need to be addressed in these sophisticated

microdevices. References [163, 164] highlight the critical design parameters for biomimetic multi-OOC platforms to develop physiologically based pharmacokinetics (PBPK) and pharmacodynamics (PD) models which have the potential to be used in the pharmaceutical industry.

Since liver and kidney are the two crucial organs in metabolism and excretion of drugs, a liver–kidney co-culture model [165] was developed on a microfluidic platform to investigate metabolism changes under drug components. HepG2/C3A cells co-cultured with kidney cells for toxicity test of a variety of molecules. This platform can be used in pharmaceutical and environmental toxicology testing. A liver-kidney model has been presented by Choucha-Snouber et al. to investigate the toxicology of an anticancer agent (Ifosfamide). By comparing the results of the liver–kidney co-culture with the kidney monoculture biochip, this study highlights the importance of multi-organ microfluidic *in vitro* models in toxicity tests and drug testing.

An integrated liver–heart–vascular microdevice developed by Vunjak-Novakovic et al. [166] incorporated liver, cardiac and blood vessel cells in a microfluidic platform which potentially can be used in toxicity tests of cardiovascular drug components.

In another interesting study which was presented by Maschmeyer at al. [167] Troglitazone, an antihyperglycemic and anti-inflammatory drug which was withdrawn from the market because of its toxicity effects on liver, has been tested on microfluidic platforms. The liver toxicity was observed in response to Troglitazone on two separate microfluidic co-culture platforms (liver-intestine and liver-skin) which highlights the efficacy of *in vitro* multi-OOC models in drug testing.

A microfluidic liver-intestine model introduced by Bricks et al. [168] demonstrates the critical role of intestine in oral medications absorption and excretion. This model emulates the interactions between HepG2 C3A cell lines and intestinal Caco-2 TC7 cell lines to assess intestinal absorption and liver metabolism of drug components. They studied the interactions between liver an intestine cells in a conventional co-culture model and a microfluidic co-culture biochip. The results demonstrated that the functionality of the liver in microfluidic biochip increased when compared with conventional models. Moreover, drug metabolism was elevated in the biochip co-culture platform when compared to co-culture in Petri dishes and with monoculture on a microfluidic platform.

A four-OOC model was presented by Maschemeyer et al. [169] to study absorption, distribution, metabolism and excretion in co-culture model of intestine, liver, skin and kidney. Other multi-OOC platforms have been reported by several research groups word wide including liver-tumor-bone marrow [170], liver-lung-adipose tissue-other tissue [171], liver-lung-kidney-adipose tissue [172], liver-vascular -adipose tissue [173, 174].

2.2.6.3 Organ-on-a-Chip Market

While various challenges [3, 59, 175] remain to be addressed before adoption of OOC technology by clinicians and pharmaceutical industry, a number of start-ups have been raised in the past few years to occupy the high-potential market by their own innovative technology. Some start-ups are more specialized in developing specific OOC, while others propose to develop an independent biochip with the possibility of developing different organs. Some others have the intention to fabricate a single organ device and some others prefer multi-organ platforms to assess interactions between organs. Each player in the field proposes its own unique technology, which has specific applications, drawbacks and strengths. However, still there is a significant gap between market needs and available technologies and it seems new players need to show noticeable progress to demonstrate the predictive validity and reproducibility of OOC platforms for disease modeling and drug discovery. The adoption of OOC technology by industry will start with contract research organizations (CROs), which support biotechnology and pharmaceutical industries in R&D services [176]. Therefore, OOC companies require abundant quantitative and qualitative research to prove that these OOC devices are true mimics of human organ functions and accelerate their adoption by CROs and consequently by industry and health care system [59]. Here, we have briefly summarized a number of pioneers in commercialized OOC devices (Table 2.3). Interested readers refer to Reference [59] for extensive details and discussion in this regard.

Table 2.3 List of some of the OOC start-ups and highlight of their technology

Company's name	Summary of specialties	Applications	Cell source	Highlight of the technology	Year
AlveoliX	OOC, Lung-on-a-chip	Drug discovery, disease modeling	Human cell lines	In vitro models inspired by nature, reproduce lung breathing motion, elastic and ultrathin membrane	2015
AxoSim	OOC, nerve-on-a-chip	Preclinical testing, 3D cell culture, neurotoxicity tests, neurodegenerative diseases	Primary cultures, Organoids	Biomimetic human tissues, combination of neurons, astrocytes, and oligodendrocytes.	2014
BEOnChip	OOC	Disease modeling, in vitro tests, drug screening	Human cells	Long-term 2D or 3D culture under flow condition, 2D-3D co-culture, simulation of physiological environments involving flow and shear stress	2016
BiomimX	OOC, heart-on-a-chip, Cartilage-on-a-chip	Drug screening, drug cardiotoxicity, anti-arrhythmic drug efficiency, discovery anti- osteoarthritic drugs	cardiomyocytes derived from human iPSCs, human cells	3D co-culture, mechanical stimulations, human cardiac tissue, human osteoarthritic cartilage, customized OOC	2017
BI/OND	OOC, BI/OND's microfluidic plate	In vitro tests, Drug discovery	Human cells, Organoids, patient derived cells or tissues	Dynamic cell culture environment by providing mechanical stimulation and continuous fluid flow, two compartments connected by a porous membrane BI/OND's plate to run up to six cultures in parallel, 3D and 2D models	2017
CN Bio Innovations	OOC,), liver-on-a-chip, Body-on-a-chip (7-OOC)	Human physiology modelling, liver diseases modelling, Preclinical drug discovery, toxicity tests, drug metabolism	Primary human cells, Tissue or Organ Slices, IPSCs, Immortalised cell lines	Multi organ studies, portable and compact device, programmable flow rate, open well plates	2009
Emulate, Inc.	OOC, Lung, Bone marrow, kidney, brain , blood vessels and intestine-on-a-chip	Personalized medicine, disease modelling, drug screening, study human physiology	-	Organ-Chips personalized with individual patients' stem cells, stretchable biochip, flexible and dynamic environment by fluid flow and mechanical stretch	2014

Company's name	Summary of specialties	Applications	Cell source	Highlight of the technology	Year
Hesperos	OOC, multi-organ-on-a-chip (heart, liver, lung, brain, skin, muscle, kidney, pancreas, bone marrow)	In vitro tests, drug discovery, toxicity tests, pharmacokinetic/ pharmacodynamic modeling	human stem cells	Pumpless platform, recreate muscle and tissue function, neural and inter-organ communication, customized human-on-a-chip platform, possibility to add immune cells in multi-organ-platform	2015
MIMETAS	OOC	Disease modelling, drug testing, toxicity tests, personalized medicine	Human cells, patient derived cells or tissues	OrganoPlates (a microfluidic 3D cell culture plate), 3D co-culture, biomimetic, compatible, easy to use	2013
Nortis	OOC, kidney, brain, heart, liver, immune system and blood vessels-on-a-chip	Disease modeling, cancer study, drug testing, study Alzheimer's disease and ageing, toxicity tests	Human derived tissue models	Perfusion system, standard cell culture incubator,	2012
SynVivo, Inc	OOC, blood-brain-barrier-on-a-chip	Drug discovery, toxicity test, targeted drug delivery, cancer researches	Human cells	Mimic microvascular environment, dynamic environment, real-time visualization, controlled condition, 3D co-culture model	2014
TARA Biosystems	OOC, heart-on-a-chip	Cardiac Toxicology, Precision Cardiology, Heart Failure Drug Discovery, Drug development, study healthy	iPSCs derived cardiomyocytes	Cardiac tissue models, patient derived disease models	2014
TissUse	OOC, body-on-a-chip	Toxicity tests, disease modeling, personalized medicine, drug development, application in pharmaceutical and cosmetic researches	Cell lines, human primary cells, biopsies	Multi-organ platforms, rapid prototyping, compatible with tissue imaging, application of physiological sheer stress, long-term performance	2010

2.2.7 Discussion and Future Perspectives

This state of art summarizes current progress regarding BioMEMS, LOC for POC applications, OOC platforms and the history of developing these technologies specially for new players in the field. Indeed, this review is dedicated to background and current advancements in LOC and OOC technologies and their applications in life. Since the main intention of developing biomedical devices is to bring the technology from academia to the market for improving human health, a list of pioneers in commercialization of LOC and OOC devices has been summed up for interested

readers. Here, having a look at developed LOC devices for POC applications and OOC platforms by considering their specifications, limitations and strengths presented above and summed up in Table 2.4 we highlight possible future perspective for OOC technologies.

Table 2.4 A summary of specifications, limitations and strength of current LOC and OOC

Technology	LOC	OOC
Applications in life science	• Recapitulate one or several laboratory functions on a single chip; • POC diagnostic devices (e.g., hormone detection, viral infection detection and etc.)	• Study human physiology; • Disease modeling; • Drug screening and development; • Toxicity tests; • Personalized medicine
Advantages	• Integration with miniaturized sensors, valves and pumps; • Use microfabtication techniques (e.g., photolithography, etching, 3D printing and etc.); • Possibility to collect data with non-trained individuals; • Small size and being portable; • Low volume of sample and reagents consumption; • Quick sample analysis; • User friendly; • Automation opportunities	• Ability to be integrated with miniaturized sensors and actuators; • Advantages linked with new microfabtication techniques (e.g., softlithography, 3D bioprinting and etc.); • Small volume of sample and reagents consumption; • Real-time and on chip analysis; • Precise control over microenvironment
Drawbacks	• Problems linked with traditional microfabrication techniques (costly, time consuming, need for highly trained experts for fabrication and etc.); • Complex configuration with multiple pumps, valves and sensors; • Problems associated with microliter scale due to surface dependent effects (e.g., capillary forces and surface roughness)	• Need well-trained experts to collect and interpret data; • Current problems with fabrication materials (e.g., absorption of small molecules by PDMS) • Current platforms mostly are not automated; • Problem linked with cell clogging and bubbles formation in microchannels; • Non-defined protocols; • cell damages due to shear stress
Size	• Few square millimeters to few square centimeters	• Few square centimeters
Materials	• Silicon, glass, metal, ceramic, polymers, thermoplastics, paper and etc.	• Biocompatible and cytocompatible materials such as polymers (e.g., PDMS); glass; biological materials (e.g., proteins, cells etc.)
Biological samples	• Body fluids (e.g., Saliva, blood, urine)	• Cells, spheroids, organoids, tissue biopsies

It has therefore been shown that materials, microengineered technologies, functionality, reproducibility, being user friendly and automation through integrated systems are the main parameters involved during development of each one of these inventions. Although many features of these technologies have been described in the literature and summarized in the present work, numerous others have to be investigated further.

MEMS based devices have a wide variety of applications from the electronic industry [30] to environmental [177] and biomedical fields [29]. Development of commercialized BioMEMS including LOC for POC devices and microfluidic biochips continue to increase consistently. Various exciting directions are expected for the future of LOC highly integrated devices for diagnostic and therapeutic are some of the interesting applications of LOC devices. For instance, rapid detection of viral infections [178, 179] and early detection of cancer biomarkers [180, 181] directly from body fluids are some of the highly attractive subjects in this area.

According to the literature, some of the LOC devices have been already commercialized years ago (e.g., home pregnancy tests, real-time glucose monitoring, etc.). Miniaturized portable LOC devices for POC applications are ideally suited for testing in developing countries where expensive and complex laboratories do not exist. These automated, accurate and cost effective diagnostic devices do not need highly trained health care experts and can be used on-site by patients. In most of the LOC devices which are categorized as a subset of BioMEMS, electrical and/or mechanical parts are integrated to the system [46, 89]. Therefore, in these platforms, normally whole patient samples (e.g., blood, saliva, urine and etc.) are introduced into a single chip and all the steps of the laboratory process including separation, filtration, analysis and read out of the results take place on the small single chip. The result of the assay usually would be available visually (e.g., yes or no in pregnancy tests or digital numbers of the blood glucose level in glucometers) and hence it does not need inferences by the experts. The global health crisis due to SARS-CoV-2 (COVID-19) [182] pandemic highlights the critical importance of LOC for POC testing for early diagnosis of suspected cases and treatment monitoring of infected people to prevent further spread of the infection. Real-time reverse transcriptase polymerase chain reaction (rRT-PCR) is the current diagnostic approach for COVID-19 [183]. However, this is a time-consuming and costly method which requires developed facilities and highly skilled staff and is

not robust in the early stages detection and can show false negatives for up to two weeks. Hence, rapid, sensitive and automated LOC devices for POC applications are urgently needed to detect COVID-19 from patient samples (e.g., saliva, plasma and etc.) [111, 184].

Since cell culture is a critical aspect in biomedical science for understanding human physiology and pathophysiology, toxicology tests, drug screening etc., microfluidic-based cell culture platforms with the aim of mimicking the *in vivo* like microenvironment for cells have strongly attracted researchers' interest in recent years worldwide. However, most of the microfluidic-based cell culture devices, which have been developed in academia, are not integrated with electrical or mechanical parts, but in terms of microfabrication technologies and principals, these platforms, which are well known as OOC platforms, have been categorized as a subset of BioMEMS systems. These platforms take advantage of microfluidic systems and microfabrication techniques to provide cell culture and tissue culture platforms which recapitulate tissue–tissue interactions, biochemical and biomechanical microenvironments of living organs. OOC systems use cells, spheroids, organoids and tissue biopsies to mimic tissue or organ level functionality *in vitro*. Hence, unlike LOC platforms, these samples are required to be prepared by trained experts and the results of the analysis need to be concluded by scientists in the field. Most of the microfluidic OOC platforms are still in the proof-of-concept stage because of some major challenges including low throughput (e.g., due to single channel designs), short lifespan of the biochip (e.g., due to channel blocking or clogging), complex sample preparation and limitations linked with material for fabrication (e.g., absorption of small molecules by PDMS). Making balance between academic research and commercialization is worthwhile to expand microfluidic based OOC platforms into clinically useful *in vitro* tools. Achieving organ physiological function *in vitro* is not an easy process. Another key point to develop commercialized OOC devices is the design of the device. An appropriate design for microfluidic OOC platform needs to be simple enough for the ease of manufacturing and operation for the end users, while having an adequate complexity to mimic the sophisticated structure and physiological function of an organ or a tissue to be adopted by the market. Although, based on the works presented above, it can be established that the state of knowledge is currently insufficient to design efficient and realistic mimics. Automation and integration of OOC devices is another important aspect to be considered for transferring OOC technology from discovery to broad availability and adoption by industry for

drug toxicity and efficacy tests. Indeed, commercialized OOC devices need to be multiple-organ-on-a-chip platforms which are integrated with various sensors (e.g., physical and electrochemical sensors) for real-time and continuous measurement of micro-environmental parameters (e.g., temperature, pH, oxygen level, soluble biomarkers, drug concentration and etc.) during a long period of an assay (7 days or more). Integration of a miniaturized microscope with such a platform, by providing in situ monitoring of morphological changes, offers a versatile tool for clinicians, biotechnology and pharmaceutical industries [175] . However, to achieve this goal, effective collaboration between clinicians, scientists and engineers is required.

Advances in OOC technology have increased the hope for personalized medicine and POC testing. Since disease modeling and drug screening are the two main goals of OOC platforms, by using patient-derived samples (cells, tissue biopsies etc.) on these platforms, we can develop individual patient-on-a-chip models for POC application. Indeed, personalized patient-derived OOC platforms have the potential to accelerate time-consuming and expensive drug discovery processes. Hence, fast detection of the best approach for treatment brings personalized health care for individuals with genetic differences[3]. For instance, targeted drug delivery [185] and combination therapy [14, 186] have gained great interest in cancer therapy to develop novel treatments. Direct and localized delivery of drug molecules to specific tissues or organs in the body enhances desired therapeutic concentration in the targeted tissue, while minimizing systematic drug side effects [185]. In combination therapy, clinicians combine two or more therapeutic agents or approaches to discover a patient's optimal treatment [14]. OOC platforms have the potential to play a critical role in the future to advance combinational therapy and targeted drug delivery assays specially for diseases like cancer, which time is crucial and there is no place for trial and error on the patient.

Finding new therapeutics for rare diseases [187, 188], which affect a small population, is another expected application for OOC devices in the future. Small market size and high expenses to develop new treatments for rare disease are the main reasons that most pharmaceutical companies are not interested in investing to develop treatments for rare diseases. However, in recent years, advances in biomedical technologies have increased the attention of governments and the pharmaceutical industry for drug discovery for rare diseases. Personalized OOC devices using

patient's samples allow us to conduct trials on a biochip to tackle the challenges of therapeutic discovery for rare diseases.

As mentioned above, automation and integration of OOC devices with different sensors and microscopes by in situ and real-time data collection decrease user interference and facilitate the device's operation. Therefore, integrated patient multi-organ-on-a-chip platforms have the potential to be used by pharmaceutical companies and clinicians for POC applications. As reviewed above, these patient-on-a-chip platforms are required to recapitulate the complexity of living organs and organ–organ interactions while keeping the device simple to promote the operation by users.

2.2.8 Conclusion

Along with advancements in microtechnologies and the development of LOC devices in life science, particularly for POC applications, microfluidics have merged seamlessly with tissue engineering to develop OOC platforms which use building blocks of human organs on biochips to mimic organ physiology and to recapitulate organ functionality *in vitro*. However, there are still many challenges to be addressed before OOC technology finds its own place among other preclinical methods used by CROs, the pharmaceutical industry and clinicians. This requires effective and close collaboration between scientists, clinicians and engineers to bring this technology to the POC.

We believe that future OOC devices for POC applications need to be multi organ platforms which are personalized and use patient-derived cells or tissue biopsies to recapitulate the complexity of each patient on a biochip while keeping this complexity clinically relevant to facilitate their adoption by clinicians and pharmaceutical pipeline to accelerate patients' treatment.

2.3 Funding

This research received a scholarship to N.A. from the Royal Bank of Canada (RBC), and financial support through NSERC discovery grants.

2.4 Acknowledgements

N.A gratefully acknowledges T. Gervais, R. J. Diaz and H. SadAbadi for fruitful scientific discussions.

2.5 Conflicts of Interest

The authors declare no conflict of interest. The funders had no role in the design of the study; in the collection, analyses, or interpretation of data; in the writing of the manuscript, or in the decision to publish the results.

2.6 Critical review

In this section, the most relevant literature regarding the main topic of this dissertation reviewed. First, a quick background about the cancer as motivation of this dissertation is presented, followed by current *in vitro* models in cancer treatment. Then relevant literature concerning spheroid formation methods briefly reviewed with the focus on microfluidic spheroid-on-a-chip platforms. Then, the influence of surface properties in cell behaviour discussed in more details. Following, surface modification of the PDMS as the most popular materials in biochip formation have been reviewed with focus on available literature on PDMS surface modifications with Pluronic and BSA as the two popular materials used in this dissertation to provide anti bio-fouling properties for PDMS.

2.6.1 Cancer

Cancer is the second leading cause of death worldwide [1, 2]. According to the 2021 annual report Cancer Research Society, over 30% of the annual total mortality in Canada is due to cancer. In the United States, cancer is the primary cause of death in people over 80 years old, after cardiac-related deaths and it is the leading cause of dead for people aged 40 to 79 [189, 190]. The number of new cancer cases and cancer-related deaths is estimated to increase yearly due to the growth in population and aging. Therefore, in 2060, cancer expected to be the first cause of mortality worldwide [1, 2].

Cancer is a very complex disease in which transmutation of genetic instabilities with random environmental factors and epigenetic perturbations empower normal cells within healthy organ to progressively generate deadly properties, including invasive behaviour, uncontrolled growth and metastatic properties [191]. Due to its asymptotic nature, cancer is often discovered in late stages and a great proportion of cancer patients who initially responded to standard chemotherapy treatments, develop resistance to these treatments during the course of cancer therapy. Therefore, despite advances in surgery and chemotherapy over the past decades, median survival rate of cancer patients is still very low. Hence, better understanding of the complex mechanisms of cancer progression and drug resistance phenomenon is crucial to develop effective and reliable cancer therapies [4]. Failure in finding effective treatments for cancer despite all efforts by researchers and clinicians is due, in part, to the reliability of pre-clinical models to predict effectiveness of drug responses and their toxicity and adverse effects in cancer patients, which can explains in part why most of the drug candidates fail to achieve clinical approval more often than they succeed.

2.6.2 Tumor microenvironment

Tumors are a diverse mixture of malignant cancer cells and non-malignant cells or stromal cells, which support the microenvironment of the tumors [103, 192]. The complex and dynamic cross-talking in the tumor microenvironment (TME) between malignant cancer cells and surrounding extra cellular matrix (ECM), immune cells, blood vessels, lymphocytes, fibroblasts, bone marrow-derived inflammatory cells and signalling molecules critically affects cancer initiation, progression, spread metastasis and tumor response to the treatments [192, 193]. Simulation of such a complex microenvironment *in vitro* will offer an in-depth understanding of the cancer cells behaviour in their TME and provide crucial insights into the biological behaviour of tumors and their responses to therapeutic agents. Fundamental understanding of TME can provide essential information in cancer study *in vitro* to develop new cancer therapeutics to target TME for controlling tumor progression [193].

2.6.3 *In vitro* models in cancer research

Here, current *in vitro* models in disease modeling and drug development have been discussed. First, the type of the cells that are usually used in preclinical study is briefly reviewed followed by *in vitro* models in cancer research.

2.6.3.1 Cell sources in preclinical research

2.6.3.1.1 Immortalized cell lines

Immortalized cell lines are a population of cells that due to genetically manipulation can keep undergoing division and proliferate indefinitely and therefore can be cultured *in vitro* for long period. Immortalized cell lines are easy to use, cost effective, provide an unlimited supply of cells and most common types of cells used in *in vitro* researches. However, they may provide different results as they can not sufficiently mimic primary cells since their phenotype, genotype, and native function can be varied over the extended time of culture [194].

2.6.3.1.2 Primary cells

Primary cells are patient cells that directly taken from the patient tissue and therefore most closely represent the tissue of origin. These cells processed to culture *in vitro* for short period under optimized culture conditions before any immortalization and genetic changes occur. Therefore, they exhibit phenotype and genotype similar to the original tumor. However, limited supply, low division rate and short survival time make them more complicated to use in *in vitro* researches when compared with immortalized cell lines [6].

2.6.3.2 Conventional 2D culture models

The culture of the cells *in vitro* is the most widely used tool to gain insights into cell biology, pathophysiology, disease modeling, and drug action. Modeling cancer *in vitro* began with growing cancer cells in two-dimensional (2D) tissue culture flasks and Petri dishes [3].

Conventional 2D cell culture which is the most common has been developed almost one hundred years ago [3]. In 2D culture model, cells grow as a monolayer attached to the plastic surface of a Petri dish or culture flask. 2D culture models are well established, simple, easy to work, and cost-

effective [6]. However, they have numerous disadvantages [3, 6]. This culture method cannot mimic the natural 3D structure of tissues and tumors including 3D cell-cell and cell-extracellular matrix interactions [3]. These micro-environmental interactions are responsible for cell functions including cellular proliferation, differentiation, gene expression and cell responses to various phenomena [3, 151]. Cell morphology, polarity, gene expression, biochemistry of the cells and cell functions changes in 2D culture systems [103, 195]. Moreover, in 2D model, the cells have unlimited access to oxygen, nutrients and metabolites[196]. However, in natural microenvironment of tumor, cancer cells experience spatiotemporal chemical gradients of nutrients, oxygen and metabolites[3]. Therefore, 2D models lack the natural tumor microenvironment and cannot mimic *in vivo* like condition and complex interactions between the cancer cells and the dynamic physicochemical microenvironment that exists within natural tumors [172]. Recapitulating this complex cellular microenvironment is essential to better understanding the cancer cell biology and behaviour. The irrelevant 2D culture in cancer research provides misleading results regarding the predicted responses of tumor cells to anticancer therapeutic agents [193, 196]. This is one of the possible causes of the failure of more than 95% of anticancer drugs in clinical trials [3]. Limitation of 2D culture models lead to development of 3D *in vitro* models to more closely mimic *in vivo* tissue/tumor microenvironment [3, 8]. These 3D models allow for better understanding of cancer biology by more effectively mimicking the natural cell structure and architectures[6].

2.6.3.3 3D culture models

To answer the limitations of 2D culture, a number of 3D cell-culture models have developed over the past 50 years where the culture environment takes into account the spatial organisation of the cells to mimic the native tissue as closely as possible [3, 6]. Compared with conventional 2D culture, 3D cell culture models more realistically bio mimicking the 3D microenvironment that cells experience *in vivo* and have an invaluable role in our understanding of tumor cells behaviour by providing important insights into cancer biology [3, 172]. 3D cell culture models can categorized into the whole animals and organotypic explant cultures, scaffold-based tissue engineered models, microcarrier cultures and multicellular tumor spheroids (MCTSs) [6, 12]. Spheroids are the most widely used 3D model in preclinical oncology researches due to their specific features to mimic natural tumor [11, 197, 198]. Since the focus of this dissertation is

spheroid between other 3D culture models, I will discuss specifically about spheroid models and various spheroid formation methods in the following section.

2.6.3.3.1 Multi cellular tumor spheroids (MCTSs)

Multi cellular tumor spheroids (MCTSs) stand out as the most widely used 3D cell culture models in oncology preclinical research [17, 199]. Spheroids defined as compact and spherical 3D cell agglomerations [10, 200]. Hence, loose cell aggregates that easily detach or other forms of spatial cells aggregates should not be considered as spheroids since the compactness and the spherical geometry of spheroids [200] are the essential spheroids characteristics, which give them *in vivo* like tumor features and make them as a reliable tool in cancer research and drug screening [10, 13].

MCTSs have proven their power of drug response prediction by more accurately reproducing the key structures of solid tumors including the formation of nutrients/waste gradients, providing different proliferation layers of cells, cell-cell and cell-extracellular matrix (ECM) interactions in 3D forms, chemoresistance, etc. [13, 201]. However, the uniformity in size and shape of the spheroids play a critical role in their response to anti-cancer drugs [12, 13]. Therefore, it is important to produce *in vitro* platforms to reduce the heterogeneity of the spheroids for accurate drug testing [13, 202]. MCTSs contained three different proliferation zones (Figure 2.9) (outer layer of proliferating cells, intermediate zone of quiescent cells, and a central necrotic zone) resembling an actual tumor [11].

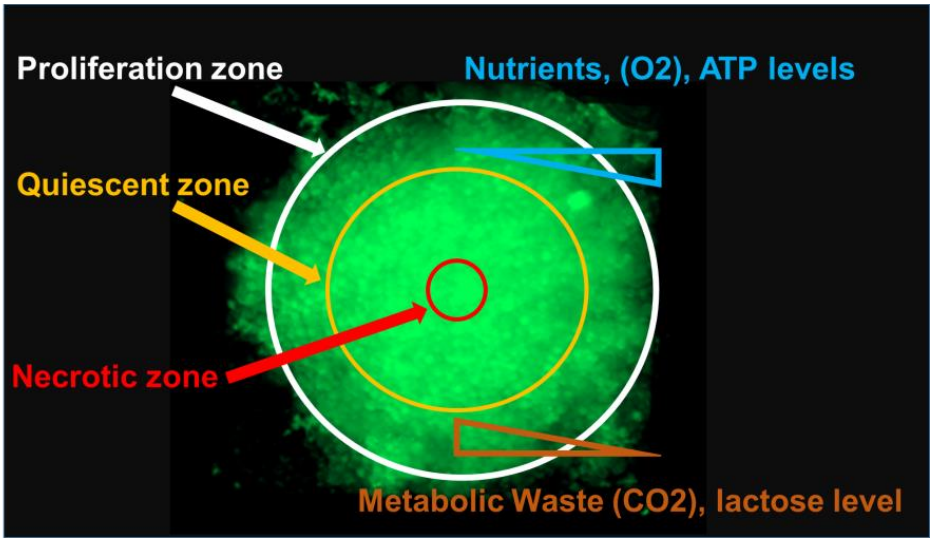

Figure 2.9 Fluorescent image of MCTS

MCTS demonstrates spherical geometry with different regions for proliferating, quiescent and dead cells. Different mass transport rates are present in the multilayer structure for oxygen, nutrients and metabolites. The spheroid presented in this image is formed from MDA-MB-231 cells. The green color is due to green fluorescent protein (GFP)

MCTSs dated back to 1970 when Sutherland et al. [203] have developed cell aggregates of Chinese hamster V79 lung cells to study the effect of chemotherapy and radiotherapy *in vitro*. These cell aggregates were compact, having uniform spherical shape [200, 203]. MCTSs mostly generate from single cell suspension from cancer cell lines [13, 204] but not often from tumor cell suspensions derived from patient tumor tissue [202, 205]. Yet, not all cell lines are able to generate MCTSs [13]. The first MCTSs developed by single cancer cell line to recapitulate the 3D tumor structure. Later, by co-culture of noncancerous cells (e.g. immune cells [206], fibroblasts [207] , and endothelial cells [208]) with cancer cells, heterotype MCTSs formed to mimic the heterogeneous interactions between tumor and stromal cells [11, 13].

Several techniques have been used for spheroid formation with the same principle in which adhesive forces between cells is prominent than cell-substrate adhesion [13, 209]. In this condition, depending on the method and the cell line, compact and spherical forms of cells self-aggregates obtain after 1 to 7 days of culture [12, 209].

2.6.4 MCTSs culture methods

Several methods used to produce spheroids. One of these methods is the hanging drop method [210] in which cell suspension drops up to 30 µl are deposited on a dish lid. Upon inversion of the dish lid, cells accumulate at the free interface between liquid and air and MCTSs will be obtained. One of the disadvantages of this technique is that MCTSs need to be transferred to another plate for further investigations [13, 208]. MCTSs can be generated by the liquid overlay technique (LOT) [13, 211] by culturing the cell suspension over plates covered with a thin inert substrate like agarose [212] or agar [211], or by seeding cells on plates with ultra-low adhesion properties without any coating to induce the cells self-aggregation instead of adhesion to the surface [213]. Spinner flasks [214] and stirred-tanks [215] are other techniques to produce MCTSs by spontaneous cell aggregation.

Each one of the above mentioned methods for spheroid formation have some deficiencies including variable sizes of spheroids, low-throughput, harmful effects on cells due to high shear stress and static microenvironment around spheroids which influence on spheroids and consequently on drug screening results [3, 12, 13].

2.6.4.1 Microfluidic biochip for spheroid culture

Recent advances in microengineering and microfabrication lead to address some of the abovementioned limitations by developing microfluidic platforms for spheroid formation and culture [3, 6]. Microfluidic devices by providing precise control over tumor microenvironment, concentration gradients, use small amount of cells and reagnets, controlled mixing, control of shear stress, possibility of continuous perfusion, perform multiple assay on a single chip, possibility to be integrated with sensors and etc. bring significant advantages over other spheroid formation methods [6, 16, 216]. Moreover, microfluidic platforms by providing a dynamic microenvironment for the cells can better mimic in-vivo like cellular microenvironment [6, 38]. For instance, spheroids in dynamic microenvironment when compared with spheroids in static condition demonstrated to be more resistant to cancer treatment [16, 217], having higher cell viability [14, 136], different gene expression profiles [218], and they better mimic tumor-like properties [3, 201]. There are numerous microfluidic-based devices for spheroids formation and studying. Some of them used only for spheroid culture, which means that the spheroids made by

other techniques will transfer and culture on-chip for drug screening or tumor study [16, 219]. Some other microfluidic devices use as spheroid formation platforms, which mean that they use different techniques (e.g. emulsion-based [220, 221], cell trapping microchamber [14, 205, 222]) to form spheroid on-chip from the cell suspension and use them for drug tests and cancer study.

Numerous microfluidic platforms have been developed for generating MCTSs using small liquid volume, as a key advantage of microfluidics [3, 16]. Torisawa et al. developed a two layers PDMS microfluidic platform separated by a semi-porous membrane for the spheroid formation and culture [223]. A multilayer microfluidic array platform containing concave microwells and flat cell culture chambers has been developed by Kang et al. for embryonic stem cell spheroids [19]. Spheroid formation using gravity oriented multi-level structured microfluidic device was performed by Lee et al. [224]. Lee et al. developed a spheroid-based 3D liver chip to study hepatocyte cell viability in static culture condition compared with the dynamic condition [136]. Lim et al. developed a microfluidic platform with pillars to generate size-controlled spheroids. The size of the spheroids can be controlled by adjusting the center-to-center distance between pillars. They have successfully formed spheroids from glioblastoma cell lines (U251 and U87) and patient-derived cells (PDCs) and performed anti-cancer drug tests on this platform [18]. Eilenberger et al. developed a microfluidic platform using live, lung, colon, and skin cells and a co-culture model of blood-brain-barrier (BBB) to assess the effect of the spheroid size on drug toxicity [20]. A multicellular spheroid skin model on-a-chip from dermal fibroblasts was developed by Chen et al. to test the active ingredients of skin care products [225]. Prince et al. developed a breast cancer spheroid-on-a-chip platform for studying the effects of drug dose and supply rate on the chemosensitivity of breast tumor spheroids [17]. Collins et al. developed a dynamic microfluidic platform under continuous perfusion conditions at a flow rate relevant to natural tumor interstitial fluid flow, to better recapitulate the dynamic of the tumor microenvironment. The viability and migratory capabilities in this device were studied and compared with static conditions [15].

One of the most common problems with spheroid culture is producing homogenous and uniform size and shape spheroids as the size, compactness level, and spherical shape of the spheroids give them special characteristics similar to *in vivo* tumors [10, 12, 13]. These specific features make spheroids more reliable tools for *in vitro* cancer study and drug testing [13]. Geometry design of

the channels and cell trapping chambers play an important role in this regard [18, 226]. Moreover, the materials used for microfluidic fabrication and their surface characteristics (e.g. wettability, chemistry, roughness and etc.) also play a critical role in regulating cell responses to the surface and quality of spheroid formation on-chip [202, 227]. Accordingly, in the past years, surface engineering has attracted great attention in cell-based biomedical applications including microfluidic platforms for cell culture [22, 26, 28].

2.6.5 Influence of surface properties on cell behaviour

Adhesive interactions between cells and their substrate are important to control cell activation, differentiation, proliferation, migration, and survival [23]. A series of physicochemical reactions between cells and the material's surface happens when cells adhere to a surface. The first step is the adsorption of the proteins to the surface [228]. This can modulate cell adhesion and send signals to the cells through cell adhesion receptors (e.g. integrin) [23]. When the cells adhere to a surface, they can release active compounds to mediate ECM deposition, cell differentiation, and proliferation [229]. Interfacial interactions between cells and surfaces are crucially important to be considered for developing biomedical devices (e.g implants) and require biologically inert materials (e.g. PDMS) to suppress non-specific adhesion and prevent immunological responses and thrombosis [230]. The culture medium, the type of cells and substrate's surface properties (e.g. stiffness, surface charge, surface chemistry, roughness and wettability) are important parameters that modulate cell behaviors in terms of adhesion, morphology, metabolism, and proliferation[23, 230].

The effect of PDMS substrate stiffness on cell adhesion and proliferation has been studied recently [231, 232]. Softer PDMS substrate was demonstrated to promote cell adhesion and growth while stiffer PDMS substrate was less compatible with cell adhesion and growth.

Mammalian cells carry negative charges [23]. Therefore, the interactions between negatively charged surfaces and cells can be employed to decrease cell-substrate adhesion by electrostatic repulsion. Several studies have demonstrated the effect of surface charge on cell adhesion and proliferation. For instance, Kim et al. demonstrated how degree of charge density of hydrogels based on 2-hydroxyethyl methacrylate (HEMA) and 2-methacryloxyethyl trimethyl ammonium chloride (MAETAC) copolymer can increase endothelial cell attachment and proliferation [233].

Surface roughness or topographical features at micro and nano scales (e.g. grooves, ridges, pores, etc.) are other important parameters to modulate cell behavior and adhesion [234]. The effect of surface roughness is depending on the cell size. For instance, the macroscopic effect of the surface roughness can modulate larger cells including osteoblasts and neurons [235]. However, the surface roughness at the nanometer scale can be used to improve cell adhesion for small size cells including human vein endothelial cells [236]. Ranella et al. [237] have studied the adhesion and viability of fibroblasts on different roughness level of 3D silicon surfaces. In this work, lower roughness ratios demonstrated higher fibroblast attachment.

Surface wettability can be considered the main controlling factor for cell behavior [23]. Water contact angle (WCA), is the key experimental tool to assess surface wettability. WCA is the angle subtended by the droplet of water and the surface[23, 238]. A surface is considered hydrophobic when WCA is between 150^{o} and 90^{o} while when it is between 90^{o} to 10^{o} the surface is considered hydrophilic[23]. Superhydrophobic surfaces have WCA higher than 150^{o} while superhydrophilic surfaces have WCA lower than 10^{o} [239]. Protein adsorption onto the hydrophobic surfaces occurs through direct interactions of hydrophobic moieties on the surface of the protein and the denaturation process, allows the proteins to expose the internal hydrophobic residues and bind to the surface [23]. When the surface is hydrophilic, minimal protein denaturation occurs because of the interaction of the hydrophilic moieties on the protein surface with the hydrophilic surface[23, 239]. The influence of coating polyester fabric at different surface wettability on mammalian cell viability has been studied [240]. Cell viability on standard tissue culture-treated polystyrene coated to rendered superhydrophobic significantly decreased. Comparing the ratio values with those observed on uncoated surfaces and more hydrophilic coating, the 3T3 or HaCaT cell line decreased their individual responses by 10 times the ratio values. The hydrophobic surfaces decreased the viability of the HeLa line when compared with the TCPS surface. These results concluded that tumor cell lines and non-tumor cells can be discriminated based on their adhesion to polyester fabrics.

2.6.6 Materials for fabrication of microfluidic biochip

As discussed above, it is been proven that surface properties including surface wettability, surface charge, and surface chemistry affects protein adsorption onto the surface and regulate cell-surface

adhesion and proliferation[23, 238, 240]. Various materials (e.g. polymers, thermoplastics, glass, silicon, paper, etc.) are used to fabricate microfluidic biochips [6, 241]. However, fabrication of most of the microfluidic devices for cell culture relies on replica molding and soft lithography due to the speed, cost-effectiveness, and ease of the process [6, 216]. In the replica molding process, microfabricated molds produce, using photolithography or stereolithography and several biochip replicas can be generated from the same mold using soft lithography. Hence, polymers, specifically PDMS due to their unique advantages are the most widely used materials in biochip fabrication [3, 6, 241].

2.6.6.1 Polydimethylsiloxane (PDMS)

PDMS is a synthetic polymeric elastomer based on silicone, which has been widely used for the fabrication of microfluidic cell culture devices due to its numerous advantages including biocompatibility, transparency, oxygen permeability, rapid prototyping, ease of processing, etc.[6]. Whitesides' group employed PDMS for micro-molding techniques in the 1990s [242, 243]. Since then, PDMS become popular in microfluidic research due to several advantages mentioned above. PDMS has Young's modulus of 2.63 MPa for the commonly used pre-polymer to curing agent ratio (10:1) [244]. This makes PDMS a flexible and high compliance material in microfluidic platforms, providing several advantages including micro-scale features preservation from a master mold imprinted in the PDMS replicas, reliable bonding to other surfaces, stretchable devices to mimic the biological movements (e.g. lung-on-a-chip) [6, 38]. However, these advantages of PDMS can be problematic in some applications. For instance, PDMS devices can be deformed under pressure conditions and initial geometry and design can vary [3, 38].

The major drawback of PDMS is its innate hydrophobic nature (water contact angle ~108° ± 7°) which is due to methyl groups present in its structure leading to biofouling, protein adsorption, cell adhesion to its surface, and bubble formation [3, 245]. It is been demonstrated that PDMS surface wettability greatly influences cell behaviors. There are pieces of evidence that surfaces with low wettability have higher levels of protein adsorption when compared with surfaces having a higher level of wettability [3, 246]. Increasing protein adsorption leads to cell adhesion on the PDMS surface. This can affect the quality and quantity of spheroid formation on PDMS-based biochips [238]. However, the uniformity in size and shape of the spheroids play a critical

role in drug test results [12, 13]. Therefore, it is important to produce *in vitro* platforms with low adherent properties to decrease cell-surface adhesion and promote homogeneity of the spheroids for accurate drug tests. Prediction of the effect of surface properties on cancer cell responses is complicated and remains unclear. To decrease cell adhesion to the PDMS surface various methods have been developed [6, 247, 248]. Surface treatment with Plasma oxygen and surface coating strategies are the most common methods for cell adhering, spreading, and proliferating on PDMS-based platforms [3, 248, 249].

2.6.7 PDMS surface modification

As mentioned above, the major limitation of PDMS is its hydrophobic nature [6, 238]. Hence, various surface treatment strategies have developed to render PDMS surface more hydrophilic to prevent non-specific protein adsorption and cell adhesion onto the surface. In this dissertation, we aimed to study the effect of PDMS surface coating with two popular materials, "Pluronic F-68 and BSA", commonly used to modify PDMS surface and provide cell repellent properties. First, I reviewed Oxygen plasma treatment as a standard inseparable step in the fabrication of closed PDMS microfluidic devices, which also increases the surface wettability of PDMS temporarily. Following, I reviewed relevant literature regarding surface coating of PDMS with BSA and Pluronic, the two popular materials to render PDMS biochip surfaces cell-repellent.

2.6.7.1 Surface activation by physical treatment of oxygen plasma

Oxygen plasma treatment is the most widely used technique for surface modification of PDMS [6, 250]. Plasma oxygen is commonly utilized in the fabrication process of microfluidic platforms to irreversibly bond PDMS layers to each other or into other surfaces (e.g. polystyrene, glass) to produce closed microfluidic devices[3, 216]. The key advantages of this technique are the fast treatment and ease of use, which make oxygen plasma treatment one of the most efficient techniques to modify PDMS surfaces[6, 25].

Under plasma conditions, electrons own high kinetic energy and break and ionize the incorporated gas molecules [251]. The photons and reactive species produced by gas discharge cause chemical reactions on the surface. The bulk properties of the polymer do not change in this process[23]. The efficiency of the plasma treatment determines by the composition of the gas,

pressure, power, and time of exposure[6]. The oxygen plasma attacks the siloxane backbone and generates reactive species that form silanol groups (Si-OH) [252]. The silanol groups of the PDMS layers, which are plasma-activated covalently bind to each other when two layers of PDMS bring into contact. Oxygen plasma by introducing hydroxyl groups on the PDMS surface temporarily render the PDMS surface hydrophilic and increase electro osmotic flow (EOF) leading to facilitate fluid flow into the microchannels [26, 252]. However, the plasma-activated silanol groups on the PDMS surface thermodynamically are not stable[253]. Therefore, the PDMS surface undergoes hydrophobic recovery by aging time due to the migration of low-molecular-weight species (oligomers) from the bulk to the surface [6, 251]. In addition to the silanol groups, oxygen plasma treatment can induce alcoholic hydroxyl groups (C-OH) and carboxylic groups (COOH) on the PDMS surface. Silanol and carboxylic groups have negative charges and induce negative charges on the PDMS surface [253].

2.6.7.2 PDMS surface modification using surface coating materials

Cell repellent property of PMDS via physical modification is temporary and recovers after a certain period [6, 253]. While chemical modifications provide a relatively stable cell repellent property for PDMS surface [254]. Surface coating of PDMS by using various materials for physical and covalent surface modification is often used to render PDMS surface more hydrophilic [26, 252]. Bovine serum albumin(BSA) [136, 223, 255], PEO-terminated triblock polymers (e.g Pluronic [14, 256, 257]), polyvinyl alcohol (PVA) [258], poly (hydroxyethyl methacrylate) [259, 260] poly(ethylene oxide) (PEO), poly(vinyl pyrrolidone) (PVP), hyaluronic acid poly(N-hydroxyethyl acrylamide) (PHEA), poly(acrylic acid) (PAA), dextran, etc. [3, 6] are some of the common examples for surface modification of PDMS [26].

Fouling derives from the non-specific adsorption of proteins into the surfaces and it is very challenging in most biomedical applications (e.g. implants, biosensors, organ-on-a-chip devices)[26]. Due to its hydrophobic nature, PDMS demonstrates biofouling problems from non-specific protein adsorption and cell adhesion[6]. The adsorption of the proteins onto the surface of PDMS can be initiated by the hydrophobic interactions between the hydrophobic methyl groups of the PDMS surface and the unfolded hydrophobic core or hydrophobic domains of the protein [253]. Hence, coating of PDMS surfaces to provide desirable anti-fouling properties for

biomedical applications have studied in many pieces of research [26, 261, 262]. Whitesides et al. [32] reported that compositions of the PDMS surfaces can influence cell adhesion and growth rates of primary human umbilical artery endothelial cells and can transform 3T3 fibroblasts, osteoblast-line MC3T3-E1 cells and Hela cells. Toworfe et al. [263] demonstrated that coating the PDMS surface with fibronectin can enhance MC3T3-E1 cellular attachment and spreading on the PDMS surface. The topography and stiffness level of PDMS surfaces influence human epidermal stem cell and mesenchymal stem cells differentiation [28].

2.6.7.2.1 Bovine serum albumin (BSA)

Bovine serum albumin (BSA) is one of the most common materials to prevent non-specific adsorption on the PDMS surface [27, 264, 265]. BSA is a heart shape carboxylic acid rich protein with having a molecular weight of approximately 66000 Da. BSA has 584 amino acids and three homologous domains connected by disulfide bonds together [264, 266]. BSA adsorb on the hydrophobic surface of PMDS by the combination of hydrophobic and electrostatic interactions between BSA molecules toward the PDMS surface [264, 265]. Surface modification with BSA coating is an effective method to decrease cell adhesion to the surface due to the presence of the anti-fouling layer of BSA on the surface [27].

Tan et al. used BSA with heparin followed by chemical crosslinking with glutaraldehyde for more stability. This surface demonstrated resistance to platelet adhesion with no thrombus forming [267]. Wang et al. coated BSA on PEM of chitosan and citrate stabilized nanoparticles of gold for prevention of protein adsorption [252]. Windvoel et al. studied surface coating of PDMS with a solution of 50mg/ml BSA for 10 minutes. Treated surfaces washed off with PBS. The surface wettability of the PDMS surface coated with BSA increased compared with the bare PDMS surfaces. (WCA=76.4^{o} for PDMS surface coated with BSA compared with WCA=105^{o} for bare PDMS surface). BSA also modified the chemical structure of PDMS by demonstrating amide peaks on the PDMS surface [268]. Schrott et al. investigated the Electrokinetic characteristics of the PDMS microfluidic chips treated with BSA molecules by a mathematical model and experimentally. AFM analysis demonstrated a “peak and ridge” structure of the protein layer and an imperfect substrate coating. AFM analysis demonstrated that average surface roughness increased from 0.68 nm to 4.28 nm when compared bare PDMS with BSA treated

PDMS. They have concluded that an increase in surface roughness provides higher resistance to the electro-osmotic flow [27]. Zhang et al. [28] studied the attachment of SUM159 and MDA-MB-468 cells on cell culture plates coated with PDMS and treated with aqueous solutions of fibronectin, BSA, or collagen. Effects of changes in stiffness level of PMDS and surface modification on cell attachment and growth have been studied in this work. This study demonstrated that PDMS surface coating with collagen and fibronectin maintain breast cancer cells phenotypes similar to the phenotypes observed over polystyrene Petri dishes. But surface coating with BSA provides a weak cell-substrate adhesion and stimulates stem cell-line phenotypes. They have observed that the surface modification of PDMS influences interactions between cells and their substrate. They have demonstrated that the stiffness level of PDMS did not significantly alter the cell phenotypic equilibrium. However, the surface coating of PDMS affects cell-substrate interactions. Therefore, depending on the research aim, an appropriate surface coating method should take under consideration.

2.6.7.2.2 Pluronic surfactants

Various coating materials including polymers have been developed to physically adsorb onto the PDMS surface via hydrophobic or electrostatic interactions [6, 269]. Non-ionic surfactants are examples of such materials, which can strongly adsorb on a hydrophobic surface and render it non-ionic and hydrophilic to prevent the interactions between proteins and the surface [239, 269].

Pluronic belongs to a group of widely used synthetic surfactants for surface coating of PDMS. Pluronic surfactants are triblock copolymers of PEO poly (propylene oxide)-PEO (PEO-PPO-PEO) [270, 271]. These molecules directly can attach to the hydrophobic surface of PDMS through spontaneous surface adsorption of their central hydrophobic heads (poly (propylene oxide) (PPO)). Their hydrophilic PEO tails extend out freely from the PDMS surface [254, 270]. Solubility of Pluronic in the PDMS matrix is less than in water. Hence, when PDMS contacts aqueous solutions, the hydrophobic PPO heads adsorb onto the hydrophobic PDMS surface via physisorption and hydrophobic interaction while hydrophilic PEO tails tend to migrate to the PDMS-water interface and render the PDMS surface hydrophilic and protein/cell resistant [254].

Several research demonstrated that Pluronic surfactants can significantly decrease protein adsorption and cell adhesion onto the PDMS surface [249, 254, 272]. Boxshall et al. [269]

studied the ability of Pluronic F-68 and F-127 and Tween 20 in preventing serum protein adsorption and adhesion of fibroblasts on PDMS surfaces. In another study, Wu et al. [249] have investigated the long-term ability of 3% Pluronic F-68 to decrease cell adhesion onto the PDMS surface. This surface showed anti-fouling properties where chondrocytes do not spread over the surface and clump together on days 2 and 6 after seeding. Pinto et al. [273] modified the PDMS surface in order to enhance the surface wettability. They have used argon plasma treatment to modify PDMS surfaces followed by coating with Pluronic F-68, or poly (ethylene glycol) methyl methacrylate (PEGMA). They have assessed the surface morphology by AFM and surface wettability by WCA measurements. Surface elemental composition was confirmed by X-ray photoelectron spectroscopy (XPS). Thrombosis and hemolysis assays were performed to assess the influence of the surface modifications on the blood compatibility of the materials. They have used mouse macrophages to evaluate the cytotoxicity of the modified PDMS.

Wu et al. studied the surface modification of PDMS by gradient-induced migration of embedded Pluronic F-127 [274]. The modified surface rendered hydrophilic and non-specific protein adsorption significantly decreased. Another study demonstrated the effects of coating of PDMS bioreactor with Pluronic and observed 85% decrease in serum protein adsorption compared with the bare PDMS [275].

Surface modification of PDMS via BSA and pluronic surfactants commonly was used as an effective method to change surface wettability of PDMS and decrease protein adsorption and consequently cell adhesion onto the surface have been proved in several studies as reviewed above. However, most of the previous works have only focused on single or binary protein models instead of on the real 3D cell culture environment in which the substrate will be employed. Moreover, to the best of our knowledge, there is no available study in the current literature to access the impact of this surface modification on spheroid formation on microfluidic devices. Since the main objective of this dissertation is producing uniform spheroids on the microfluidic biochips, we have studied the effect of BSA concentration and duration of surface treatment with BSA on modulating surface properties of the PDMS and accordingly on quality of spheroid formation on microfluidic devices in terms of spheroid compactness level, spherical shape and uniformity.

CHAPTER 3 STRUCTURE AND ORGANIATION OF THE ARTICLES

In this chapter, the relation between the articles and each specific research objective is stated to present the coherence of the articles in order to reach the main objective of this PhD dissertation. The scientific contributions of this dissertation were presented in the form of a comprehensive literature review and three original articles. This review paper presented in Chapter 2, is entitled Evolution of biochip technology: A review from lab-on-a-chip to organ-on-a-chip and more than 100 peer-review publications in the field were covered in this work. In this review article, I have discussed the background of biochip development and the advancements in the field of microfluidics toward its novel biomedical application in recent years as cell/tissue culture platforms to more relevantly mimic the microenvironment of living cells/tissues. This work is published in the journal micromachines and it was ranked within the first 10 highly cited articles in this journal in 2020. To the best of our knowledge, this is the first existing comprehensive review that covers the background and evolution of microfluidic devices toward the recent biochip platforms for studying human pathophysiology and drug screening. Performing this review guided me to better design my experimental research and to address my research questions during my PhD. Chapters 4 to 6 present the core of this dissertation and cover the research work conducted to fulfill the research objectives in this work.

The first objective of this work was to optimize the PDMS surface of the microfluidic biochip platform to increase cell repellent properties and accordingly enhance cells self-aggregations to form uniform spheroids in a repeatable manner. The results of this work are presented in detail in Chapter 4 in the article entitled Uniformity of spheroid-on-chip by surface treatment of PDMS microfluidic platforms is published in the journal Sensors and Diagnostics. I consider this publication to be one of my most significant research contributions to date. In this work, we aimed to by modifying the PDMS surface wettability and microstructure provide an optimized biochip surface to reduce cell adhesion. To this purpose, I have developed and fabricated PDMS microfluidic platforms for spheroid production on-chip. I have used bovine serum albumin (BSA) and Pluronic F-68, which are well-known for their cell repellent properties, to treat PDMS surfaces. In this work, I have investigated the effect of the concentration of the material and their incubation time with the surface as the two important variables to alter PDMS surface wettability and microstructure. Following, the roles of surface wettability on MDA-MB-231 breast cancer

responses and adhesion to the surface were investigated. Characteristics of spheroids produced in biochips with different degrees of wettability have been studied in this work.

Considering surface wettability as one of the main regulators modulating cell-surface responses and since different cell lines can response differently to various degrees of surface wettability due to their specific cell surface proteins, the second objective was to address if the optimized PDMS surface for spheroid formation from the specific cell line used in the first study (MDA-MB-231 breast cancer cell line) can be expandable as an optimal surface for various cancer cell lines. Therefore, spheroid formation from five cancer cell lines (MDA-MB231, C4-2B, H1299, A549 and U251) and Fibroblasts IRM-90, plus hetero-type multi-cellular tumor spheroids (MCTSs) by co-culture of IRM-90 cells with A549 cells to mimic the heterogeneous tumor microenvironment have been studied. In this work, we have also modified the design of microfluidic cell trapping chambers in order to assess the synchronous impact of design and surface of biochip in homogenous spheroid production. This constitutes the second objective, which is addressed, in the article entitled Surface optimization and design adaptation toward spheroid formation on-chip which is published in journal Sensors, and presented in Chapter 5.

The objective of my third study was to produce homogenous and compact spheroids from patient biopsy samples on the surface-optimized biochip in order to assure reproducibility of drug screening on-chip. In this study, three types of spheroids were produced in order to compare their drug resistance. Spheroids from patient bone metastasis secondary to lung, mono-type of MCTSs from A549 human lung carcinoma, epithelial cell line, and hetero-type MCTSs from a co-culture A549 cells with osteoblasts have been produced in this study. Changing in the cellular metabolic activities under different concentrations of anticancer drug (Doxorubicin) has been studied to assess integrity and reproducibility of data, which can represent homogeneity of spheroids. In addition, the drug tests have been studied in 2D culture model of the same cell lines in terms of comparing drug resistance in 3D and 2D models. This study is described in details in Chapter 6 in article entitled Uniform tumor spheroids on surface optimized microfluidic biochip for reproducible drug screening and personalized medicine. This article is published in journal Micromachines.

CHAPTER 4 ARTICLE 1: UNIFORMITY OF SPHEROID-ON-CHIP BY SURFACE TREATMENT OF PDMS MICROFLUIDIC PLATFORMS

Neda Azizipour [1], Rahi Avazpour[2], Mohamad Sawan[3 4 5], Derek H.Rosenzweig[6 7 *] and Abdellah Ajji [3 8 *]

[1] Institut de génie biomédical, Polytechnique Montréal, Montréal, QC H3C 3A7, Canada; neda.azizipour@polymtl.ca

[2] Department of Chemical Engineering, Polytechnique Montréal, Montréal, QC H3C 3A7, Canada; Info@recutex.ca

[3] Institut de génie biomédical, Polytechnique Montréal, Montréal, QC H3C 3A7, Canada ;

[4] Polystim Neurotech Laboratory, Electrical Engineering Department, Polytechnique Montréal, QC H3T 1J4, Canada;

[5] CenBRAIN Laboratory, School of Engineering, Westlake University, and Westlake Institute for Advanced Study, Hangzhou 310024, China, sawan@westlake.edu.cn

[6] Department of Surgery, McGill University, Montréal, QC H3G 1A4, Canada; derek.rosenzweig@mcgill.ca;

[7] Injury, Repair and Recovery Program, Research Institute of McGill University Health Centre, Montréal, QC H3H 2R9, Canada

[8] NSERC-Industry Chair, CREPEC, Chemical Engineering Department, Polytechnique Montréal, Montréal, QC H3C 3A7, Canada, abdellah.ajji@polymtl.ca

*Authors contributed equally.

The article is published in the journal Sensors & Diagnostics in May 2022

4.1 Abstract

Spheroids have emerged as a reliable model in preclinical oncology researches. Uniformity of spheroids is the key parameter in reproducibility and precision of drug test results. Microfluidic-based biochips have many advantages over other spheroid formation methods, including a better control over the size of spheroids. Decreasing of cell adhesion into the surface is one of the most important challenges in microfluidic platforms, which could be controlled by appropriate surface engineering methods. We have studied the effect of surface modification of PMDS microfluidic biochips by two commonly used anti-fouling coating materials, BSA and Pluronic F-68, on uniformity of spheroids production on-chip. The optimized PDMS surfaces effectively inhibited cell adhesion into the surfaces and promoted cells self-aggregations to produce homogenous and uniform spheroids on-chip. This work highlights the importance of surface modification on quality and quantity of spheroid formation on microfluidic-based biochips.

Keywords: microfluidic, 3D cell culture, spheroid, surface modification, PDMS, cancer

4.2 Introduction

The tumor microenvironment is known to play a crucial role in the development of cancer [3, 7]. It is therefore important to mimic the *in vivo* like tumor microenvironment *in vitro*, to better study the mechanisms of cancer progression and enhance new therapeutics. Studies of the cancer mostly rely on 2D cell culture models using immortalized cell lines [3]. However, it is known that signals from extracellular matrix and 3D tumor microenvironment play crucial role in the maintenance of tissue specifications [103]. Nevertheless, tumor cells respond to chemotherapy and environmental cues differently when they are cultured in 3D microenvironment [3, 276]. 3D cell culture has gained much attention over the past decades with its evident advantages of more physiologically relevant data and more predictive responses in drug discovery and disease modelling [216]. Among various 3D cell culture models, spheroids are cell aggregations formed by self-assembly which act as excellent physiologically relevant models to provide more reliable therapeutic readouts [197, 277]. Spheroids can be made by cancer cell lines or cells isolated from patients [11, 278]. These *in vitro* models can reproduce some physiological aspects of *in vivo*

tumors such as non-uniform distribution of nutrients and oxygen, limited availability of nutrients and/or drugs in their center, various metabolism and proliferation of cells in different part of the spheroids and being drug resistance [197]. They also have gene expression profiles similar to native tumors when compared with 2D models [196]. Size, geometry and compactness level of spheroids directly influence spheroid viability and drug uptake profile [10, 201]. However, production of spheroids with uniform and homogenous spheroids is the main challenge for broad use in cancer researches [10, 201, 203].

[201]Accordingly, developing platforms to simply provide size-controlled spheroids are crucially important. Microfluidic, which is the science of working with fluids in very small quantities (between 10^{-9} to 10^{-18} liters) in a set of micro-channels with dimensions in the range of tens to hundreds of micrometers, have recently been employed by various research groups worldwide to generate spheroid-based tumor-on-chip models [204, 256, 259]. However, quantity and quality of spheroids formed in these platforms and the ability to provide long-term monitoring of cellular activities are still among the remaining challenges.

Spontaneous spheroid formation occurs when cell-cell interactions dominate over cell-substrate interactions. Numerous studies have demonstrated that material surface properties (e.g. surface wettability, surface chemistry, surface charge and roughness) influence protein adsorption on the surface, which consequently regulates cell adhesion, cellular communications and their proliferation [247]. Different materials have been used to fabricate microfluidic-based cell culture devices [6, 241]. In the past few years, polydimethylsiloxane (PDMS) has attracted more interest in microfluidic biochip fabrication due to its unique properties and particularly because of its biocompatibility, transparency, ease of fabrication and rapid prototyping [6, 279, 280]. However, cell culture results on the PDMS biochips greatly depend on the physicochemical properties of the PDMS surfaces [22]. PDMS is inherently hydrophobic due to a high surface energy barrier, which may cause challenges for the flow of aqueous solutions into the channels [3, 281]. It is mostly believed that hydrophobic surfaces have higher levels of protein adsorption than that of hydrophilic surfaces [3, 246, 280]. Protein adsorption will promote cell adhesion on PDMS surface, which consequently results in channel clogging in microfluidic based cell culture platforms [26, 246]. Various methods have been used by researchers to reduce cell attachment on the PDMS surfaces, yet full optimization remains to be determined.

Plasma oxygen is widely used in microfluidic devices to permanently bond PDMS layers to each other or into another surface (e.g. glass slide). Plasma oxygen introduces hydroxyl groups on the PDMS surface temporarily to render the surface hydrophilic and increase in electroosmotic flow (EOF). This leads to facilitated fluid flow into the micro channels. However, the treated PDMS surfaces can undergo hydrophobic recovery by aging time due to the migration of low-molar-mass PDMS species from the bulk to the surface [6]. Alternatively, surface modification with non-ionic surfactants including poly(ethylene oxide) (PEO)-terminated triblock polymers (e.g. Pluronic) [254] and modification with blocking molecules with strong anti-fouling properties (e.g. bovine serum albumin (BSA)) [282] has been widely used to "block" protein adsorption and cell adhesion on the PDMS surface. PDMS chemical surface modifications to reduce protein adsorption and cell attachment have been studied earlier elsewhere [22, 28, 254, 269, 283] [22, 254, 282, 284, 285]However, the impact of PDMS surface modification on spheroid formation remained unclear.

Here, the impact of PDMS surface modification on uniformity of spheroid production on microfluidic biochip platforms has been investigated. In this work, BSA and Pluronic F-68 used as the two most common materials to treat PDMS surfaces of biochips before cell culture to decrease cell adhesion into the surface. By changing the incubation time and concentration of the BSA and Pluronic F-68, various surface wettability and microstructure produced on PDMS surface. We have observed that surface properties of PDMS drastically affect spheroid formation on-chip. Overnight treatment of PDMS surfaces with 10% BSA provides a moderate surface wettability (around 62 ^{o}) and desirable surface morphology to provide optimized surfaces with anti-fouling properties, which enhance uniform spheroid production. We believe that surface modification is an easy to use and cost-effective method to produce homogenous spheroids for reliable and reproducible data in drug assays and cancer researches.

We anticipate that this method can lead to efficient surface treatment in microfluidic-based biochips for cancer studies.

4.3 Materials and methods

4.3.1 Fabrication of PDMS layer

Constant three-millimeter thick PDMS layers were cured by mixing elastomer base and curing agent with the ratio of 10:1 (w/w) (Sylgard 184 Silicone elastomer kit, Dow Corning). The PDMS mixture was poured into petri dishes. Then, they degassed for 1 hour under vacuum to remove bubbles and cured at 65 ◦C in the oven for 2 h. When the PDMS samples were cured, they were cut into approximately 2.5 cm × 2.5 cm pieces.

4.3.2 Surface Modification of PDMS layer

Surface modification process was performed in two steps as described below:

4.3.2.1 PDMS surface treatment with oxygen plasma

The cured PDMS layers were exposed to oxygen plasma (liquid air, alphagaz 1, 99.999% purity) which was set at a flow rate of 20 sccm (standard cubic centimeters) controlled by a mass flow controller (MKS 247C channel readout MKS 1259B-00100RV (0-100 sccm). The pressure in the chamber (Cylindrical with a 9” diameter and 1.25” height) was set at 600 mTorr (80 Pa) and fixed using a butterfly valve during the process. The plasma was initiated by radio frequency plasma at 13.56 MHz (ENI model HF-300 impedance matching unit Plasma therm AMNS 3000-E) and the applied power was set at 20 Watts, with a plasma exposure time of 20 seconds per sample.

4.3.2.2 PDMS surface treatment with chemical coatings

To repeat each experiment in a minimum of three replicates, numerous PDMS pieces have been fabricated with soft lithography and have been treated with oxygen plasma as described above. The hydrophobic recovery of PDMS after treatment with oxygen plasma occurs by the aging time of plasma treatment due to the migration of lower molecular weight species to the surface [250]. Therefore, all PDMS pieces have treated with chemical coating on the day 7^{th} after plasma exposure to provide the same physicochemical properties for all the samples before coating with chemicals. Samples surfaces were washed gently with Ethanol 99% and then, samples were

washed with chemical coating solutions and were immersed in their chemical coating solutions. In this study, we have chosen two different coatings with three different concentrations of each (6 different coatings in total). BSA and Pluronic F-68 which are commonly used surface coatings to reduce cell adhesion into the surfaces have been chosen for this purpose. Chemical coatings were prepared in concentrations of 3% w/v, 5% w/v, and 10% w/v of each, to treat sample surfaces. Two time points have been used in this study. One set of samples has been treated by immersion in freshly prepared BSA solution and Pluronic F-68 solution for approximately one hour at 37 °C, and another set of samples has been treated over night at 37 °C to ensure maximum time for adsorption.

4.3.3 Surface characterisation

4.3.3.1 Water contact angle (WCA) measurement

After surface treatment, each sample was gently washed with HBSS (Wisent Bioproducts, St-Bruno, QC) to remove the excess BSA and Pluronic on top of the PDMS, also to access if the WCA changes and morphology changes on the PDMS surface were long term or just visible due to excess Pluronic and BSA crystals on the surface. Then, surfaces have been washed with complete cell culture media, in order to follow the same procedure which we use before the cell culture on PDMS biochips.

WCA were measured directly on clean and flat surfaces with a goniometer (Data Physic OCA, SCA20 software) using the sessile drop technique. An intermediate equilibrium of water-air-solid contact angle was obtained by depositing a 2 µl water droplet on the surface using the calibrated syringe. A photograph of each droplet was taken 30 sec after contact with the surface by using the VCA Optima contact angle analyzer (AST products, Billerica, MA) to study the hydrophobicity. Water contact angle measurements were measured in triplicate for each sample on the contact side.Atomic force microscopy (AFM) measurement

The surface morphology of treated PDMS surfaces along with non-treated surfaces was studied using an Atomic force microscopy (AFM). All AFM images were captured in the air at room temperature using tapping mode on a (Dimension ICON AFM, Bruker/Santa Barbara, CA). Intermittent contact imaging (i.e., "tapping mode") was performed at a scan rate of 0.8Hz using

etched silicon cantilevers (ACTA from AppNano) with a resonance frequency around 300kHz, a spring constant of ≈ 42 N/m, and tip radius of 'lt;10 nm. All Images were obtained with a medium tip oscillation damping (20-30%).

4.3.4 Fabrication of microfluidic device to form spheroids on biochip

Each microfluidic device is composed of two PDMS layers obtained from 3D printed master mold. Design of the channels is adapted from Astolfi et al. [33] and the parameters of each channel and wells are broadly the same as the device described by them [33], except that the height of the wells have been increased to 540 μm to optimize device operation [226]. The bottom layer of the device consists of 2 open channels with a 600 μm wide square cross-section. Each channel is containing of five 600 μm-wide square-bottom micro- wells of 540 μm in height. The top layer PDMS with 3mm diameter inlet and outlet holes bonded with Plasma Oxygen (same conditions described above for PDMS surface treatment with plasma oxygen) to the bottom layer. The polymeric resin molds (HTM 140 resin, EnvisionTEC GmbH, Gladbeck, Germany) have 3D printed using stereolithography printer (Freeform Pico and Pico 2 HD, Asiga, Alexandria, Australia).

Briefly, a mixture of PDMS (Sylgard 184 polydimethylsiloxane elastomer kit; Dow Corning, Midland, USA) base polymer to curing agent at a mass ration of 10:1 prepared and mixed well, degassed and poured into each resin mold and allowed to crosslink and cure for 2 hours in 65 °C oven [284-287]. When it is cured, the PDMS layer is gently peeled off from the mold. Following surface treatment with oxygen plasma, the two layers of the PDMS have bond together to form closed microfluidic channels and assembled into the microfluidic device.

4.3.5 Surface treatment of the microfluidic channels

Each microfluidic device was sterilized and air bubbles were removed from each channel by using 99.9 % ethanol (Sigma-Aldrich). Then, the channels were washed a minimum of three times with chemical coating solutions (BSA or Pluronic F-68) to clean the channels surface from ethanol residues. After, the channels were treated with relevant chemical coating solutions (BSA or Pluronic F-68) in order to assess the role of surface coating to reduce cell adhesion into the

channels and facilitate spheroid formation on-chip. As described above, two chemical coatings have been used in this study for surface treatment of PDMS. Triblock copolymer surfactant Pluronic F-68 (Sigma-Aldrich) and BSA (Sigma-Aldrich) which are the most commonly used materials for surface treatment in PDMS-based microfluidic devices to decrease cell adhesion into the surface, have been prepared in three different concentrations of 3% w/v, 5% w/v and 10% w/v of each to incubate with PDMS surface. We have divided the devices into two groups to be treated with the same surface coating for two different incubation times. One group of devices have been treated with each chemical coating for approximately one hour at 37 °C, and the second group of devices have been treated over night at 37 °C. Simply, by using P1000 micropipette, each one of the chemical coatings has been introduced through each channel inlet and washed the channel for three to four times. Then each channel was filled with the chemical coating for the specific time designed for each group (Less than one hour for group one and overnight for group two of devices) and placed in the incubator ((37 °C, 5% CO2, 95% ambient air).

4.3.6 Cell culture and spheroid formation on-chip

MDA-MB-231-GFP cells (human mammary gland adenocarcinoma) were donated by the laboratory of Professor M. Park (McGill University) and were maintained in high glucose Dulbecco's Modified Eagle Media (DMEM, Sigma Aldrich) supplemented with 10% (v/v) Fetal Bovine Serum (FBS) (Sigma-Aldrich) and 1% (v/v) penicillin–streptomycin (Sigma-Aldrich) at 37 °C, 5% CO2 and 95% relative humidity (RH). Cells were seeded and passaged one or two times into 75 cm^2 tissue culture flasks (Corning Inc., New York, USA) before spheroid formation on chip. 80–90% confluent cell cultures were used for the experiments on biochip. For spheroids culture on biochip, cells were washed with sterile phosphate buffered saline (PBS, Sigma Aldrich) and trypsinized with 0.25% Trypsin-EDTA solution (Sigma-Aldrich) to create a cell suspension right before the cell culture on chip. Then, microfluidic devices removed from the incubator and channels were rinsed three times with sterile HBSS (Wisent Bioproducts, St-Bruno, QC) to clean the channels from chemical coating residues. Then, cell suspension with the concentration of 5×10^5 cells/mL was introduced into the channels inlet by using P200 micropipette. Cell suspension flowed into the channels using gravity-driven flow. The tube

connected to the outlet will be lowered to approximately 10-15 cm below the inlet during cell seeding process. Accordingly, gravity resulted from this difference in height, will create a force to facilitate cell seeding. When the channels were completely filled with the cell mixture, flow was stopped and allowed cell sedimentation into the wells. The devices were then incubated under static conditions at a humidified incubator with 5% CO_2 at 37 °C for 24 hours. Spheroid formation was occurred by on-chip sedimentation and containment [204, 259]. During the cell loading process into the inlet of the channels, a portion of the cells were trapped and settled down into the wells and the rest flowed into the rest of the downstream wells or were ejected through the outlet. Since the surface of the channels were treated and became cell-resistant, cells self-aggregation to form spheroids occurred inside each well within one day after the cell seeding process. On the first day post-seeding, non-adherent cells were washed off by gently rinsing the channels with complete media and cell aggregated spheroids remained inside the wells. Inlets and outlets of the devices filled with complete media and devices were kept in the incubator under static conditions for a period of 7 days for daily monitoring and media exchange by using P200 micropipette.

4.3.7 On-chip observation of spheroid formation and growth tracking

Spheroid formation and growth were imaged directly through the thin PDMS layer by using Epifluorescence inverted microscope (Axio Observer.Z1, Zeiss, Oberkochen, Germany) and sCMOS camera (LaVision, Göttingen, Germany) and the objective lens EC Plan-Neofluar 5x / 0.15 for duration of 7 days incubation. The size of the spheroids was determined by measuring their diameters after they were imaged by fluorescent microscopy.

4.3.8 Image J and data analysis

As explained above, spheroid images were recorded by using Epifluorescence inverted microscope (Axio Observer.Z1, Zeiss, Oberkochen, Germany) and sCMOS camera (LaVision, Göttingen, Germany) with the objective lens EC Plan-Neofluar 5x / 0.15. To analyze the fluorescent images of spheroids, Image J (National Institute of Health, Maryland, USA) was used. The fluorescence intensity of green fluorescent has been obtained by a digit value from zero to maximum 255 with Image J. The analyzing area of the spheroid cell culture has been carefully selected on their 2D fluorescence image. All images had high resolution of more than 1900 dpi.

The average mean diameter were calculated as Dm= (Dmax+Dmin)/2 [288]. Dm, Dmax, and Dmin are representing mean diameter, maximum diameter, and minimum diameter of the spheroid, respectively. The average of spheroids size for each types of surface treatment on days 1, 3, and 7 after cell seeding was reported as average of mean diameter for 10 spheroids per each condition ± standard error (SE). The circularity of the spheroids has been calculated as circularity=Dmin/Dmax ×100. Dmin, and Dmax are representing the minimum diameter and maximum diameter around a single spheroid, respectively. The circularity of spheroids for each types of surface treatment on days 1, 3, and 7 after cell seeding was reported as average of circularity for 10 spheroids per each condition ± standard error (SE). Brightness level ratio (BLR) is calculated as BLR=Brightness level/255 × 100. By using Image J, fluorescent signals obtained from fluorescent images of spheroids as the function of cell density in the spheroids were used as brightness level for BLR calculations. All Data have been reported as the mean ± standard error (SE) of minimum three independent replicas. All error bars in figures indicate SE. Experiments were repeated at least three times per each condition. One representative image is presented where the same trends were observed in multiple trials.Results and discussion

Previous studies have demonstrated that surface treatments with BSA and poly (ethylene oxide)-poly (propylene oxide)-poly (ethylene oxide) (PEO/PPO/PEO) co-polymers (Pluronics) strongly have anti-fouling characteristics [270, 289]. Liu et el. [270] were demonstrated that PEO/PPO/PEO co-polymers can modify the surface to completely prevent cell attachment. But in the present study, we have observed that the success in the surface treatment highly depends on the concentration of the chemical coating and their incubation time with the surface. The objective of this work was to study the impact of PDMS surface modification on spheroid formation on-chip. To reach this objective, we have modified the PDMS surfaces with the two popular and commonly used materials with anti-fouling properties to decrease or inhibit cell adhesion into the PDMS surfaces of microfluidic biochips. We have assessed surface wettability and surface morphology of PDMS on treated surfaces compared with bare PDMS surfaces. Following, spheroid formation in various surface treated biochips were compared in terms of spheroid size, spherical form, and compactness level of the spheroids measured or estimated to assess the impact of surface properties on spheroid production.

4.3.9 Water contact angle

Contact angle measurements were performed for bare and treated PDMS surfaces with BSA and Pluronic F-68 coatings. Plasma treatment is an inseparable step in microfluidic biochip fabrication to permanently bond the two PDMS layers together or into another surface (e.g. glass slide) to form closed microfluidic channels [3]. WCA decreases immediately after plasma treatment due to the temporarily present of polar groups (e.g. SiO2, Si–OH and Si–CH2OH) on the PMDS surface [25, 250]. However, PDMS surfaces undergo hydrophobic recovery by the aging time due to the migration of low-molar mass PDMS species from the bulk of PDMS onto the surface [243, 250]. Usually, there is few days/weeks gap between fabrication of biochip and use them for cell culture experiments. Therefore, the PDMS surfaces go through hydrophobic recovery after this certain time and before cell culture experiments. We have mimicked this condition to provide the exact steps, which PDMS surfaces of microfluidic biochips go through before cell culture. Therefore, first, we have treated PDMS surface with plasma oxygen. Then, surface treatment with chemical coatings carried out on day 7^{th} after plasma treatment to have the integrity in all data and to provide the same conditions for PDMS pieces similar to biochip surfaces before cell culture. [25]. It is observed that for both surface treatments with BSA and Pluronic F-68, WCA decreased when the incubation time and concentration of chemical coatings increased. The results showed that WCA for BSA coated surfaces decreased to close to 60 degrees, while WCA for Pluronic F-68 coated surfaces decreased to around 82 degrees.

We have observed that WCA of PDMS surfaces treated with BSA and Pluronic F-68 is lower than that of the bare PDMS surface, which means that both of these surface coating materials reduced the hydrophobicity of PDMS (Figure 4.1)

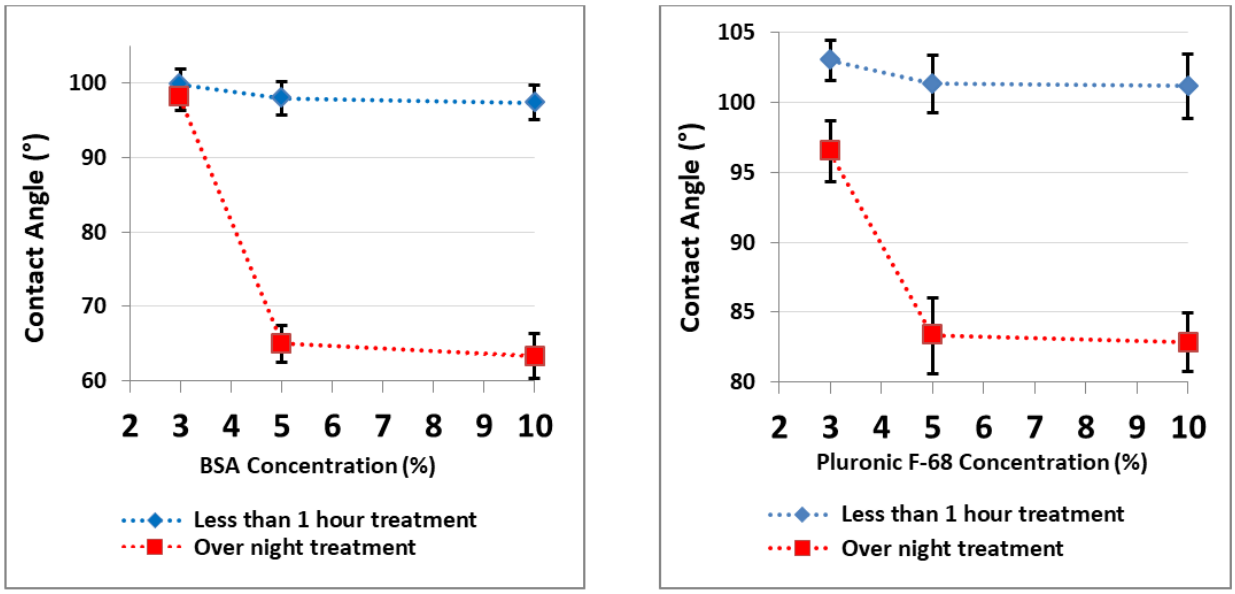

(a) (b)

Figure 4.1 Measurement of WCA on the treated PDMS surface

(a) with BSA, (b) with Pluronic F-68 demonstrate the WCA of PDMS layers in the contact side vs different concentrations of chemical coatings: A) The difference between water contact angles of PDMS coated after 1 hour and 24 hours of incubation with three concentrations of BSA, B) The difference between water contact angles of PDMS coated after 1 hour and 24 hours of incubation with three concentrations of Pluronic F-68. Error bars represent SE for 3 independent sets of experiments. Within each experiment, WCA was calculated by averaging data points on the same sample (n = 3)

Previous studies have demonstrated the effect of surface wettability on protein adsorption and consequently cell adhesion into the surfaces [237, 251, 290]. Here, we have observed that surface treatment of PDMS with BSA and Pluronic F-68 has changed PDMS surface wettability. Following, we have assessed the impact of this change on cell responses to the surface and spheroid formation on-chip.

4.3.10 PDMS surface topology and AFM analysis

Surface microstructure and topology are among key parameters to affect protein adsorption and unwanted cell adhesion into the surfaces [237, 251, 269]. In the present study, we have used AFM to assess the possible topological effects on cell adhesion into the surface. The topology and microstructure of PDMS surfaces before and after treatment with BSA and Pluronic F-68, as two commonly used surface coating materials in the microfluidic-based devices to reduce cell adhesion into the surfaces were characterized. In this regard, we have studied if surface morphology of PDMS changes by surface treatment when compared with the bare PDMS. Moreover, we have investigated if this change is repeatable and reproducible in several trials. Clear changes have been observed on surface treated PDMS layers compared with the bare PDMS. First we have assessed the impact of incubation time. To do this, 5% BSA and 5% Pluronic F-68 incubated with PDMS layers in two different groups. The first group was treated in less than one hour and the second group was treated overnight with surface coating materials.

AFM images of PDMS surfaces for bare PDMS and treated surfaces have plotted in Figure 4.2

Time	Less than 1 hour treatment	Overnight treatment
PDMS surface treated with 5% Pluronic F-68	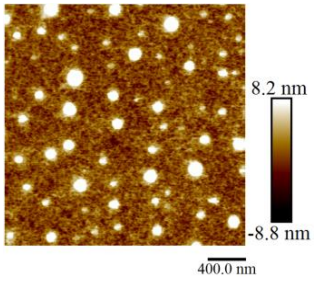	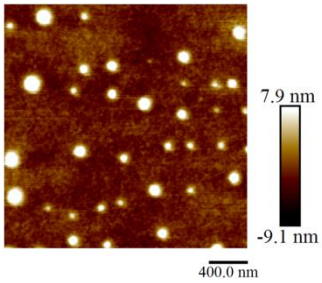
PDMS surface treated with 5% BSA	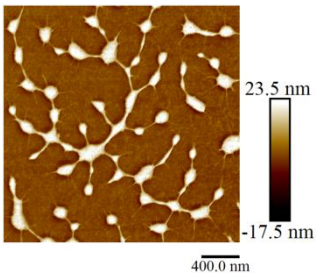	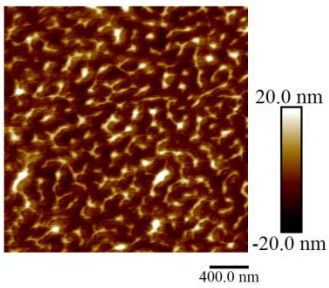
Bare PDMS surface	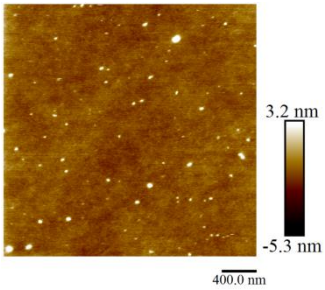	

Figure 4.2 AFM images of the chemical coated and bare PDMS surfaces
Surface treatment for less than one hour and overnight treatment with 5% BSA and 5% Pluronic F-68, vs bare PDMS compared

AFM images of treated PDMS layers have demonstrated changes in surface microstructure compared with bare PDMS. The results obtained from AFM indicate that bare PDMS surfaces have homogenous and smooth surfaces with smaller vertical height for pick and valley structures [25, 28, 291]. Increasing the incubation time decreased the maximal vertical height for pick and valley structures. We assume this could be related to more surface coverage by increasing the

incubation time. It means that BSA or Pluronic molecules have more time to adsorb into the surfaces and cover the gaps between heights and depths on the surfaces [27].

Table 4.1 summarized the average of maximal vertical height value for pick structures formed on PDMS surfaces after surface treatment with BSA and Pluronic in short term (less than one hour) and long term (overnight treatment). Three AFM images considered to calculate the average of maximal vertical height of the peaks.

Table 4.1 Average maximal vertical height value for pick structures formed on PDMS surfaces after short term and long term treatment with chemical coatings (Average ± SD, n=3)

Material	**Short treatment with 5% agent**	**Long treatment with 5% agent**
Average maximal vertical height for pick structures (nm) for surface treatment with Pluronic F-68	8.3±0.8	7.9±0.5
Average maximal vertical height for pick structures (nm) for surface treatment with BSA	19.1±0.8	18.3±0.6

To assess the impact of concentration of the coating materials, in another set of experiment, PDMS surfaces have been treated with three different concentrations of BSA and Pluronic F-68 overnight (3% w/v, 5% w/v, and 10% w/v of each). AFM images obtained from PDMS surfaces treated with different concentration of BSA and Pluronic clearly showed the formation of peak and valley structures which proved that surface modification occurred. AFM images have demonstrated that by increasing the concentration, maximal vertical height for pick and valley

structures have been decreased. We assume that increasing in concentration provided more molecules to cover the PDMS surfaces. Therefore, more gaps and free spaces between the heights and depths on the surface have been covered. Accordingly, the height differences between height and depths on the surface decrease (Table 4.2 and Figure 4.3)

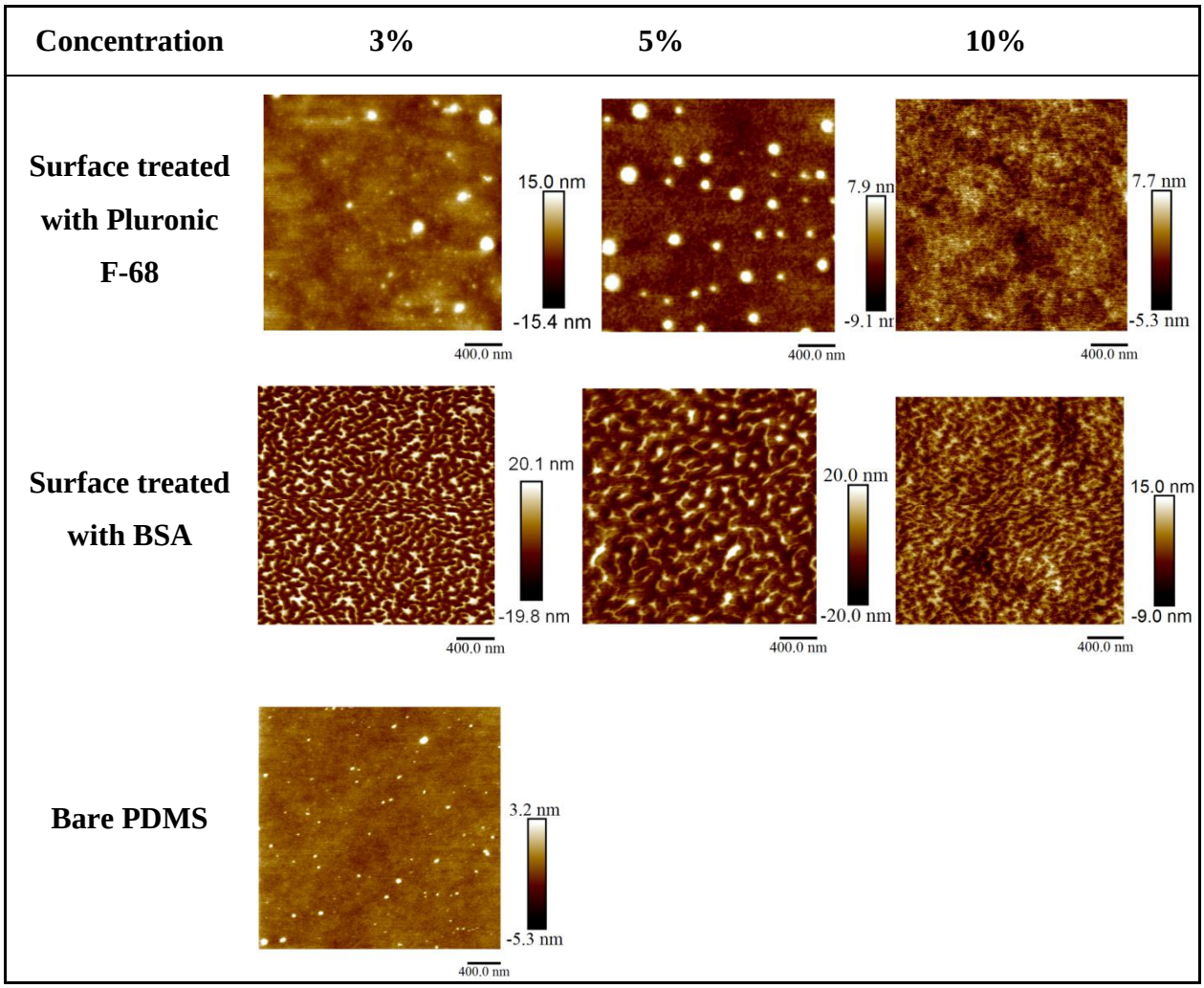

Figure 4.3 AFM images of the three concentrations of chemical coated PDMS surfaces with BSA and Pluronic F-68 vs bare PDMS

Table 4.2 summarized the average of maximal vertical height value for pick structures formed on PDMS surfaces after surface treatment with different concentration of BSA and Pluronic F-68. Three AFM images considered to calculate the average of maximal vertical height of the peaks.

Table 4.2 Average maximal vertical height value for pick structures formed on PDMS surfaces treated with three concentration of chemical coatings (Average ± SD, n=3)

Material	**PDMS + 3% agent**	**PDMS + 5% agent**	**PDMS + 10% agent**
Average maximal vertical height for pick structures (nm) for treatment with Pluronic	13.4±0.6	7.9±0.5	7.8±0.5
Average maximal vertical height for pick structures (nm) for treatment with BSA	25.1±0.7	18.3±0.6	16.8±0.4
Average maximal vertical height for pick structures (nm) for Bare PDMS		4.6±0.4	

As explained above and as summarized in increasing the incubation time and concentration of chemical coating clearly change the surface morphology of treated PDMS compared to the bare PDMS. This morphological change was repeatable and showed the formation of peaks and valleys structures on the PDMS surfaces which proved that surface modification occurred and BSA and Pluronic molecules adsorbed into the PDMS surfaces [25, 250, 273].

4.3.11 Spheroid formation on microfluidic biochips

Microfluidic devices have been used in this work to assess the impact of surface modification on homogenous spheroid production were inspired by design developed by Astolfi et al. [33]. The design has been modified to have two separate microfluidic channels in each device. The height of each well is also modified according to the theoretical simulation [226] for optimal cell trapping. The cell mixture of MDA-MB-231 cells is introduced into the inlet of each channel. A portion of cells trapped and settled down into the micro-wells by sedimentation [204, 259]. Since the surfaces were modified and became cell-repellent [25, 26], cell-cell adhesions became dominant over cell-substrate adhesions [13, 201, 292].The sizes of the spheroids were relatively uniform in each group and it mostly depends on the initial cell concentration of the cell mixture. We have experimentally optimized the initial cell concentration to 5×105 cells/mL in cell mixture for our device (Figure 4.4).

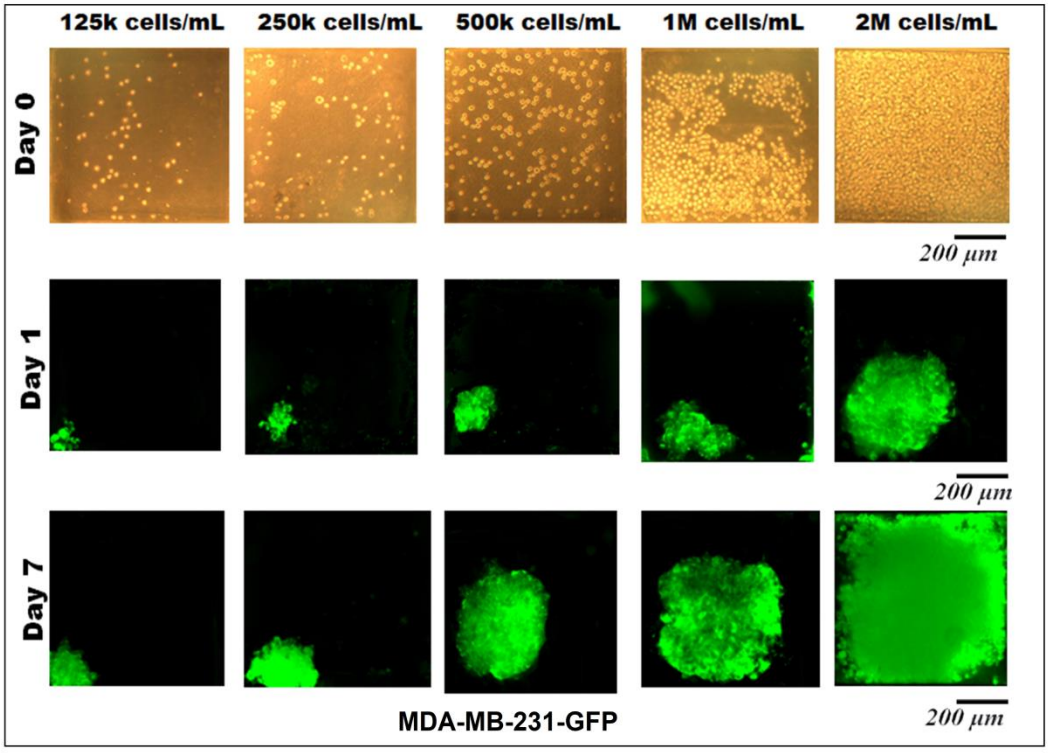

Figure 4.4 Spheroid formation on-chip with different initial cells concentration and their growth during 7 days

Fluorescent images of MDA-MB-231-GFP spheroid formation within microchannels. Different initial cells concentration applied to adjust the optimal initial cells concentration. (Size of chambers: 600, 600, 540 μm, Size of microchannel: 600 μm width, 600 μm height. Scale bar is 200 mm. The green color is due to green-fluorescent protein (GFP) in MDA-MB-231 cells. Images of the cells in day 0 (cells injection inside the microfluidic channels) were captured by bright field microscopy. Images of the spheroids on day 1 and 7 were captured by fluorescent microscopy

Microscopic observations have demonstrated that there is no significant difference between the spheroids formed in different micro-wells through the channel and have confirmed the uniform distribution of cells along the length of each channel. Fluorescent images of spheroids have shown the progressive development of spheroid sizes through 7 days of culture. Cells are capable to self-aggregating and form cellular clusters after one day of culture and transform into compact

uniform-sized spheroids after the second day of culture. Figure 4.5 demonstrates the cell aggregation process on non-treated biochips compared with devices which have been treated with chemical coatings (BSA or Pluronic F-68) to be resistant to cell adhesion into the PDMS surface. In contrast with biochips which have been treated overnight with chemical coatings, devices without any surface modifications and devices which only have been treated for a maximum of 1 hour of incubation with chemical coating were favourable for the attachment of MDA-MB-231 cells. In these devices, cells tended to attach to the walls of the microfluidic channels and exhibited spread morphology which was propagated to adherent cell clusters attached to the surfaces of the micro-wells.

The spheroids morphology on the BSA-coated and Pluronic F-68-coated devices was observed to be very similar and it seems to be mostly depends on the concentration of the chemical coating. As a control, cells were seeded on a PDMS device without any surface treatment. A significantly greater number of cell adhesions qualitatively were observed on non-treated PMDS channels as demonstrated in the Figure 4.5 which illustrate the impact of surface treatment in reducing cell adhesion into the PDMS surfaces. When the PDMS surfaces of microfluidic biochips were treated with BSA or Pluronic F-68, surfaces became cell-repellent. According to the surface characterisation experiments, explained above, we assume that the changes in surface wettability and microstructure of PDMS due to surface modification affected cell responses into the surface. Therefore, cell-substrate interactions decreased while cells self-agglomerations have been promoted to facilitate spheroid production. On the other side, cells tend to attach to hydrophobic surfaces of non-treated PDMS biochips. Therefore, in most of the micro-wells they have been proliferated randomly without formation of spherical cells clusters. The growth pattern of the MDA-MB-231 cells within the 3D environment over the course of 1 week is shown in this figure.

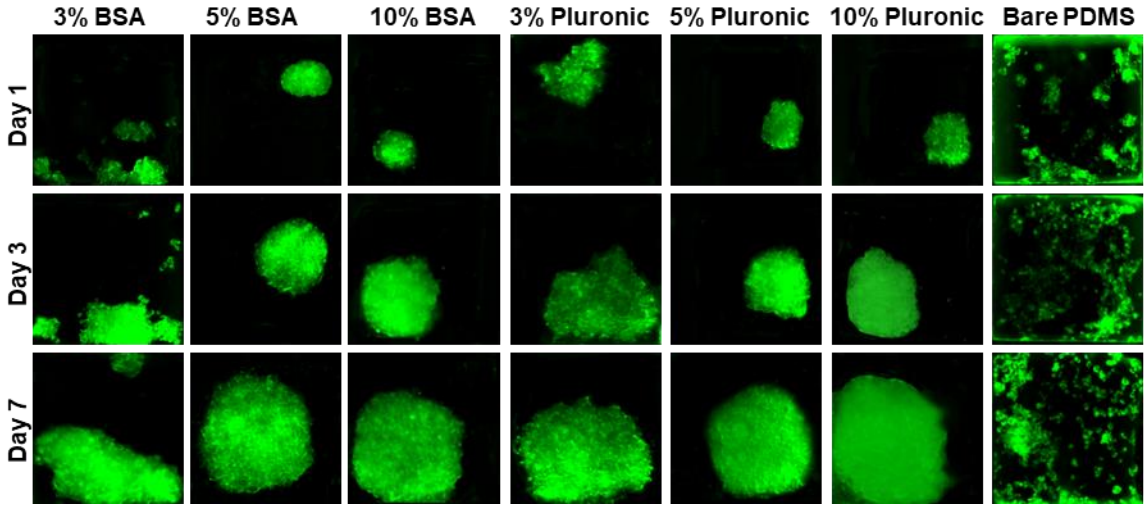

Figure 4.5 MDA-MB-231-GFP Spheroid formation on-chip

MDA-MB-231-GFP Spheroid formation on-chip surface treated with various concentrations of chemical coatings (BSA and Pluronic F-68) compared with non-treated PDMS biochips. Each square in this image is representing 600 μm ×600 μm. Green color is due to green fluorescent protein GFP. (n=3)

4.3.12 Monitoring of spheroids growth

Daily growth of spheroids has been performed by using fluorescent microscopy. In this work, we have observed that surface modification of PDMS biochips is a simple and cost-effective method to produce uniform spheroids on-chip. Our observations indicated the key role of surface modification of biochips on cell responses into the surfaces and accordingly on spheroid formation on-chip. More specifically, this work highlights the impact of incubation time and concentration of the chemical coating to modify PDMS surface wettability and microstructure. These two demonstrated to play critical role on spheroid production on PDMS biochips. We need to take in the consideration that non-uniform cell aggregations, lobular structures, and loose cell-cell connections should not be considered as spheroids [10, 203]. Hence, this work, highlight the crucial impact of surface modification to produce uniform and compact cell clusters, known as spheroids.

In Figure 4.6 Image J has been used to analyze size, spherical shape, and compactness level of spheroids during 7 days of culture. The average of 10 spheroids has been used per condition. All

experiments have been repeated in three independent replicas. The brightness level of the green fluorescent color obtained by a digit value from zero to maximum 255 which respectively corresponds to darkest and brightest pixels in image J. The analysing area of the spheroids have carefully selected on 2D fluorescent images of spheroids. Brightness level ratio was presented as BLR=Brightness level/255 × 100 in our calculations. This number qualitatively can be representative of compactness level of spheroids. This means that when the fluorescent image is brighter, BLR value obtained by image J is a higher number. This can be representative of more cells in the spheroids that have been produced more intense fluorescent signals captured by fluorescent microscopy. BLR increased from day 1 to day 7. As explained in detail in Methods, we have calculated the spherical shape of the spheroids as Circularity=Dmin/Dmax × 100 around a single sphere. Spheroids size have been presented as the average mean diameter calculated as Dm=(Dmax+Dmin)/2.

Figure 4.6 demonstrate changes in size, shape and compactness level of the spheroids during 7 days of culture.

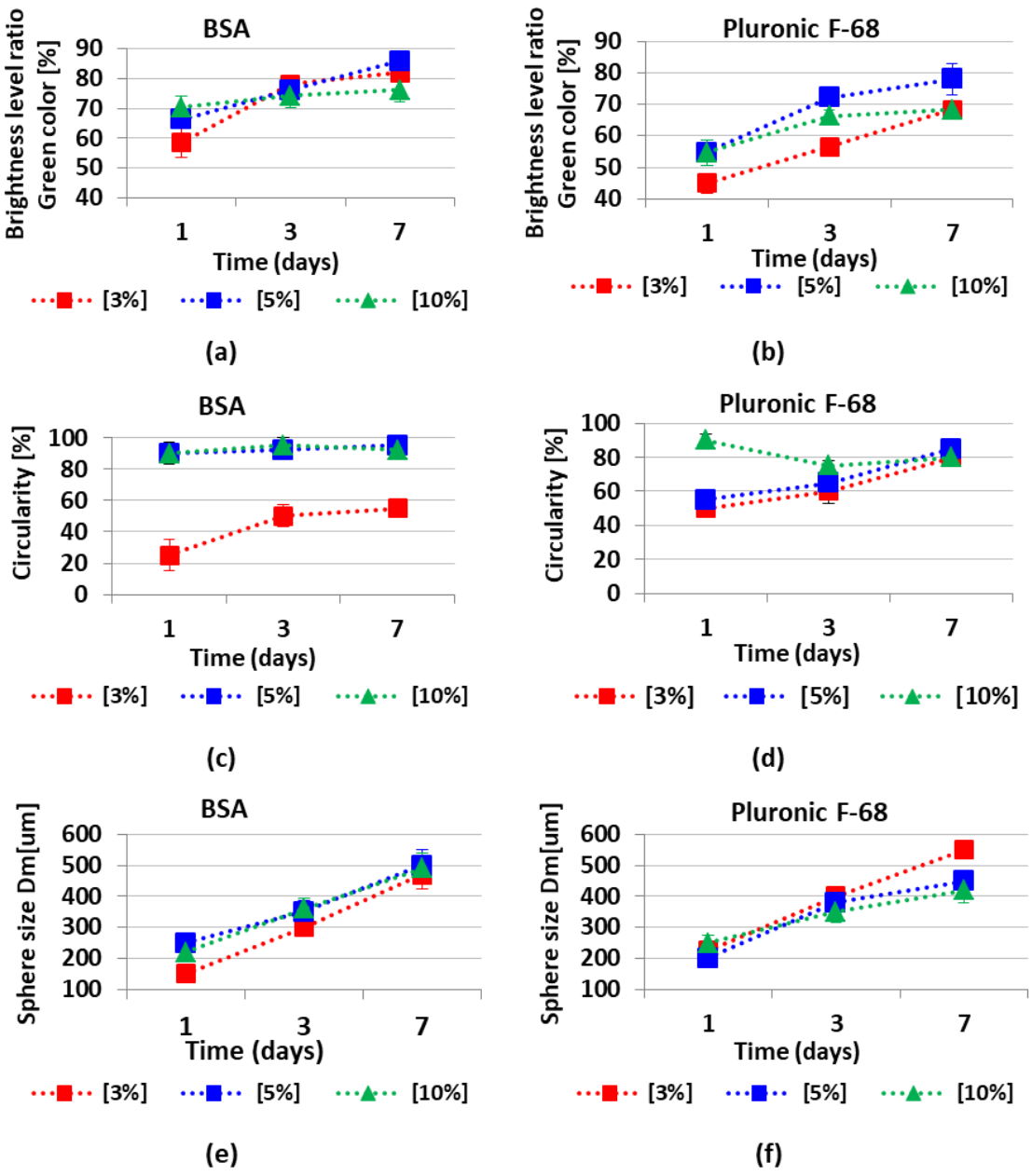

Figure 4.6 Image J analysis of spheroids formed in biochips treated with different concentrations of BSA and Pluronic F-68 overnight

a) and b) show the brightness level ratio of green fluorescent for BSA and Pluronic F-68 respectively. Brightness level ratio demonstrated the intensity of green fluorescent measured by Image J. This can be representative of the cellular concentration or compactness level of the cells inside the spheroids that produced fluorescent signals. c) and d) show the circularity of the

spheroids formed in BSA and Pluronic F-68 treated biochips, respectively. Circularity can demonstrate how spheroids are spherical shapes or homogenous. e) and f) show the spheroid size measured as the average mean diameter in um. 10 spheroids were used for calculations per condition. Experiments have been repeated in three independent trials (Error bars represent ± SE, n=3)

Our data reveal that the BSA coating produced a cell repellent pattern similar to that observed following Pluronic F-68 surface treatment. However, BSA was more effective starting at the concentration of 5% and the optimized results have been recorded at the concentration of 10% to reduce cell adhesion to the surfaces. On the other hand, Pluronic F-68 has been shown to be effective in reducing cell adhesion to surface starting at the concentration of 3%. According to our observations we believe that 5% is the optimal concentration for Pluronic F-68 to achieve higher percentage of uniformly sized spheroid formation on-chip as it seems that with 5% of Pluronic F-68, we are going to have enough surface coverage to prevent cell attachment into surfaces.

In our experiments, spheroid formation on surface treated with 10% BSA and 5% Pluronic F-68 was greater than to the other surfaces, suggesting that the moderate wettability (62-88 degree water contact angle) shared by these two surface coatings promoted higher cell repellent properties for PDMS surfaces.

We believe that the concentration of the chemical coatings and the incubation time are the two important factors to regulate surface wettability and morphology of PDMS surfaces, which are providing optimal anti-fouling property for PDMS surfaces.. In this study, we only have focused to investigate the impact of PDMS surface wettability and microstructure on spheroid production on-chip. However, we need to take in the consideration that the impact of surface properties on cellular responses into the surfaces is very complicated and it is not completely understood yet [22, 23, 251]. Further investigations required for better understanding the influence of various surface properties on cell responses into the PDMS surfaces.

4.4 Conclusion

Understanding the correlation between surface properties and cellular responses into the surfaces is essential to design optimal surfaces in biomedical applications including microfluidic based biochip platforms. Although enormous studies have been performed concerning PDMS surface modifications, a systematic study on the effect of anti-fouling coating on the PDMS surface properties and its impact on spheroid production on PDMS microfluidic biochip platforms was still missing in the literature. As the cells behaviour is deeply influenced by the cellular microenvironment and their substrates, the objective of this study was to investigate the influence of PDMS surface properties (specifically surface wettability and microstructure), on uniform and homogenous spheroid production on microfluidic biochips.

In this work, we have used BSA and Pluronic F-68 as the two commonly used materials to decrease cell adhesion into the surfaces of microfluidic platforms. We have studied the effects of incubation time and concentration on changing the PDMS surface wettability and microstructure. Then, the impacts of PDMS surface properties on spheroid formation from MDA-MB-231-GFP cells on PDMS microfluidic biochips have been investigated.

This study provides not only fundamental understanding about control of cell behaviour in PDMS-based microfluidic platforms, but also a simple and cost-effective method to effectively enhance spheroid formation on-chip for *in vitro* assays. Our observations have been demonstrated that moderately hydrophilic surfaces (62-88 degree water contact angle) promoted the highest level of cell repellent properties. Here, we have observed that overnight PDMS surface modification with 10% BSA provided an optimized surface to effectively supress cell adhesion into the PDMS surfaces and promote spheroid formation on-chip.

In this study, we have produced homogenous and uniform-sized and shaped spheroids in a repeatable manner. In this work, we have used breast cancer cells lthough the technology described here is versatile. In our future work, we will use other cell lines to assess the capability of this surface optimized biochip to effectively capture cells from various cell lines and produce uniform spheroids on-chip. On the whole, the results of this work indicated the importance of the surface properties to modulate cell responses into the surfaces and decrease non-specific cell adhesion.

In summary we have shown a simple, effective, practicable and repeatable method to modify the PDMS surface of biochips to effectively enhance spheroid formation on PDMS biochips without the need of using expensive additive materials (e.g. hydrogel, matrigel, etc.) into the cells mixture to produce uniform spheroids for drug testing and cancer studies.

4.5 Author contributions

Conceptualization: N.A., R.A., M.S., D.H.R. and A.A.; Data curation: N.A. and R.A.; Formal analysis: N.A., R.A., D.H.R. and A.A.; Funding acquisition: D.H.R., M.S. and A.A.; Investigation: N.A., R.A., M.S., D.H.R. and A.A.; Methods: N.A., R.A., D.H.R. and A.A.; Project administration: M.S., D.H.R., and A.A.; Resources: M.S., D.R. and A.A.; Supervision: M.S., D.R., and A.A.; Validation: N.A., M.S., D.H.R., and A.A.; Visualization: N.A; Writing original draft: N.A.; Writing—review and editing: N.A., R.A., M.S., D.R. and A.A.; N.A. should considered as first author; D.R. and A.A. contributed equally to this work and should considered as co-corresponding authors. All authors have read and agreed to the published version of the manuscript.

4.6 Conflicts of Interest

The authors declare no conflict of interest.

4.7 Acknowledgements

The authors gratefully acknowledge funding support from the Natural Sciences and Engineering Research Council (NSERC) of Canada discovery grants. The authors also gratefully acknowledge Professor Thomas Gervais (Polytechnique Montréal) for fruitful scientific discussions for the design and fabrication of the biochip, and Professor Morag Park (McGill University) for kindly providing the cell line used in this study. N.A gratefully acknowledges the scholarship from Fondation et Alumni de Polytechnique Montréal donated by Royal Bank of Canada (RBC).

CHAPTER 5 ARTICLE 2: SURFACE OPTIMIZATION AND DESIGN ADAPTATION TOWARD SPHEROID FORMATION ON-CHIP

Neda Azizipour [1], Rahi Avazpour[2], Mohamad Sawan[3 4 5], Abdellah Ajji [3 6 *] and Derek H.Rosenzweig [7 8 *]

[1] Institut de génie biomédical, Polytechnique Montréal, Montréal, QC H3C 3A7, Canada; neda.azizipour@polymtl.ca

[2] Department of Chemical Engineering, Polytechnique Montréal, Montréal, QC H3C 3A7, Canada; Info@recutex.ca

[3] Institut de génie biomédical, Polytechnique Montréal, Montréal, QC H3C 3A7, Canada;

[4] Polystim Neurotech Laboratory, Electrical Engineering Department, Polytechnique Montréal, QC H3T 1J4, Canada;

[5] CenBRAIN Laboratory, School of Engineering, Westlake University, and Westlake Institute for Advanced Study, Hangzhou 310024, China, sawan@westlake.edu.cn

[6] NSERC-Industry Chair, CREPEC, Chemical Engineering Department, Polytechnique Montréal, Montréal, QC H3C 3A7, Canada, abdellah.ajji@polymtl.ca

[7] Department of Surgery, McGill University, Montréal, QC H3G 1A4, Canada; derek.rosenzweig@mcgill.ca;

[8] Injury, Repair and Recovery Program, Research Institute of McGill University Health Centre, Montréal, QC H3H 2R9, Canada

* Co-senior authors, equal authorship and corresponding authors

The article is published in journal Sensors in April 2022

5.1 Abstract

Spheroids have become an essential tool in preclinical cancer research. The uniformity of spheroids is a critical parameter in drug test results. Spheroids form by self-assembly of cells. Hence, the control of homogeneity of spheroids in terms of size, shape, and density is challenging. We have developed surface-optimized PDMS biochip platforms for uniform spheroid formation on-chip. These biochips were surface modified with 10% bovine serum albumin (BSA) to effectively suppress cell adhesion on the PDMS surface. These surface optimized platforms facilitate cells self-aggregations to produce homogenous non-scaffold-based spheroids. We have produced uniform spheroids on these biochips using six different established human cell lines and a co-culture model. Here, we have observed that the concentration of the BSA is important in blocking cell adhesion to the PDMS surfaces. Biochips treated with 3% BSA demonstrated cell repellent properties similar to the bare PDMS surfaces. This work highlights the importance of surface modification on spheroid production on PDMS-based microfluidic devices.

Keywords: microfluidic, 3D cell culture, spheroid, surface modification, PDMS, cancer

5.2 Introduction

Cancer is among the top causes of death in developed countries. According to the statistics Canada [293], cancer causes over 30% of the total deaths in Canada annually. Major issues for successfully treating cancer include early diagnosis and proper radio-, chemo-, and/or surgical therapy. Chemotherapy has long stood as the adjuvant for radiation and surgical approaches; however, not all cancer types or patients respond to chemotherapy. One reason for this can be linked-to methods used for developing the chemotherapies, which rely heavily on *in vitro* two-dimensional cell culture and animal models which do not recapitulate the physiological human tumor microenvironment. Spheroids, tumoroids, and tumorospheres have been developed compact and spherical three-dimensional (3D) cell agglomerations widely used advanced in preclinical oncology *in vitro* models [11, 12, 209]. Hence, loose cell aggregates that easily detach or other forms of spatial cells aggregations should not be considered spheroids since the compactness and the spherical geometry of spheroids are the essential characteristics giving them

in vivo-like tumor features to make them more reliable tools in cancer research and drug safety assessment [10, 200, 209].

Focusing on spheroids, various techniques have been used for their formation with the same principle in which adhesive forces between cells are more prominent than cell-substrate adhesion [13, 209]. Producing uniform and homogenous spheroids in terms of size, shape, and compactness level has proved to be challenging using conventional spheroid formation methods such as liquid overlay technique (LOT) [13, 211], hanging drop method [210], spinner flasks [214] and stirred-tanks [215]. Recent advances in microengineering and microfabrication aim to address this limitation by developing microfluidic cell culture systems to generate more uniform, reproducible spheroids by providing better control over the cellular microenvironment [3, 6]. These devices are particularly useful for capturing small numbers of circulating tumor cells from patient liquid biopsies[294].However, most of the developed platforms only rely on the design of the channels and cell trapping chambers geometries to effectively direct cell aggregations [21, 226, 257, 295]. Surface engineering has become more popular in the past decades due to the importance of substrate surface properties to alter cellular responses (e.g. cell adhesion) [222, 227]. However, there remains ample room for surface optimization toward spheroid-on-a-chip technology. PDMS has a long history of use in microfluidic biochip platforms [3, 216] The hydrophobic nature of the PDMS [3], which is associated with the methyl groups present in the PDMS structure [245, 296], leads to protein adsorption and consequently cell adhesion to the PDMS surface is problematic specifically in the cell culture-based platforms [3, 216]. Therefore, the optimal surface engineering approach to render PDMS more hydrophilic remains to be determined for tumor-on-a-chip studies and drug screening [3, 136, 202, 258, 259].

We previously designed a PDMS-based tumor-on-a-chip model for capturing tumor cells and generating uniform spheroids [238]. We observed that 10% BSA can render PDMS surface hydrophilic and block adhesive properties, leading to higher cell-cell interactions compared to cell-substrate interactions. This resulted in homogenous spheroid production from MDA-MB-231 breast cancer cells conducive to future co-culture experiments and therapeutic screening. The objective of the present study was to expand the use of the microfluidic platform to multiple tumor cell types in an effort to broaden the scope of therapeutic screening. In this work, the

impact of surface modification of PDMS on the uniform and homogenous spheroid production from several tumor cell lines and the co-culture model of tumor-stromal cells has been studied.

5.3 Materials and methods

5.3.1 Fabrication and surface treatment of the microfluidic devices

5.3.1.1 Fabrication of microfluidic biochip to produce spheroids

The general design of the channel is similar to our previous work which is adapted from the design developed by Astolfi et al. [33] In this work, the shape of the micro-wells was modified to the cylindrical form instead of the cube shape to prevent sticking the cells to the corners of the micro-wells and promote spheroid formation on the device (Figure 5.1). This device is composed of two PDMS layers. The bottom layer of the device consists of two open channels with 840 μm × 840 μm wide square cross-sections. Each channel is containing five 840 μm in diameter circle-bottom micro-wells of 756 μm in height. The top layer PDMS has 3mm diameter inlet and outlet holes bonded with Plasma Oxygen to the bottom layer as described before. 3D-printed molds (HTM 140 resin, EnvisionTEC GmbH, Gladbeck, Germany) have been kindly printed by Prof.D.Juncker's lab, Biomedical engineering department, McGill University, using a stereolithography-based printer (Perfactory MicroEDU, EnvisionTEC Inc., Germany).

To obtain microfluidic devices from the 3D-printed mold, we have made PDMS replicas by soft lithography. To prevent sticking of the PDMS to the resin mold, we have pre-treated molds with a silicone spray (Ease Release 200®, Mann Formulated Products, USA) prior to replication of PDMS. To make PDMS replicas, as described before[238], elastomer base and curing agent (Sylgard 184 polydimethylsiloxane elastomer kit, Dow Corning, Midland, USA) were mixed properly in a 10:1 ratio. The mixture then was degassed for about 1 hour and poured into the 3D-printed mold while placed in a petri dish. PDMS replicas were cured for 2 hours in a 65 °C oven and then peeled off from the mold. Due to the presence of the silicone spray residues, the first PDMS replicas from each mold were discarded and subsequent replicas were used to fabricate microfluidic devices. The two PDMS layers have bonded together to form closed microfluidic devices following surface treatment with oxygen plasma at Prof.M.Wertherimer's lab, Engineering Physics department, Polytechnique Montréal. An oxygen gas (air liquide, alphagaz

1, 99.999% purity) was set at a flow rate of 20 sccm (standard cubic centimeters) controlled by a mass flow controller (MKS 247c channel readout + MKS 1259B-00100RV (0-100 sccm). The pressure in the chamber (cylindrical with a 9" diameter and 1.25"height) was set at 600 mTorr (80 Pa) and fixed using a butterfly valve during the process. The plasma was initiated by radiofrequency plasma at 13.56 MHz (The power source: ENI model HF-300 + impedance matching unit, plasma therm AMNS 3000-E) and the applied power was set at 20 Watts, with a plasma exposure time of 20 seconds.

5.3.1.2 Surface treatment of PDMS biochips

Before introducing the cells to the devices, by using 99.9% ethanol (Sigma-Aldrich) microfluidic channels were sterilized and the air bubbles were removed from the channels. In order to reduce cell adhesion to the PDMS surfaces and promote the spheroid formation, we have performed surface coating with BSA. BSA (Sigma-Aldrich) solutions in two different concentrations of 3% w/v and 10% w/v in sterile phosphate buffered saline (PBS, Sigma Aldrich) have prepared [238] and were sterilized by filtration through a 0.2 μm filter (Millipore Sigma). The microfluidic channels were flushed out 3-4 times with the BSA solutions to remove the ethanol residual.

Then, by incubation of freshly prepared BSA solutions with biochips, their surfaces were modified to assess spheroid formation on-chip. One group of biochips was surface treated with 3% BSA, and, another group of biochips was surface treated with 10% BSA to assess the impact of surface treatment on spheroid production. Only 10% BSA was used for co-culture model assays. All the devices were incubated overnight in the incubator (37 °C, 5% CO 2, 95% ambient air) right after cell seeding process.

5.3.1.3 Cell culture and spheroid formation on-chip

Six different cell lines have been used in this study: The epithelial breast cancer cell line MDA-MB231 (Green-fluorescent protein, GFP), stromal connective tissue cells including IRM-90 mCherry Fibroblasts (Red-fluorescent protein, RFP), Derivative subline of human prostate cancer LNCaP-derived C4-2B cells, the human non-small lung adenocarcinoma cell line H1299, human lung carcinoma epithelial cell line A549 and Human glioblastoma cell line U251. MDA-MB231,

IRM-90, and C4-2B were kindly provided by the laboratory of Prof.M. Park at McGill University. H1299 and A549 were generously provided by the laboratory of Prof.M.Lavertu at Polytechnique Montréal. U251cell line was a generous gift from the laboratory of Dr.R.J.Diaz at The Montréal Neurological Institute-Hospital, McGill University. C4-2B, H1299, A549, and U251 cells were fluorescently labeled with cell-labeling solution (Vybrant Dio, V22886; Molecular Probes, Invitrogen) in accordance with the manufacturer's protocol.

H1299 and C4-2B cells were cultured in RPMI-1640 medium supplemented with 10% v/v fetal bovine serum (FBS) and 1% v/v penicillin/streptomycin (PS). All the other cell lines were cultured in high-glucose Dulbecco's Modified Eagle's Medium (DMEM) supplemented as above. (All products from Gibco, Thermofisher). All the cell lines (less than 5 passages) were seeded in T-75 flasks (Corning Inc., New York, USA) at the density of 1.5×10^{6} cells per flask and placed in the incubator at 37 °C, 5% CO 2 and 95% relative humidity (RH). After reaching 80%–90% confluence, cells were washed two times with sterile phosphate buffered saline (PBS, Gibco, Thermofisher), and trypsinized with 0.25% Trypsin-EDTA solution (Gibco, Thermofisher. Then supplemented fresh culture medium (Gibco, Thermofisher) was added to the cell suspensions and centrifuged for 5 min at 1500 rpm to collect the cells. Prior to cell seeding, microfluidic channels were rinsed properly with sterile PBS (Gibco, Thermofisher) three times to clean the channels from the BSA residues, then the fluid within the channels was replaced with a fresh supplemented culture medium. Then, cell suspensions with the concentration of 1×10^{6} cells/mL were injected into the microfluidic channels inlets by using a micropipette (P200) and at the same time, 100 µl of the medium were removed from the channel's outlet. Consequently, the cell suspension was pipetted into the outlet, and 100 µl of cell suspension inside the channel was removed from the inlet. To provide uniform and homogenous cell distribution across the channels, we have repeated this process on both sides (inlet and outlet) of the channels three times. Following the cell seeding process, microfluidic devices were put in the incubator. The culture medium was refreshed every 24 hours using a micropipette (P200).

5.3.2 On-chip observation of spheroid formation and growth

Using Epifluorescence inverted microscope (Axio Observer.Z1, Zeiss, Oberkochen, Germany) and sCMOS camera (LaVision, Göttingen, Germany) and the objective lens EC Plan-Neofluar 5x

/ 0.15 Spheroids formation and growth were imaged directly through the thin PDMS layer for the duration of 7 days. The size of the spheroids, their compactness, and their spherical geometry was quantitated on day 1, 3, and 7 using Image J software.

5.3.3 Image J and data analysis

The images of the spheroids which were recorded as explained above have been used for analysis with Image J (National Institute of Health, Maryland, USA) to assess spheroid growth. All images had a high resolution of more than 1900 dpi. The brightness level of fluorescent images was assessed by a digit value from zero to a maximum of 255. The average mean diameter of each spheroid can be written as D m= (D max+D min)/2 from 10 repeats. We have reported the average size of the spheroids as mean diameter ± standard deviation. We have defined the circularity of the spheroids by the Circularity= 100 × (D min/D max around a single sphere). Brightness level ratio is equal to BLR= (Brightness level/255) × 100. We have used fluorescent signals as the function of increasing the number of cells in the spheroids. All Data have been reported as the mean ± SE of minimum of three independent tests. All error bars in figures indicate SE. One representative experiment is presented where the same trends were seen in multiple trials.

5.3.4 Assessment of multicellular spheroid co-culture model on-chip

We have assessed spheroid morphology and growth in co-culture models. 3D tumor model consisting of a co-culture of A549 cells and IRM-90 cells (Ratio of 1:1, 1:2, 2:1) have been used to form hetero-type MCTSs in comparison with a monoculture of either A549 or IRM-90. The initial cell suspension had a concentration of 1×10^{6} cells/mL in all the experiments. Process of cell seeding and spheroid formation on-chip repeated as described above for mono-type MCTSs.

5.3.5 Adhesion and morphology assays on biochips treated with 3% BSA

As a comparison and a control model for spheroid formation assays on PDMS biochips which were surface treated with 10% BSA, spheroid formation and cell adhesion were assessed on biochip treated with 3% BSA.

5.3.6 Statistical analysis

All experiments were repeated in three independent biological replicates (n=3) in order to evaluate the reproducibility of the data. For each experiment, a minimum of 10 spheroids were analyzed per condition. Statistical analyses were performed using Microsoft Excel 2016 (Version 1803, Build 9126.2259). All data is represented as mean ± standard error of the mean. One-way ANOVA was performed to assess statistical significance between means, with post-hoc Tukey tests for comparison between means. A $p \leq 0.05$ was considered statistically significant.

5.4 Results and discussion

To generate compact and uniform spheroids adhesive forces between cells and their substrate need to be weaker than adhesive forces between the cells. Our previous work [238] has demonstrated the impact of surface properties of the PDMS in uniform spheroid formation on-chip. Our observations have indicated that PDMS biochips surface modified with 10% BSA provide optimal cell repellent properties characterized by greater surface wettability (moderate contact angle between 70° to 60°) when compared with the bare PDMS (contact angle ≥ 100°). The PDMS surface modification with 10% BSA has illustrated a desirable surface microstructure upon which MDA-MB 231 cells reproducibly do not tend to adhere. Hence, PDMS surface treatment with 10% BSA has promoted cell self-aggregations and homogenous spheroid formation on-chip. On the other hand, the biochips that were surface treated with 3% BSA have demonstrated lower surface wettability (contact angle ≥ 90°) when compared with 10% BSA upon which MDA-MB 231 cells tend to adhere to the surface. The microstructure of PDMS surfaces treated with 3% BSA was less smooth with less surface coverage when compared with PDMS surfaces treated with the 10% BSA. Therefore, the quantity and quality of cellular self-aggregations and spheroid formation on devices drastically were reduced. We have previously studied the impact of PDMS surface modifications on spheroid formation using MDA-MB 231 cells. Since cells' adhesive interactions with the surfaces are complicated due to the different cells' surface receptors and various surface properties [297-299], in the present study, we have investigated the impact of our surface-optimized biochips treated with 10% BSA on the uniform and homogenous spheroid production from several cell lines.

5.4.1 Design and fabrication of the microfluidic biochip

The physicochemical properties of the microfluidic biochips play a crucial role in spheroid formation on devices[238]. In the present study, we have optimized the design of the micro-wells to improve the chance of spheroid formation on our surface-treated device. We have developed a design[238], adapted from Astolfi et al. [33] [226]. We have observed that the cube shape of the wells could increase the chance of cell adhesion to the corners of the cell trapping micro-wells and could affect the quality of spheroid formation by increasing the chance of producing lobular shapes and non-spherical cell aggregations. To overcome this limitation, in this work we have modified the form of the cell trapping micro-wells to cylindrical shapes which have resulted in more effective cell aggregation and centered position of resulting cell clusters (Figure 5.1).

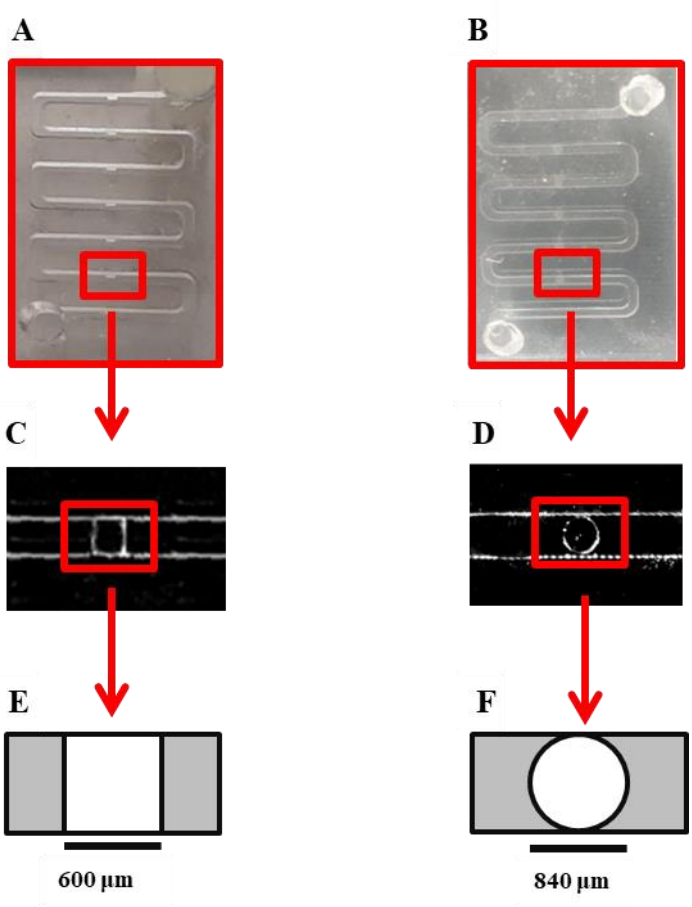

Figure 5.1 Microscopic image and schematic of the cube shape cell trapping microwell

A) Image of the channel in previous design with cube shape cell trapping chamber Each channel has 78 mm length with a cross-section of 600 µm ×600 µm with five cube shape cell trapping chambers for cell sedimentation and spheroid formation, B) Image of the modified design used in this work with cylindrical shape cell trapping chambers. Each channel has a 109.2 mm length with a cross-section of 840 µm ×840 µm with five cylindrical cell trapping chambers for cell sedimentation and spheroid formation, C) Top view of microscopic image of cell trapping chamber of the previous design, size of the chamber is 600 µm×600 µm and the height of the chamber is 540 µm D) Top view microscopic image of modified cylindrical shape cell trapping chamber in the present study, the radius of the chamber is 840 µm and the height of the chamber is 756 µm E) Schematic top view of cube shape cell trapping chamber in previous design, F)Schematic top view of cylindrical shape cell trapping chamber in the current design used in this work

5.4.2 Spheroid formation on model surfaces treated with 3% and 10% BSA

The uniform spheroid formation on surface-modified PDMS biochips has been studied. [238][238] [238]We have observed that biochips treated with 10% BSA solution boosts a greater number of spheroid formation on-chip and increase the quality of spheroids for various cell lines studied here, in a reproducible manner.

The principle of spheroid formation is the same for all the cell lines studied in this work. After micro-channels were filled with the cell suspension, cells began to sediment into the cylindrical micro-wells. When the surfaces of the channels are pre-treated with 10% BSA, cell-cell adhesive forces become dominant over cell-substrate adhesive forces. Hence, during the first 24 hours of incubation, cell aggregations were occurred for all the cell lines and the co-culture models, except for C4-2B cells spheroid formation did not observe during the first 72 hours of culture. After 24 hours, non-aggregated and aggregated cells inside the channels were rinsed with a fresh medium. During the second day of incubation (48 hours post-seeding), growth and spheroid compaction were observed for all the cell lines and co-culture models, except for C4-2B cells. For C4-2B cells, spherical cell agglomerations were observed on day 3 (72 hours) post-seeding. All the cell lines were successfully made spheroid on biochips pre-coated with 10% BSA and spheroid growth was assessed over a period of seven days (Figure 5.2).

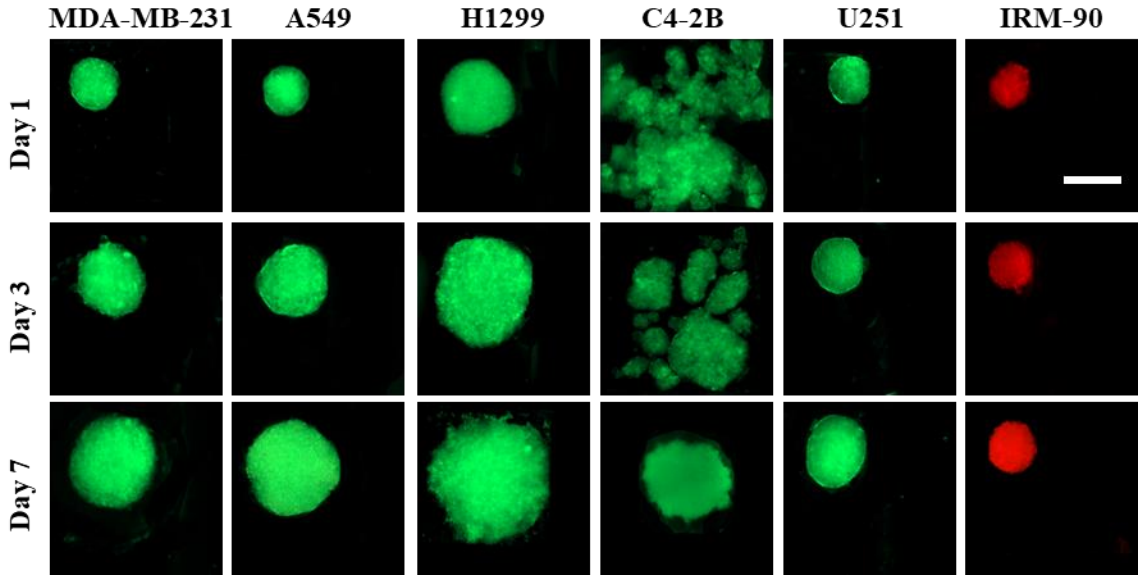

Figure 5.2 Spheroid formation on PDMS biochips pre-coated with 10% BSA

Fluorescent images of spheroids captured on days 1, 3, and 7 showed that each cell line had its own growth rate in 3D model. All cell lines studied here were able to form spheroid during 7 days of culture. The red color is due to red-fluorescent protein (RFP) in IRM-90 cells and the green color is due to green-fluorescent protein (GFP) in MDA-MB-231 cells. For other cell lines, green color is due to fluorescently labeled with cell-labeling solution Vybrant Dio V22886. Scale bars: 200 μm

Laminar flow in microfluidic channels provided protection of spheroids from the shear stress caused by exchange of medium, while the diffusion-based mass exchange is quick enough to effectively remove cellular waste and provide nutrition for spheroids [33, 226, 300]. We have observed that the growth pattern is different in 3D for different cell lines which leads to different sizes of spheroids on day 7 post-seeding while the initial cell concentration is the same (1×10^{6} cells/mL) in all groups. As a control model, we have studied the spheroid formation on biochips pre-coated with 3% BSA (Figure 5.3). When the cell suspension is introduced to the channels, due to the higher protein adsorption to the surface, cell-substrate interactions are greater than cell-cell interactions. This leads to cell adhesion to the surface depending on the cell type which can influence the quality of cells' self-aggregations and spheroid production.

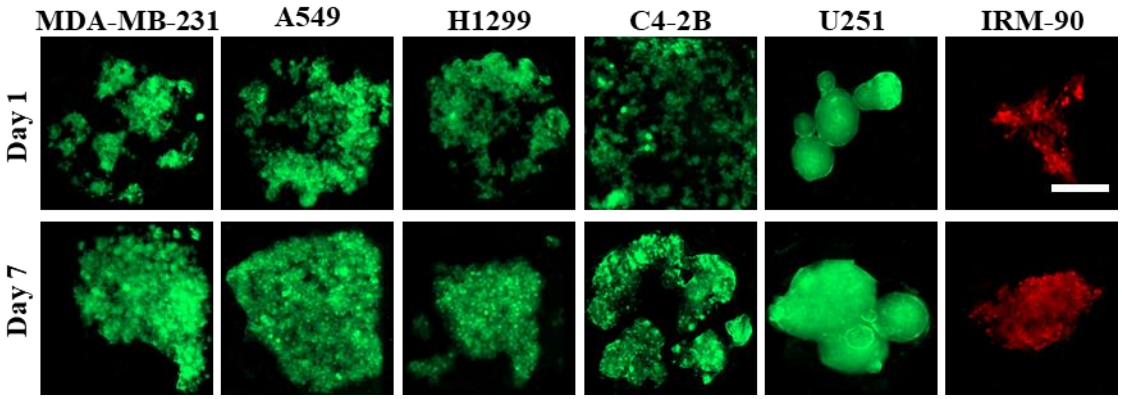

Figure 5.3 Culture of different cell lines on PDMS biochips pre-coated with 3% BSA

Cell adhesion pattern to the surface is different and it depends on the cell type. In some cell lines like C4-2B cell-substrate interactions are dominant over cell-cell interactions, therefore they cannot form compact cell clusters on surfaces treated with 3% BSA. On the other hand, some cell lines like U251 demonstrated to have greater cell-cell interactions when compared with cell-substrate interactions, therefore this leads to the formation of more compact cell clusters. The red color is due to red-fluorescent protein (RFP) in IRM-90 cells and the green color is due to green-fluorescent protein (GFP) in MDA-MB-231 cells. For other cell lines, the green color is due to fluorescently labeled with cell-labeling solution Vybrant Dio V22886. Scale bars: 200 μm

5.4.3 Spheroid characterization

Routine monitoring of the spheroids was performed for 7 days. Fluorescent images of the spheroids were recorded directly from the thin PDMS layers. By using Image J software, morphometric parameters including minimum and maximum diameter, spheroid size, BLR, and circularity were obtained. Various parameters (e.g. flow rate, cell density during seeding, duration of cell seeding) modulate spheroid size [209] on the same design/size of channels/chambers of a microfluidic platform. Here we have studied the influence of cell type in the spheroid size, growth and spherical shape on our optimized design treated with 10% BSA.

Figure 5.4 shows the seven day growth pattern of the spheroids cultured on biochips pre-coated with 10% BSA.

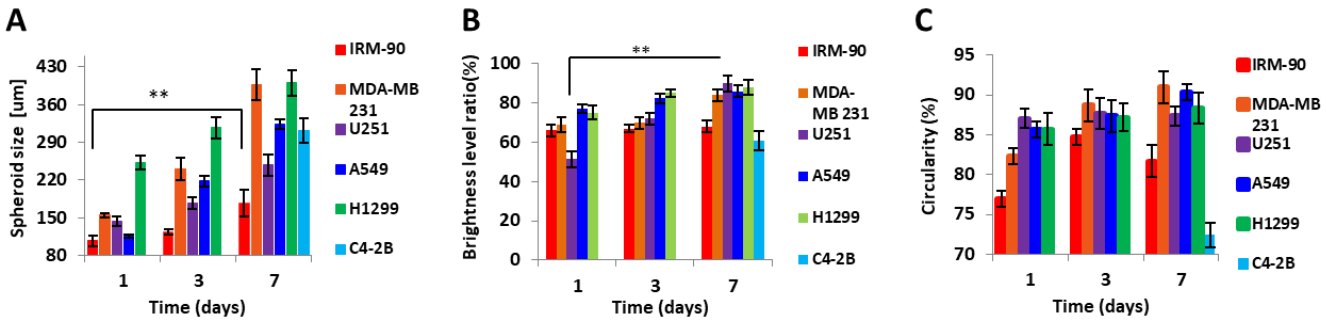

Cell line	Size	BRL
IRM-90 D1 Vs. D7	**	NS
MDA-MB 231 D1 Vs. D7	***	NS
U251 D1 Vs. D7	***	**
A549 D1 Vs. D7	***	*
H1299 D1 Vs. D7	***	*

Figure 5.4 Growth pattern for spheroid production on biochip pre-coated with 10% BSA

(A) Spheroid size over the seven days of culture. Spheroid size varied and was significantly increased on day 7 compared to day 1 for all cell lines (D1 Vs. D7 **$p<0.001$ and ***$p<0.0001$). C4-2B cell line only was able to produce spheroid after day 3 of culture, we only saw the size on day 7 accordingly. (B) BRL for U251, A549, and H1299 significantly increased on day 7 compared to day 1 (D1 Vs. D7 *$p<0.05$ and **$p<0.001$) and for IRM-90 and MDA-MB 231 varied non significantly (NS=non-significant). (C) Circularity is representative of the spherical or circular shape of spheroids. Circularity increased non-significantly on day 7 compared to day 1 for all of the cell lines. C4-2B cell line only was able to produce spheroid after day 3 of culture, as previously mentioned. All assays were performed as triplicates per trial in three independent experiments. (Error bars represent ± SE, n=3)

Here, we have observed that contrary to 2D cultures which grow exponentially, spheroids were characterized by an exponential growth phase followed by a decrease in growth with an increase in non-growth rate. According to our observations duration of each phase is depending on the type of the cell line.

5.4.4 Study of co-culture multicellular spheroids

Spheroids can also be formed from a co-culture of tumor cells with stromal cells [11, 209]. These co-culture models are advantageous for cancer research as they better mimic the complexity of the tumor microenvironment [11, 201].

We have developed scaffold-free multicellular spheroids consisting of tumor cells (A549) and fibroblast (IRM-90) to provide the crosstalk between tumor and stroma cells.

Figure 5.5 shows the images of the co-culture models for three ratios of tumor-stromal cells including 1:1, 1:2, and 2:1 for the total number of 1×10^{6} cells/mL in each experiment.

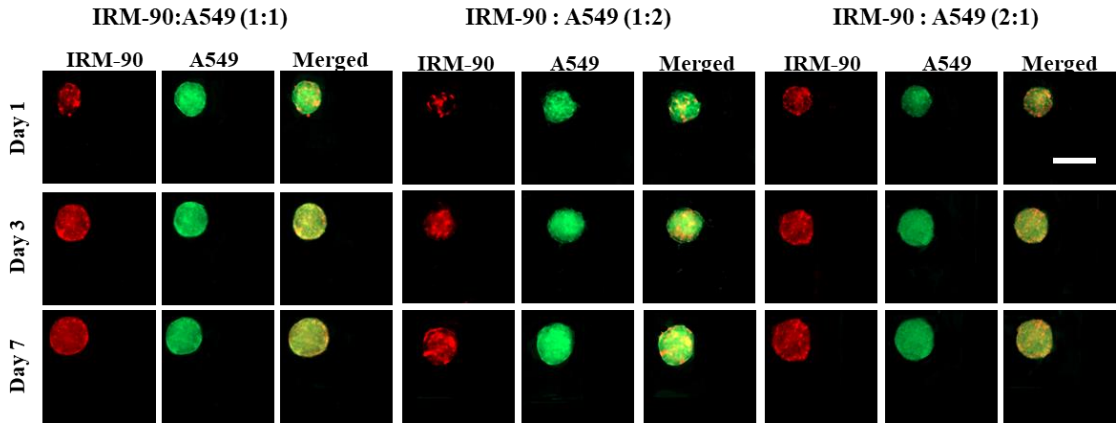

Figure 5.5 Image of co-culture A549 and IRM-90 cells with different ratios between the two cell lines

The total initial cell concentration is 1×10 6 cells/mL for all experiments. Our observations demonstrated that there are no remarkable differences in terms of the growth pattern including the size and the shape of the spheroids by varying the ratio between tumor and stromal cells. The red color is due to red-fluorescent protein (RFP) in IRM-90 cells and the green color is due to fluorescently labeled with cell-labeling solution Vybrant Dio V22886 for A549 cells. Scale bars: 200 μm

We have studied the effect of changes in the ratio of tumor cells and stromal cells in the size and growth pattern of the co-culture models. In terms of spheroid size, circular shape, and the chance

of spheroid formation on-chip no significant changes were observed by changing the ratio between the tumor and stromal cells in this study (Figure 5.6).

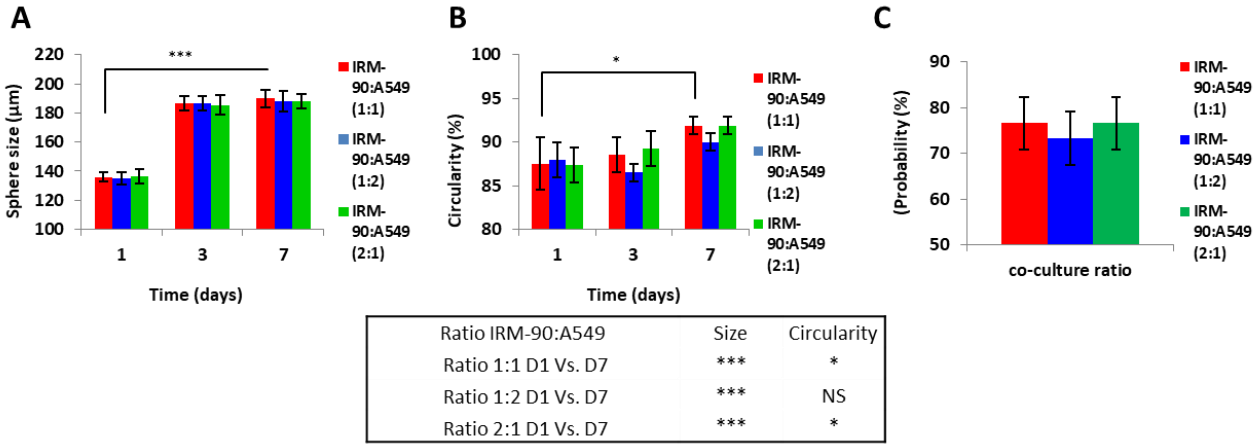

Ratio IRM-90:A549	Size	Circularity
Ratio 1:1 D1 Vs. D7	***	*
Ratio 1:2 D1 Vs. D7	***	NS
Ratio 2:1 D1 Vs. D7	***	*

Figure 5.6 MCTSs produced from different ratio of tumor (A549) and stromal (IRM-90) cells (A) Spheroid size in day 1, 3 and 7 of culture. In all three ratio between tumor and stromal cells, size of the spheroids significantly changes in day 7 when compared to day 1 (D1 Vs. D7 ***$p<0.0001$). However, spheroids from different ratio of tumor-stromal cells (1:1, 1:2, and 2:1) on day 7 do not have statistically significant difference in size. (B) Circularity of spheroids for stromal-tumor ratio of IRM-90:A549 1:1 and IRM-90:A549 2:1 is increased significantly on day 7 when compared to day 1 (D1 Vs, D7 *$p<0.05$) and for IRM-90:A549 1:2 is not statistically significant (non-significant= NS). However spheroids from different ratio of tumor-stromal cells (1:1, 1:2 and 2:1) on day 7 do not have statistically significant difference in terms of circularity. (C) Probability of spheroid formation on-chip. By changing the ratio of tumor and stromal cells probability of spheroid production does not change statistically significant. Total number of cells is 1×10^{6} cells/mL for all three ratio. $p<0.05$ is considered statistically significant. All assays were performed as triplicates per trial in three independent experiments. (Error bars represent ± SE, n=3)

According to our data presented in Figure 5.6 since remarkable differences in terms of size, geometry, and the chance of spheroid formation did not observe by changing the ratio between A549 and IRM-90 cells in our experiments, we have chosen the ratio of 1:1 between tumor cells

(A549) and fibroblasts (IRM-90) for further experiments. In this regard, we have studied the effect of the presence of the stromal cells in the tumor microenvironment on spheroid size, morphology, and chance of spheroid formation.

Spheroid size on day 7 of culture had a significant difference when comparing mono-type MCTSs with hetero-type MCTSs which are consisting stromal cells in their microenvironment (***p<0.0001). However, the circularity of the mono-type and hetero-type MCTSs did not show a statistically significant difference. Moreover, the chance of spheroid formation on the device by adding the stromal cells into the tumor microenvironment significantly increased (**p<0.001) (Figure 5.7). We have considered the images from spheroids having the ratio of 1:1 between the tumor and stromal cells as the co-culture model in our calculations.

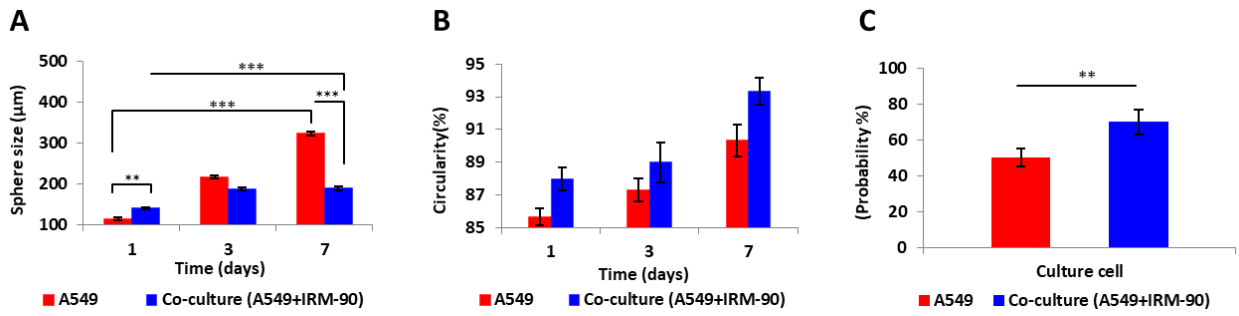

Figure 5.7 Comparing mono-type MCTSs with hetero-type MCTSs

Mono-type MCTSs were produced from tumor cells (A549) and hetero-type MCTSs were produced from tumor: stromal (A549:IRM-90, ratio 1:1) cells (A) Spheroid size over 7 days of culture changes. In both conditions (mono-type and hetero-type MCTSs) size of the spheroids on day 7 was significantly increased when compared to day 1 (D1 Vs. D7 ***p<0.0001). Spheroid size on day 1 was significantly different when comparing mono-type with hetero-type MCTSs (**p<0.001). The size of mono-type MCTSs compared with hetero-type MCTSs on day 7 was significantly different (***p<0.0001). The size of spheroids in the co-culture model did not change significantly after day 3 of culture while in mono-culture spheroids size increased significantly on day 7 when compared to day 3 (D3 Vs. D7 ***p<0.0001). (B) Circularity of the spheroids is not significantly different in mono-type MCTSs when compared to the co-culture model. (C)Probability of spheroid formation on-chip is greater in the co-culture model when

compared with the monotype MCTSs model (**p<0.001). The total number of cells is 1×10^{6} cells/mL for all three ratios. p<0.05 is considered statistically significant. High-resolution images of 10 spheroids in each independent experiment have been considered for calculations per each condition. All assays were performed as triplicates per trial in three independent experiments. (Error bars represent ± SE, n=3)

It is proven that the presence of the stromal cells in the tumor microenvironment increases the physiological relevance of the spheroid models and influences the cellular responses to therapeutic agents [11, 13]. Our observation demonstrated that the presence of the fibroblasts cells (IRM-90) in the tumor microenvironement provides dynamic interactions and strong adhesion between tumor cells and stromal cells.. This can explain why we do not see a remarkable change in the size of the heterotype MCTSs after day three while they proliferate and become more compact with uniform and spherical shapes.

5.5 Conclusion

Spheroid size and morphology influence the robustness of *in vitro* assays [209]. Therefore, the generation of homogenous spheroids in terms of size, compactness, and spherical morphology is important for reliable drug testing [12, 13, 209]. The relationship between surface properties and cell adhesion is complex, and it depends on various factors including but not limited to surface wettability, charge, morphology, roughness, and also to the type of the cells and cell's surface receptors [23, 26, 247, 289]. In this work, we have used 10% BSA to develop surface-optimized biochips with having optimal cell repellent properties. We have studied the effect of surface modification on the uniformity of spheroid production from several cell lines.

The microenvironment, including multicellularity, can drastically influence the formation of spheroids [11, 199]. Recapitulating this microenvironment is highly important for assessing physiological responses to therapy [13]. We have observed that cell behavior is deeply influenced by their cellular microenvironment and the surface properties of the substrate on which they grow.

Here, we conclude that surface treatment with 10% BSA is a simple, effective and reproducible method for surface modification of PDMS-based biochips to promote the formation of scaffold-free spheroid models on-chip for various cell lines studied in this work. This platform holds the possibility to be used as a tool for the assessment of the efficacy of various therapeutic strategies *in vitro*. A fundamental understanding of interactions between cell-surface is particularly important for directed control of cell function for biomedical applications. Future work will explore capturing patient-derived circulating tumor cells from liquid biopsies, as well as assess the impact of spheroid formation from patient-derived solid-tumor and stromal cells. The continued research effort in the field of biomaterials and surface engineering in microfluidic platforms will help to create desirable surfaces for lab-on-a-chip and organ-on-a-chip applications.

5.6 Author contributions

Conceptualization: N.A., R.A., M.S., D.H.R. and A.A.; Data curation: N.A.; Formal analysis: N.A. and R.A.; Funding acquisition: D.H.R., M.S. and A.A.; Investigation: N.A.; Methods: N.A., R.A., D.H.R. and A.A.; Project administration: M.S., D.H.R. and A.A.; Resources: M.S., D.H.R. and A.A.; Supervision: M.S., D.H.R. and A.A.; Validation: N.A., R.A., M.S., D.H.R. and A.A.; Visualization: N.A.; Writing original draft: N.A.; Writing—review and editing: N.A., R.A., M.S., D.H.R. and A.A.; N.A. should considered the first author; D.H.R. and A.A. contributed equally to this work and should considered co-corresponding authors. All authors have read and agreed to the published version of the manuscript.

5.7 Funding

This research was funded by the Natural Sciences and Engineering Research Council (NSERC) of Canada discovery grants (A.A. and M.S.) and Fonds de Recherche du Quebec Sante (FRQS) Junior 2 Research Scholar Award (D.H.R.).

5.8 Acknowledgements

The authors gratefully acknowledge funding support from the Natural Sciences and Engineering Research Council (NSERC) of Canada discovery grants (A.A and M.S) and Fonds de Recherche

du Quebec Sante (FRQS) Junior 2 Research Scholar Award (D.H.R.). The authors also gratefully acknowledge Prof.Morag Park (McGill University), Prof.R.J.Diaz (McGill University) and Prof.M.Lavertu (Polytechnique Montréal) for kindly providing the cell lines used in this study and Prof.M.Wertheimer (Polytechnique Montréal) and Prof.D.Juncker's Laboratory (McGill University) for kindly providing the access to plasma oxygen equipment and support to fabricate the molds, respectively. N.A gratefully acknowledges the scholarship from Fondation et Alumni de Polytechnique Montréal donated by Royal Bank of Canada (RBC).

5.9 Conflicts of Interest

The authors declare no conflict of interest.

CHAPTER 6 ARTICLE 3: UNIFORM TUMOR SPHEROIDS ON SURFACE OPTIMIZED MICROFLUIDIC BIOCHIP FOR REPRODUCIBLE DRUG SCREENING AND PERSONALIZED MEDICINE

Neda Azizipour [1], Rahi Avazpour[2], Michael H. Weber [3, 4], Mohamad Sawan[5, 6, 7], Abdellah Ajji [5,8 *] and Derek H.Rosenzweig [4, 9 *]

[1] Institut de génie biomédical, Polytechnique Montréal, Montréal, QC H3C 3A7, Canada; neda.azizipour@polymtl.ca

[2] Department of Chemical Engineering, Polytechnique Montréal, Montréal, QC H3C 3A7, Canada; Info@recutex.ca

[3] Montréal General Hospital, Division of Orthopedic Surgery, McGill University C10.148.6, 1650 Cedar Ave, Montréal, QC H3G 1A4, Canada

[4]Injury, Repair and Recovery Program, Research Institute of McGill University Health Centre, Montréal, QC H3H 2R9, Canada

[5]Institut de génie biomédical, Polytechnique Montréal, Montréal, QC H3C 3A7, Canada;

[6] Polystim Neurotech Laboratory, Electrical Engineering Department, Polytechnique Montréal, QC H3T 1J4, Canada;

[7] CenBRAIN Laboratory, School of Engineering, Westlake University, and Westlake Institute for Advanced Study, Hangzhou 310024, China, sawan@westlake.edu.cn

[8]NSERC-Industry Chair, CREPEC, Chemical Engineering Department, Polytechnique Montréal, Montréal, QC H3C 3A7, Canada, abdellah.ajji@polymtl.ca

[9] Department of Orthopaedic Surgery, McGill University, Montréal, QC H3G 1A4, Canada; derek.rosenzweig@mcgill.ca;

* Co-senior authors, equal authorship and corresponding authors

The article is published in journal Micromachines in April 2022

6.1 Abstract

Spheroids are recognized for resembling the important characteristics of natural tumors in cancer research. However, the lack of controllability of the spheroid size, form, and density in conventional spheroid culture methods reduces the reproducibility and precision of bioassay results and the assessment of drug-dose responses in spheroids. Nonetheless, the accurate prediction of cellular responses to drug compounds is crucial for developing new efficient therapeutic agents and optimizing existing therapeutic strategies for personalized medicine. We have developed a surface optimized PDMS microfluidic biochip to produce uniform and homogenous multicellular spheroids in a reproducible manner. This platform is surface optimized with 10% bovine serum albumin (BSA) to provide cell repellent properties. Therefore, weak cell-surface interactions lead to promoting cell self-aggregations and produce compact and uniform spheroids. We have used lung cancer cell line (A549), a co-culture model of lung cancer cells (A549) with (primary human osteoblasts, and patient-derived spine metastases cells (BML, bone metastasis secondary to lung). We have observed that the behavior of cells cultured in three-dimensional (3D) spheroids within this biochip platform more closely reflects *in vivo* like cellular responses to chemotherapeutic drug, Doxorubicin, rather than on 24 well plates (two-dimensional (2D) model). It is also observed that the lung spheroid co-culture and patient-derived spheroids exhibit resistance to anti-cancer drugs more than the mono-culture spheroids. The repeatability of drug test results in this optimized platform is the hallmark of reproducibility of uniform spheroids on-chip. This surface-optimized biochip can be a reliable platform to generate homogenous and uniform spheroids to study and monitor tumor microenvironment and drug screening.

Keywords: spheroid-on-a-chip, spheroid, cancer, drug test, microfluidic, personalized medicine

6.2 Introduction

Lung cancer has been one of the leading causes of cancer death worldwide for several decades [301, 302]. Notwithstanding all efforts to develop new cancer therapies, the overall survival rate of patients with lung cancer is still very low [303, 304]. Most frequently patients with advanced lung cancer develop bone metastases during the course of their disease [305]. Although these patients have a relatively short survival time, they are likely to experience debilitating bone lesions and a significant reduction in their quality of life [305, 306]. One of the most challenging issues in cancer treatment is developing effective drugs in a timely manner [3]. Failure to develop novel therapies to tackle lung cancer has multiple reasons, but one of the most important reasons is the reliability of pre-clinical models to predict drug response and their side effects in humans [3, 35, 307], which explains in part why drug candidates fail to achieve clinical approval more often than they succeed.

Traditionally, established cancer cell lines in two-dimension (2D) monolayers on flat plastic substrates (e.g. Petri dishes) are used for the first phase of drug screening [3]. These culture models can not reflect many critical characteristics of an actual tumor [3, 35]. They often lack spatiotemporal chemical gradients [308], three-dimension (3D) cell-cell [309, 310] and cell-extracellular matrix (ECM) interactions [311] which are all essential to maintain cellular functions [3] and define cell phenotypes [195, 312]. 3D cell culture models have been developed over the past decades to avoid certain drawbacks of 2D culture models [3, 256], by bio-mimicking the 3D microenvironment of the tumor [35, 313], at least in part.

Multicellular tumor spheroids (MCTSs) stand out as the most widely used 3D cell culture models in oncology preclinical research [11, 314]. MCTSs have proven their power in drug response prediction by more accurately reproducing the key structures of solid tumors [201, 315, 316]. However, the uniformity in size and shape of the spheroids play a critical role in their responses to anti-cancer drugs [12, 13]. Therefore, it is important to produce *in vitro* platforms to reduce the heterogeneity of the spheroids for accurate drug testing. Various techniques have been developed for spheroid production including the hanging drop method, liquid overlay technique (LOT), spinner flasks, and stirred-tanks [3, 16, 257]. Advancements in microfluidics have led to the

development of numerous microfluidic biochip devices to generate spheroid-on-a-chip platforms using a small liquid volume of cell suspension, as a key advantage of microfluidics [3, 17, 317].

Spheroids' size, shape, and compactness level play a critical role in responses to drug compounds [10, 13]. However, one of the most common problems with spheroid culture is producing uniform size and shape spheroids [13]. Geometric design of the channels and cell trapping chambers play an important role in this regard [18, 226, 257]. However, the materials used for microfluidic fabrication and their surface characteristics (e.g. wettability, chemistry, roughness, etc.) also play a critical role in regulating cell responses to the surfaces [202, 227]. Accordingly, in the past years, surface engineering has attracted great attention in cell-based biomedical applications including microfluidic cell culture platforms [6, 22, 23, 262].

In our previous work [238], we have designed a surface-optimized PDMS spheroid-on-a-chip platform to capture tumor cells and produce uniform spheroids. We have used 10% BSA to block cell adhesion to the surface and promote cell aggregations to form homogenous spheroids. We have demonstrated the impact of surface modification of PDMS on the uniform and homogenous spheroid production on-chip [238]. In the present study, we have investigated the reproducibility of uniform spheroids formation on optimized biochips. We have used the repeatability of drug test on-chip as a hallmark of reproducibility and homogeneity of produced spheroids. Patient-derived cells were demonstrated to retain the heterogeneity and complexity of the original tumor [6, 318]. Therefore, in the present study we have investigated the capability of our surface-optimized biochip to capture tumor cells from the patient biopsies and produce uniform MCTSs from patient-derived bone metastasis secondary to lung (BML) cells. Lung cancer bone metastases involve complex communications between tumor cells and the bone microenvironment [6, 305]. Cross-talking between tumor cells and their surrounding microenvironment is important in cancer progression and drug resistance [309, 310]. [320, 321][6, 307] Hence, to mimic such a structure, a co-culture model of lung cancer cells (A549) and primary human osteoblasts was also developed on our optimized biochip. A 3D monotype MCTSs model of lung cancer cells (A549) was produced in this study to compare with patient-derived and co-culture spheroids. We have studied the efficacy of the anti-cancer drug, Doxorubicin (Dox) [319], on patient-derived MCTSs, MCTSs from lung cancer cell line A549, and a hetero-type MCTSs model (A549-primary human osteoblasts, 1:1). Here, we have

observed that hetero-type MCTSs and patient-derived MCTSs exhibited drug resistance to Dox more than the monotype MCTSs. In our model, we conclude that microscale interactions within sophisticated MCTSs made by patient-derived cells or hetero-type co-culture of cell lines strongly support its usefulness as a preclinical tumor model for drug screening and for studying interactions in the cancer microenvironment. To investigate the superiority of this 3D culture model in testing the therapeutic agents, we have compared the drug efficacy in the 3D MCTSs models with 2D culture models using the same cells cultured on 24 well plates. We have observed that drug resistance is significantly reduced in 2D culture models compared with 3D MCTSs. Our observations were in a positive correlation with a growing body of evidence conferred by various studies [3, 11, 217, 320] suggesting that 3D MCTSs models compared with 2D conventional culture more accurately replicate the tumor microenvironment and therefore cellular behavior in 3D will reflect their *in vivo* responses more relevantly.

6.3 Materials and methods

6.3.1 Fabrication and surface treatment of microfluidic biochip

Microfluidic biochips were made using polydimethylsiloxane (PDMS) (Sylgard 184 PDMS elastomer kit, Dow Corning, Midland, USA) as previously explained [238]. The biochips then were used for cell culture experiments 7 days or more post-fabrication. Right before starting cell culture on-chip, channels and chambers were sterilized and the air bubbles were removed by using 99.9% ethanol (Sigma-Aldrich). In order to decrease cell adhesion to the PDMS surfaces and increase uniformly sized spheroids, microfluidic channels were treated overnight in the incubator (37 °C, 5% CO2, 95% ambient air) with sterile 10% BSA (Sigma-Aldrich) solution in phosphate buffered saline (PBS, Sigma Aldrich) as previously reported.

6.3.2 2D Cell culture and on-chip spheroid formation

6.3.2.1 Preparation of cell lines and patient derived cells

We have used three types of the cell for the spheroid formation and 2D culture experiments: Human lung carcinoma epithelial cell line A549 was kindly provided by the laboratory of Prof.M.Lavertu at Polytechnique Montréal. Primary human osteoblasts and Patient-derived spine

metastases cells secondary to lung cancer (BML) were kindly provided by Dr.M.H.Weber's laboratory at the Research Institute of McGill University Health Centre (RI-MUHC). The ethics approval for patient sample collection is through McGill Scoliosis and Spine Group, RI MUCH REB Extracellular Matrix Protocol # 2020-5647. Resected metastatic spine tumors secondary to lung cancer were collected with consent from a patient undergoing surgery at the Montréal General Hospital. By washing tissue samples in PBS (Gibco, Thermofisher) and then cutting them into 5 mm × 5 mm sections samples were processed. Then samples were incubated at 37 ◦C overnight in a collagenase type II (Thermofisher, Gibco, Burlington, ON, Canada). Digested cells were strained in a 100 µM cell strainer and then pelleted for five minutes in a centrifuge at 300× g. Isolated cells consisting of a mixed population of bone metastasis-derived patient cells and bone cells were cultured in high-glucose Dulbecco's Modified Eagle's Medium (DMEM) (Gibco, Thermofisher) supplemented with 10% v/v fetal bovine serum (FBS) and 1% v/v penicillin/streptomycin (PS), 1% glutamax (Gibco, Thermofisher), and 1% fungizone (Gibco, Thermofisher) at 37 ◦C in a humidified atmosphere of 5% CO2.

Before processing spheroid formation on-chip, A549 cells and primary human osteoblasts (passage less than 3) were seeded in T-75 flasks containing DMEM (Corning Inc., New York, USA) supplemented with 10% v/v fetal bovine serum (FBS) and 1% v/v penicillin/streptomycin (PS) at the density of 1.5×10^{-6} cells per flask, then incubated in the incubator at 37 °C, 5% CO2 and 95% relative humidity. When they reached 80–90% confluence, cells were washed two times with PBS (Gibco, Thermofisher), and trypsinized with 0.25% Trypsin-EDTA solution (Gibco, Thermofisher). Then supplemented fresh culture medium (Gibco, Thermofisher) was added to the cell suspensions and centrifuged for 5 min at 1500 rpm to collect the cells.

6.3.2.2 Construction of MCTSs on the biochips

Prior to the cell seeding process, the channels were gently rinsed a minimum of three times with sterile PBS (Gibco, Thermofisher) to remove the BSA residues, and then the fluid within the channels was replaced with a fresh supplemented culture medium and warmed by placing them in a CO2 incubator. Then, the cell seeding process started by introducing a cell suspension (concentration of 1×10^{6} cells/mL) into the inlet of the microfluidic channel using a micropipette (P200) and removing 100 µl of the medium from the channel's outlet. Then the process was

repeated in the other direction by pipetting the cell suspension through the outlet and removing 100 µl from the inlet. By injecting and removing the cell suspension at the same time, we need to make sure that channels are filled with the suspension all the time (to prevent bubble formation inside the channels). For homogenous cell distribution across the channels, this process was repeated in both directions at least three times. Microfluidic devices were put in the incubator after the cell seeding process. Culture medium was refreshed every 24 hours using micropipette P200.

Three types of MCTSs formed on biochip for further experiments: A mono-type MCTSs model containing tumor cells A549, a co-culture of hetero-type MCTSs model containing A549, and primary human osteoblasts (1:1 ratio), and spheroids produced by patient-derived cells (BML). The cell concentration in cell suspension keeps to 1×10^{6} cells/mL in all three types of spheroids.

6.3.2.3 2D cell culture

Three types of cell suspensions mentioned above were seeded separately for the 2D culture in triplicate on 24 well plates (Falcon Tissue Culture 24 Well Plate, Thermofisher) with the initial cell seeding of 0.03×10^{6} cell/well in DMEM supplemented as mentioned above for spheroids.

6.3.2.4 Cells/spheroids microscopic monitoring

Cell growth in 2D and uniformity of spheroid formation on biochip platforms were monitored daily from day one post-seeding by bright field (BF) microscopy. The culture media was refreshed every day.

6.3.3 Drug testing evaluation

To assess cell sensitivity to anti-cancer drugs, doxorubicin (Dox, Sigma-Aldrich) was chosen as an anti-cancer drug model. Dox was stored at 1000 mM aliquots in PBS at -20 ^{o}C and diluted to the desired concentrations in PBS. Right before the drug test experiments 3 concentrations of 0.1 mM, 1 mM, and 10 mM of Dox in low-serum media (1% FBS) were prepared. As a control group, 0 mM concentration of Dox in media was prepared using PBS.

Three days after cell seeding in the microfluidic biochip, compact and uniform size spheroids were treated by either sterile PBS vehicle or drug (Dox) in low-serum conditions (1% FBS) for

two days. Culture medium containing the drug or PBS was introduced into the channels inlets and placed in the incubator for 24 hours. The medium was exchanged after 24 hours with a freshly prepared medium containingthe relevant dose of drugs or PBS and incubated for another 24 hours (a total of 48 hours of drug treatment).

To compare differences and similarities in 2D and 3D culture responses to Dox treatments, we have compared their sensitivities to Dox. For this purpose, monolayer 2D cell cultures were treated with either the sterile PBS vehicle or Dox 48 hours after cell seeding in 24 well plates for a duration of two days. The media containing the drugs or PBS were refreshed every day during the two days of drug treatment. For each concentration of Dox at least three independent experiments were performed for both 2D and 3D models.

6.3.3.1 Metabolic activity assays post drug treatment

To assess 2D and 3D cell viability after exposure to the selected concentration of drugs for 48 hours, Alamar Blue (Thermofisher) assay was carried out according to the manufacturer's instructions. Briefly, after removing the drugs from the cells/spheroids, Alamar Blue dye was added to the culture media in 10% vol on the last day of drug treatment (48 hours after drug exposure) and incubated with cells/spheroids in the incubator (37 ^{o}C, 5% CO2) for 4 hours. After incubation, the fluorescence intensity at excitation wavelengths 560 and emission wavelengths 590 were recorded using the Tecan Infinite M200 Pro microplate reader (Tecan Trading, AG, Männedorf, Switzerland). The metabolic activity was presented as a percentage of the negative control (cells/spheroids untreated with Dox) from the same series of experiments. Three independent experiments (with three replicates each time) were performed for each cell type and each concentration of Dox.After the measurements, spheroids were washed with PBS for further fluorescence-based Live/dead assay.

6.3.3.2 Differential staining

To visualize the distribution of the live and dead cells in the spheroids on the last day of the experiments a fluorescence-based live/dead assay was performed using the Live/dead Viability/Cytotoxicity kit (Invitrogen, Sigma-Aldrich) according to the manufacturer's instruction. Two days after drug exposure and right after the Alamar Blue assay, spheroids were

washed with PBS and incubated with the live/dead staining solution for 20 minutes protected from light at 37 ^{o}C incubator. By using Epifluorescence inverted microscope (Axio Observer.Z1, Zeiss, Oberkochen, Germany) and sCMOS camera (LaVision, Göttingen, Germany) and the objective lens EC Plan-Neofluar with respective fluorescence filter for Calcein AM (ex 485 nm, em 530 nm) and ethidium bromide EthD-1 (ex530 nm, em 645 nm) spheroid images were captured.

6.3.4 Statistical analysis

All experiments were repeated in three independent replicates (n=3) in order to evaluate the reproducibility of the data. For each experiment, a minimum of 10 spheroids were considered for analysis at each time point per condition. Statistical analyses were performed by using Microsoft Excel 2016 (Version 1803, Build 9126.2259). All data are represented as mean ± standard error of the mean. We have performed one-way ANOVA to assess statistical significance between means, with post-hoc Tukey tests for comparison between means. A $p \leq 0.05$ was considered statistically significant.

6.4 Results and discussion

Cells randomly aggregate to form spheroids in conventional spheroid culture methods (e.g. 384 well plate) [18]. As a result, the spheroid size and shape can be heterogeneous which leads to the difference in diffusion distance of the drug within various spheroids [18, 319]. However, to accurately evaluate the drug efficacy on spheroids, the generation of uniform-sized, compact, and spherical spheroids are essential for comparison of the responses under various drug concentrations [10, 12, 13].

6.4.1 Biochip fabrication and surface treatment

Microfluidic platforms by providing relatively uniform spheroids compared to conventional spheroid formation methods demonstrated to be a reliable *in vitro* platform for testing drug efficacy [17, 18, 201]. We have developed an optimized microfluidic biochip surface treated with 10% BSA which is statistically demonstrated to be successful to form uniform and compact spheroids compared to non-treated devices [238]. This optimized surface treatment by decreasing

the cell-surface interactions [13], promote tumor cells to self-aggregate more tightly, and produces compact and homogenous spheroids. We have used stereolithography to fabricate the resin mold and consequently soft lithography was performed as explained before for the fabrication of PDMS biochips. Each device has two layers of PDMS which are permanently bonded with oxygen plasma. Figure 6.1 represents the images of the biochip, microfluidic channel, and an image of lung tumor A549 spheroid captured inside the cylindrical chamber by a bright field microscope.

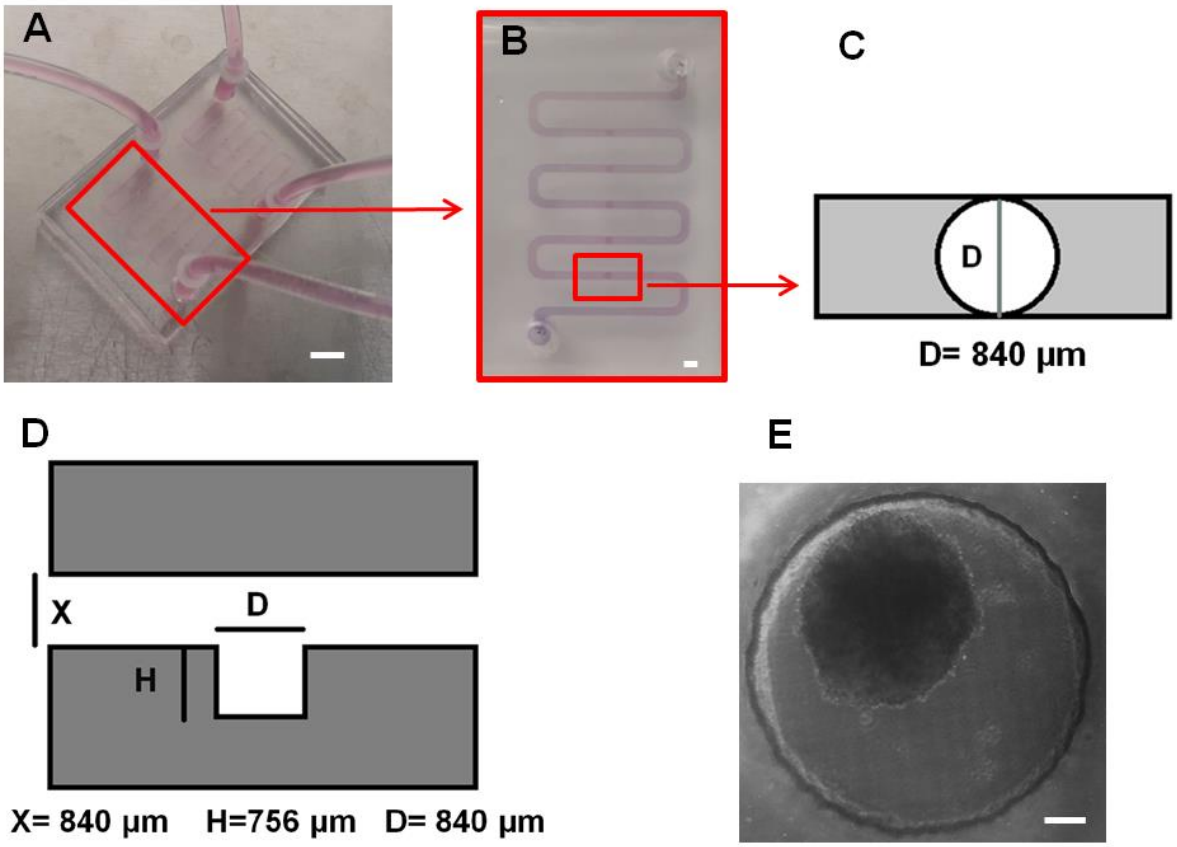

Figure 6.1 Microfluidic biochip design and spheroid formed in cylindrical cell trapping chamber

A) Image of two layers PDMS microfluidic device fabricated by the soft lithography technique. Each device has two independent channels of 109.2 mm in length with a cross section of 840×840 µm. Each channel has five cylindrical cell trapping chambers for cell sedimentation and spheroid formation. Error bar represents 1 cm. B) Top view image of a single channel with inlet,

outlet, and five cylindrical cell trapping chambers. Error bar represents 1mm. C) Schematic of the top view of the cylindrical cell sedimentation trap. The Diameter is 840 μm D) Side view schematic of the cell trapping chamber. The diameter of the cylindrical chamber is 840 μm and the height of the chamber is 756 μm. X represents the size of the cross-section of the channel which is 840 μm. E) Microscopic image from day five of a lung tumor (A549) spheroid formed in the cell trapping chamber. The scale bar represents 100 μm

6.4.2 Cell culture and spheroid formation experiments

6.4.2.1 Spheroid formation on biochips and drug test

In this work, we have produced a mono-type MCTSs (A549) (name as group A), a hetero-type MCTSs (A549: primary human osteoblasts, ratio 1:1) (name as group B) and a patient-derived MCTSs model (BML) (name as group C). Our main goal was to investigate the capability of this optimized biochip to produce uniform and homogenous spheroids on-chip. The chemosensitivity of the anti-cancer drug, Doxorubicin (Dox), was studied as a hallmark of the reproducibility and uniformity of the spheroids. Prior to investigating the drug sensitivities of these three cell conditions, the ability of these cells to form uniform-sized and compact MCTSs on our surface optimized biochip was assessed in accordance with our previous work [238].

Figure 6.2 demonstrates changes in the size and circularity of the spheroids. We have used the same method as our previous work to calculate circularity. Accordingly, circularity defines as the percentage of minimum diameter (Dmin) divided by maximum diameter (Dmax) around a single spheroid. This parameter shows if spheroids are uniformed-shape and spherical. By qualitatively monitoring the three groups of cells (A, B, C), we observed that mono-culture and co-culture spheroids demonstrated a significantly increases in size on day 5 when compared with day 1 ($p<0.05$). The size of BML spheroids did not significantly increase from day 1 to day 5. This difference can be explained by the fact that primary cells mostly grow slower than the cell lines. Moreover, in spheroids made by primary cells more dynamic cellular interactions and strong adhesion within the tumor microenvironment are expected to play a role to form tight cell-cell connections. This could be some of the reasons for no remarkable changes in their size when comparing day 5 to the first day of culture. Since the PDMS layers are transparent, the size and

shape of each spheroid can be easily observed using an optical microscope without the need for fluorescence cell labelling before spheroid formation.

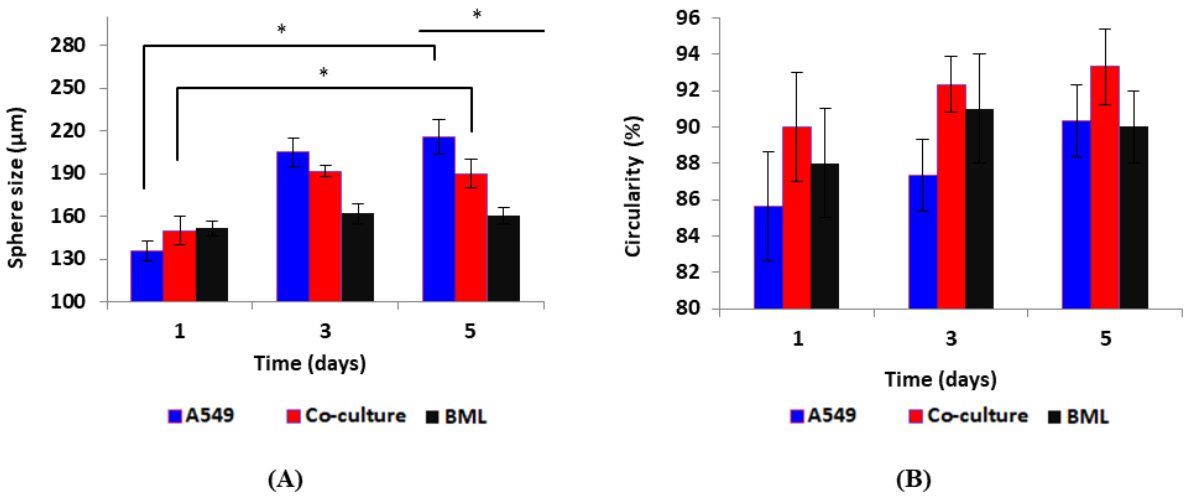

Figure 6.2 Spheroid size and circularity during the 5 days of culture

A) Spheroid size changes in three groups during the 5 days of culture. Spheroid size increased significantly on day 5 compared to day 1 for mono-culture and co-culture spheroids (D1 Vs. D7 *$p<0.05$). The size of BML spheroids did not changed statistically significant when compared day 5 to day 1. On day 5, the size of 3 groups of spheroids was significantly different when compared to each other (*$p<0.05$). B) Change in circularity in the spheroids during the 5 days of culture. This shows how the spheroids' shape is spherical and uniform. Spheroids in all three groups have a homogenous circularity and spherical form. Circularity did not change statistically significant when compared day 5 to day 1 for the 3 groups. Circularity is not significantly different on day 5 when comparing 3 groups to each other. Total initial number of cells is 1×10^6 cells/mL in all 3 groups. $p<0.05$ is considered statistically significant. All assays were performed as triplicates per trial in three independent experiments. (Error bars represent ± SE, n=3)

Spheroid formation on-chip has been achieved due to the gravity by sedimentation and containment [33, 259]. As the PDMS surfaces are pre-coated with 10% BSA, cell repellent

properties of the surface [136] and the cylindrical shape of each cell trapping micro-well enabled the precise and quick cell agglomerations. Due to the adhesive interactions between cells surface proteins and extracellular matrix, the spheroids were formed [13, 209]. The cell aggregation of A549, co-culture of A549: primary human osteoblasts (1:1), and the spine metastasis patient-derived cells (BML) were observed 24 hours after the cell culture on-chip. However, the compact spheroid formation was observed three days after the cell seeding (Figure 6.3.A). The drug screening on-chip was performed according to this timeline: the day of the cell seeding was considered day 0, 24 hours after the cell seeding was considered day 1. On day 3 the spheroids are more compact, spherical, and bigger in size when compared with day 1. Therefore, drug administration was performed on day 3 for 48 hours. Then, on day 5 drugs were removed from the devices and the Alamar Blue assay was performed followed by live/dead viability staining on the same day. We have monitored spheroid growth and culture medium was exchanged on a daily bases. For the two days of drug treatment, the culture medium with the corresponding concentration of the drug was refreshed once a day. Figure 6.3.B represents the timeline of the experiments.

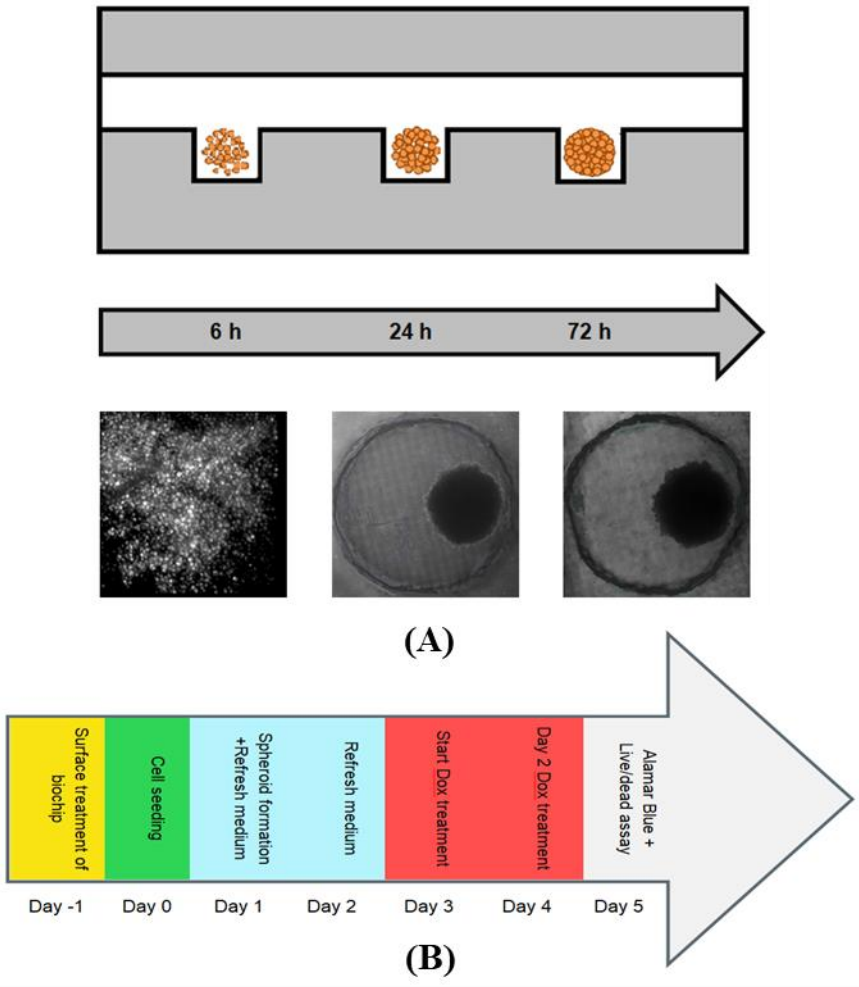

Figure 6.3 Spheroid formation and the experimental timeline for drug test

A) Cell suspension introduces through the channel's inlet and some of the cells will settle down into the cell trapping chambers due to the gravity. As the PDMS surface of the channel is treated with 10% BSA and became cell repellent, cells effectively agglomerate and form compact and uniform spheroids on day three after cell seeding. At the bottom of the figure, we see images of A549 lung cancer cells that produced spheroids captured by bright field microscopy. B) Experimental timeline for the spheroid formation and drug test on the biochip. The start of the drug dosing is on day 3 post-seeding and on day 5 post-seeding (after 48 hours of drug exposure) drug response analysis were performed

6.4.2.2 2D culture model as comparison with 3D MCTSs

In the drug development process, having appropriate *in vitro* pre-clinical tools provide a major contribution to more precisely predicting drug responses in clinical trials. To assess drug sensitivity in 3D MCTSs compared with the 2D model, we have compared our optimized microfluidic platform with a 2D monolayer culture model on 24 well plates for all three cell conditions.

Here, we have evaluated Doxorubicin (Dox) sensitivity on three groups of cells: mono-type A549 cells, hetero-type A549: primary human osteoblasts and patient-derived cells using both 2D (24 well plate) and 3D (MCTSs) *in vitro* models. Doxorubicin [319] is known as one of the most widely used chemotherapy agents in the early and advanced treatment of several types of cancer. However, tumor resistance has limited the effectiveness of Dox in single-drug treatment [18]. The mechanism of drug resistance is poorly understood [319].

6.4.3 Drug testing evaluation

6.4.3.1 Metabolic activity testing post-drug treatment using the Alamar Blue assay

To assess the metabolic activity after drug exposure, the Alamar Blue assay has been performed due to nontoxicity of Alamar Blue to cells [321]. 48 hours after drug administration, culture media was removed from the microfluidic channels and 24 well plates and replaced with Alamar Blue solution which was incubated with spheroids in microfluidic channels and with the cells in 24 well plates to measure the metabolic activity of the cells/spheroids. Alamar Blue assay [320] defines the viability of the cells/spheroids and the toxicity effect of the Dox on cells. Resazurin [321] is an oxidation-reduction (REDOX) indicator of Alamar Blue which undergoes colorimetric change (from blue to red) when reduces to fluorescent Resorufin by metabolically active cells. Resorufin can be reduced to non-fluorescent hydroresorufin later. Cells and spheroids untreated with the drug (0 mM Dox) were considered as a control group. Cells/spheroids viability after drug treatment was calculated in the relation to the control group. A Blank sample was prepared by using only dye solution (10%vol Alamar Blue). The incubation time with Alamar Blue was adjusted experimentally by incubation of 10%vol Alamar Blue with cells/spheroids at 37 ^{o}C for 1, 2, 3, 4, 5, 6 hours. After each time the fluorescence intensity was

recorded. 4 hours of incubation were selected for all experiments as the highest fluorescence intensity signal was detected after 4 hours of incubation. Fluorescence intensity was measured using fluorescence spectrophotometry and red fluorescence while excitation and emission wavelength were set as 560 nm and 590 nm, respectively.

The metabolic activity of mono-type spheroids A549 significantly decreased compared to the control group when exposed to 1 μM and 10 μM of Dox (1 μM Dox Vs. control *$p<0.05$ and 10 μM Dox Vs. control *$p<0.05$). However, co-culture and patient-derived spheroids exhibited more resistance to Dox administration and metabolic activity did not change statistically significant. This drug resistance could be related to tumor-stromal cells interactions which consider as a crucial factor of cancer cell growth and their resistance to anti-cancer therapies [276, 322]. The interactions between the tumor cells and its microenvironment modulate cellular signaling which has an effect on tumor cells' responses to chemotherapeutic agents [322]. Our results can demonstrate that the co-culture models and using patient cells can better reflect the *in vivo* like tumor conditions *in vitro*.

Alamar Blue assay results show when the cells were exposed to Dox in the 3D model, they demonstrated greater resistance than the cells in the monolayer in all three cell conditions. Most of the spheroids in all groups treated with Dox maintained a spherical shape but many of the spheroids in high drug concentrations displayed a rough surface and could be considered dead. A similar trend was observed in all three groups. In all three groups, spheroids treated with all concentrations of Dox (0.1, 1, and 10 mM Dox) showed lower metabolic activity compared with the spheroids in the control group (0mM Dox) (Figure 6.4). In the 2D model, all three groups of cells show a decrease in metabolic activity by increasing the drug concentration. This decrease is non-significant when cells were exposed to 0.1 μM Dox. However, metabolic activity significantly decreased compared to the control when the cells exposed to 1 μM and 10 μM of Dox (1 μM Dox Vs. control *$p<0.05$ and 10 μM Dox Vs. control *$p<0.05$ and **$p<0.001$) in all groups (Figure 6.4).

At the high concentration of Dox (10 mM), most of the spheroids became loose and lost their compact and circular shape which can be related to general cell death. Spheroids subjected to lower concentrations of Dox (0.1 μM, and 1μM) maintained their integrity but their growth was limited and therefore detected fluorescent signal was lower compared with the control group.

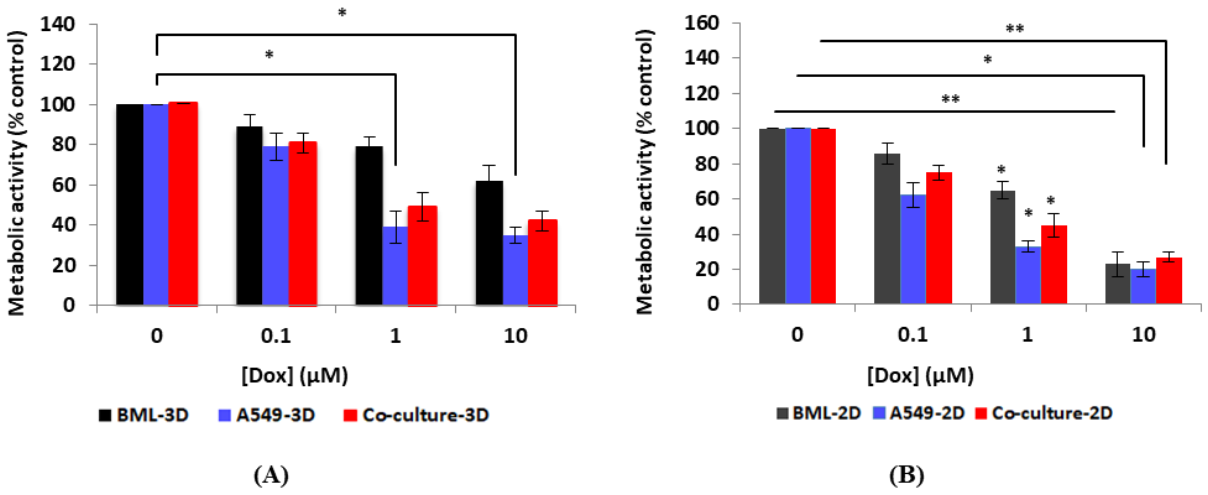

Figure 6.4 Metabolic activities of treatment groups compared to the control group

A) Metabolic activity of MCTSs measured after 48 hours of drug exposure (Dox). Metabolic activity of mono-type spheroids A549 has been decreased statistically significant compared to the control when exposed to 1 μM and 10 μM of Dox (1 μM Dox Vs. control *$p<0.05$ and 10 μM Dox Vs. control *$p<0.05$). MCTSs from patient-derived cells demonstrate more resistance to Dox when compared with the other two groups. B) Metabolic activity measured in the 2D model (24 well plates). Metabolic activity significantly decreased compared to the control when the cells were exposed to 1 μM and 10 μM of Dox (1 μM Dox Vs. control *$p<0.05$ and 10 μM Dox Vs. control *$p<0.05$ and **$p<0.001$).$p<0.05$ is considered statistically significant. All assays were performed as triplicates per trial in three independent experiments. (Error bars represent ± SE, n=3)

We have observed that treatment of cells with Dox in the 2D culture for two days inhibited cell growth and survival dramatically. Compared with the 2D models, MCTSs in all three groups represent more resistance to Dox and better demonstrate *in vivo* like interactions between drugs and cancer tissues. The slower growth rate of cells grown in the 3D conditions compared to the 2D monolayer culture plays an important role in drug resistance. Since the cytotoxicity may be

less effective in cells with a slower growth rate when compared to cells with a higher growth rate. When the cells grow in 2D, cells spread in monolayer on a culture surface. Therefore when a drug is tested in 2D, the drug components need to only diffuse the distance across the cells to reach its target. However, in 3D cells arrange in multilayers and the drug needs to diffuse across layers of cells to reach its target. This could be one explanation for higher drug resistance in 3D MCTSs compared with the 2D model. Figure 6.5 shows the comparison of metabolic activity between 3D MCTSs and 2D for each group of cells.

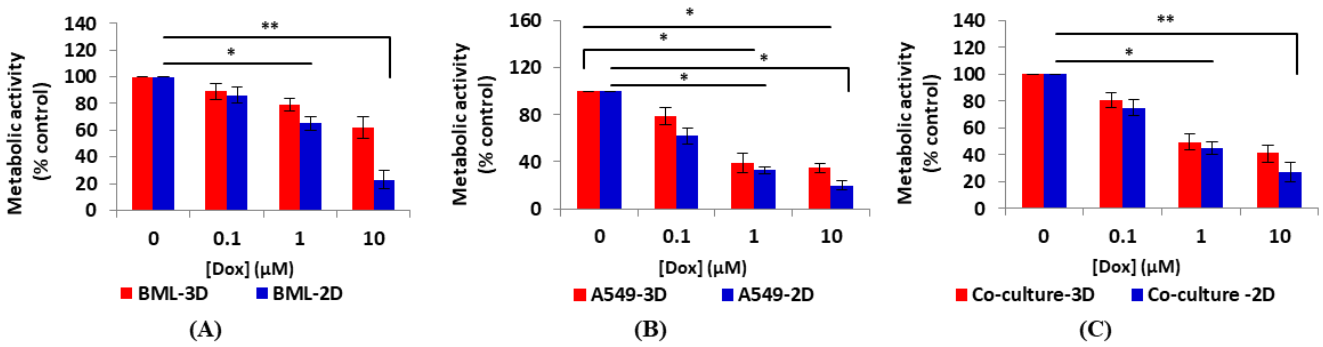

Figure 6.5 Metabolic activity after drug exposure in 3D and 2D culture

A) Patient-derived cells metabolic activity in 3D MCTSs and 2D model. Spheroids are drug resistant as drug penetration is harder in 3D form. Therefore the metabolic activity of spheroids did not changed statistically significant compared to the control group when they were exposed to various concentrations of drugs. On the other hand cells in 2D demonstrated statistically significant decrease compared to the control group when exposed to 1 μM (*$p<0.05$) and 10 μM (**$p<0.001$) of Dox. B) Established lung cancer cells A549 show a significant decrease in metabolic activity when exposed to 1 μM of Dox and higher in both 3D and 2D conditions (*$p<0.05$). C) Co-culture of lung cancer cells A549 and primary human osteoblasts with the ratio of 1:1 to mimic the tumor-stromal reaction. Metabolic activity in spheroids did not changed statistically significant when compared to the control group by increasing the Dox concentration. In the 2D model, metabolic activity decreased statistically significantly compared to the control when the cells were exposed to 1μM (*$p<0.05$) and 10 μM (**$p<0.001$) of Dox. $p<0.05$ is

considered statistically significant. All assays were performed as triplicates per trial in three independent experiments. (Error bars represent ± SE, n=3)

Our results demonstrate that our surface optimized biochips by providing a cell repellent surface produce homogenous MCTSs that can be served as a reliable *in vitro* tool for drug sensitivity assays. These observations were supported by live/dead assay images presented in the following section.

6.4.3.2 Differential staining (live/dead assay)

On the last day of experiments, differential staining and microscopic observation were performed to observe the live and dead cells distribution in the spheroids. As these compounds are toxic to cells, this experiment was carried out as the last point additional reference method to confirm the results obtained in the Alamar Blue assay. A mixture of PBS containing Calcein AM and ethidium bromide EthD-1 according to the manufacturer guideline was introduced into the microfluidic channels and incubated at 37 ^{o}C for 20 minutes. After this time, spheroids images were captured using a fluorescence microscope. Living cells (green fluorescence) and dead cells (red fluorescence) were observed in recorded images. Figure 6.6 shows how the number of live (green color) and dead (red color) cells changed for spheroids exposed to different concentrations of Dox compared to the control group in all three groups of cells.

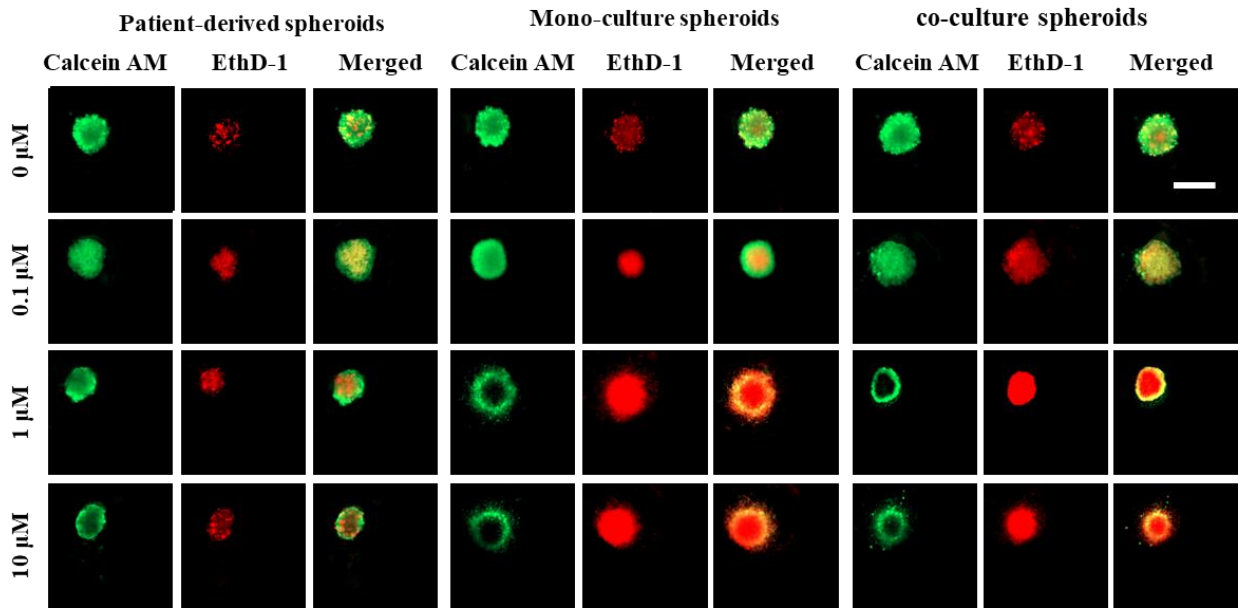

Figure 6.6 Images of differential staining (Live/dead assay)

The green color is due to the Calcein AM and it is representing the distribution of the live cells in the spheroids. The red color is due to the EthD-1 and it is representing the dead cells in the spheroids. In all the three groups of cells, increasing in the area of dead cells and a decrease in the area of the live cells were observed by increasing the drug concentrations. The initial total number of cells keeps as 1×10^{6} cells/mL for all experiments. The ratio of 1:1 considered for the co-culture model of lung tumor cells A549 and primary human osteoblasts by keeping the total initial cells of 1×10^{6} cells/mL. All assays were performed as triplicates per trial in three independent experiments. Images represent when a repetitive phenomenon observed in three independent experiments. Scale bar represents 200 µm

Changes in the cellular viability and spheroids morphology can be associated with the cell's death as apoptotic and necrotic cells lose their ability to stay tightly connected with other cells. The phenomenon of spheroids showing more drug resistanceOne of the challenges in using of the

live/dead assay in the 2D culture compared to the 3D model is that the dead cells usually detach from the surface in monolayer (2D) culture plates. Therefore they are easily removed during the pipetting of the live/dead solutions. Hence, the results demonstrate higher viability compared to its actual viability due to the under-representation of the dead cells in the monolayer culture. Therefore, for 2D models, other methods (e.g. flow cytometry) is more appropriate to determine live/dead cell populations when we can first remove all the cells (live and dead) from the culture plates and then stain and image/count them to reduce the under-counting effect of dead cells. Accordingly, in this work, we have only used the live/dead staining method as a complementary technique for the Alamar Blue assay for spheroid models only. Since, the main objective of this work is to assess the repeatability of these surface-optimized biochips to produce uniform spheroids for reliable drug test.

The co-culture and patient-derived spheroids have a higher sensitivity to Dox. These spheroids are more compact (dense) due to the stronger cellular interactions inside the spheroids [10]. There is some evidence that the increase in the hypoxic center inside the spheroids has a positive correlation with the compactness level of the spheroids [323, 324]. Hypoxia is known to be one of the important factors in drug resistance in spheroids [324]. Hence, we can conclude that hypoxic status in patient-derived and co-culture spheroids can be one of the causes of their resistance to the chemotherapeutic drugs. The phenomenon of spheroids showing more drug resistance compared with monolayer culture has been attributed to various mechanisms. These can be including decreased drug penetration to the cells, hypoxia inside the spheroids, and up-regulation of genes giving drug resistance.

From our results, we can conclude that mono-type MCTSs cannot accurately recapitulate the *in vivo* like tumor microenvironment. As tumor cells' interactions with stromal cells play a critical role in mimicking tumor microenvironment *in vitro*, co-culture models of tumor cells with stromal or patient-derived 3D MCTSs models might better represent the tumor features *in vitro*.

MCTSs represent the *in vivo* like features of the tumor microenvironment, with respect to gradient distribution of oxygen, nutrients, metabolites, and drug penetration. Therefore, having the other key components of tumor tissue (e.g. immune cells, fibroblasts, osteoblasts, etc.) will increase the *in vivo* like characteristics of MCTSs models. We assume that MCTSs can significantly contribute to the development of optimized cancer treatment for patients. Our results

showed the potential of our surface-optimized biochips for reproducible production of uniform and homogenous spheroids toward reliable and repeatable drug testing.

6.5 Conclusion

The fact that numerous anticancer drugs are eliminated during the clinical phase of drug development demonstrates that current 2D culture models are not efficiently predictive. The 3D tumor spheroids showed to recapitulate the feature of the tumor microenvironment more precisely and to better estimate the efficacies of the chemotherapeutic drug compounds compared to the 2D models. However, one of the most important challenges in using spheroids for drug testing is producing uniform spheroids [10, 12, 13].

In the present work, we have developed surface-optimized microfluidic biochips for uniformly sized MCTSs formation, culture, and drug testing. Uniform spheroids from lung cancer cell lines A549, co-culture of lung cell lines A549 and primary human osteoblasts, and patient-derived spine metastasis secondary to lung (BML) cells has been produced in these optimized platforms in a repeatable manner. The modified PDMS surfaces of the biochips provided cell repellent properties. Therefore, cell-cell interactions became dominant over cell-surface interactions. This leads to the reproducible formation of compact and uniform spheroids on-chip. We have observed that drug test results are repeatable which is a hallmark of reproducibility and

Overall, the present study highlights the importance and suitability of our *in vitro* model for drug testing. In conclusion, these surface optimized microfluidic platforms, may be convenient *in vitro* tools for uniformly sized and homogenous spheroid formation and culture from established tumor cell lines, co-culture models, and patient-derived cells. Further surface optimization of these biochips is subject of work in progress to better elucidate the efficacies of these platforms and to serve as a reliable drug testing device for developing new therapeutic agents and optimizing the existing drug compounds in personalized medicine.

6.6 Author Contributions

Conceptualization: N.A., R.A., D.H.R., and A.A.; Data curation: N.A.; Formal analysis: N.A., and R.A.; Funding acquisition: D.H.R., M.S., and A.A.; Investigation: N.A.; Methods: N.A.,

R.A., D.H.R., and A.A.; Project administration: D.H.R., and A.A.; Resources: M.S., M.H.W., D.H.R., and A.A.; Supervision: M.S., D.H.R., and A.A.; Validation: N.A., R.A., D.H.R., and A.A.; Visualization: N.A.; Writing original draft: N.A.; Writing—review and editing: N.A., R.A., M.S., M.H.W., D.H.R., and A.A.; N.A. should considered the first author; D.H.R., and A.A. contributed equally to this work and should considered as co-corresponding authors. All authors have read and agreed to the published version of the manuscript.

6.7 Funding

This research was funded by the Natural Sciences and Engineering Research Council (NSERC) of Canada discovery grants (A.A. and M.S.) and Fonds de Recherche du Quebec Sante (FRQS) Junior 2 Research Scholar Award (D.H.R.).

6.8 Institutional Review Board Statement

The study was conducted in accordance with the ethics approval for patient sample collection through McGill Scoliosis and Spine Group, RI MUCH REB Extracellular Matrix Protocol # 2020-5647.

6.9 Acknowledgements

The authors gratefully acknowledge the McGill Spine and Scoliosis group for helping obtain the patient samples. The authors also gratefully acknowledge M. Lavertu (Polytechnique Montréal) for kindly providing the lung tumor cells used in this study and M. Wertheimer (Polytechnique Montréal) and D. Juncker's Laboratory (McGill University) for kindly providing the access to plasma oxygen equipment and support to fabricate the molds, respectively. N.A gratefully acknowledges the scholarship from Fondation et Alumni de Polytechnique Montréal donated by the Royal Bank of Canada (RBC).

6.10 Conflicts of Interest

The authors declare no conflict of interest.

CHAPTER 7 GENERAL DISCUSSION

7.1 Discussion

The fact that the majority of the successful chemotherapeutic drug candidates in the preclinical stage fail when they reach to clinical phase is mainly due to the inefficiency of current preclinical models. To increase the predictive power of *in vitro* preclinical models, 3D culture spheroids have been developed to more precisely recapitulate the characteristics of the tumor microenvironment and accordingly more efficiently predict drug responses in human. The lack of reproducibility of the spheroids in terms of size and morphology is one of the most significant limitations in conventional spheroid culture platforms, which drastically influence on robustness of drug screening assays. Using microfabrication and microfluidics, helped to increase the uniformity of the spheroids by having better control over the spheroid size and growth. However, most of the current researches focus on modifying the microfluidic design to control the homogeneity of the spheroids, which can increase the cost and complication of manufacturing process and the increase the need for involvement of highly educated experts.

The main goal of this PhD dissertation was to produce uniform spheroids on-chip in terms of size, compactness level and spherical morphology for standardized and reproducible data from drug testing to accelerate drug development process. Out main hypothesis was that surface modification of microfluidic biochip can modulate spheroid formation on-chip toward uniform and homogenous spheroids production for repeatable drug testing. In this chapter, I present a general discussion by reviewing the articles in terms of each specific research objective. Here, the limitations of this work are discussed as well.

Study 1: Uniformity of spheroid-on-chip by surface treatment of PDMS microfluidic platforms

To design an optimal surface with effective anti-fouling properties for spheroid-on-a-chip platforms, understanding the correlation between the surface characteristics and cell responses is crucially important. Accordingly, ***the first objective of this dissertation, as explained in detail in Chapter 4, was to optimize the PDMS surface of biochip in order to decrease PDMS hydrophobicity and increase its anti-fouling properties.*** Therefore, ***our first hypothesis was that***

by changing the concentration of the anti-fouling materials to treat the PDMS surface and by changing the incubation time, we may modify the surface wettability of the PDMS. Our second hypothesis was that changes in surface wettability might have an impact on modulating cellular responses to the surface and promote cell self-aggregations.

The originality of the first part of this PhD dissertation was that for the first time, the impact of the surface wettability of the PDMS and its microstructure on quality and quantity of spheroid formation on microfluidic platforms was investigated.

In this work PDMS surface wettability and its microstructure by modifying with the two well-known anti-fouling materials, BSA and Pluronic F-68, have been studied. Here, I have studied the effect of two important variables: "concentration and time of incubation" on PDMS surface wettability and microstructure. Water contact angle measurements, SEM and AFM analysis demonstrated that by changing the concentration of the surface modifying materials to "3%, 5% and 10%" and modifying the duration of surface treatment in two different time points of "one hour treatment" or "overnight treatment" various degrees of surface wettability and microstructure for PDMS surface have been observed. Our observations demonstrated that by increasing the concentration and incubation time, better surface coverage will be provided and accordingly, the hydrophobicity of the PDMS surface decreases. Then, spheroid formation from MDA-MB-231 cells on PDMS biochips following surface treatment with six different degrees of wettability and morphology was compared. Microscopic observations showed that a moderate hydrophilic surface in the range of 88^{o} to 62^{o} provides optimized surface repellent properties which lead to effective cell self-aggregations and compact and uniform spheroid production.

This study highlights the important role of surface properties of microfluidic-based spheroid culture platforms in effectively blocking non-specific cell adhesion to the surface. Our observations reveal that surface optimization is a simple, powerful and cost-effective method to enhance homogenous and uniform spheroid production on microfluidic platforms just from a simple cell suspension without the need of using expensive additive materials (e.g. hydrogel, matrigel).

Study 2: Surface optimization and design adaptation toward spheroid formation on-chip

After confirming the role of PDMS surface wettability and its morphology on cell adhesion to the surface and spheroid formation on-chip, the versatile capability of the optimized PDMS surface in the first study was investigated using 6 different cell lines and co-culture models. Accordingly, ***my second objective was to optimize the surface and design of a biochip for homogenous spheroid production from various cancer cell lines and co-culture of tumor cells with stromal cells.*** In the second part of this dissertation, as explained in Chapter 5 in detail, ***I have first hypothesized that design optimization and surface modification are the two important parameters in altering the cell orientation in the microfluidic device.*** Therefore, the design of cell trapping chambers modified to cylindrical shape instead of cube shape toward enhancing central cell-aggregations, which can result in more spherical shape of cell clusters. To fully fit reach to our second objective, ***the second hypothesis of this work was that the optimal PDMS surface from the first study may possess strong enough anti-fouling properties to deter various cell types from the PDMS surface.*** In the other words, I was interested to see if this optimized surface is cell line-dependent or can be considered as an optimized surface for several cell lines to enhance uniform spheroid production. In this regard, cell adhesion to the PDMS biochip surface and spheroid formation from 6 different cell lines and co-culture models on biochips treated with 10% BSA as an optimal surface have been investigated. The microscopic results have been analyzed in comparison with cell adhesion and spheroid formation on biochip pre-coated with 3% BSA, which demonstrated the least cell repellent properties in our first study.

The originality of the second part of this PhD dissertation was that in this work I have investigated the effect of two crucial parameters on spheroid-on-a-chip platforms: microfluidic design and surface properties. This is the first optimized platform assessing spheroid formation from several cell lines and co-culture models with considering the effect of surface wettability and morphology to enhance uniform scaffold-free spheroids in a repeatable manner.

Study 3: Uniform tumor spheroids on surface optimized microfluidic biochip for reproducible drug screening and personalized medicine

The final research objective was to produce uniform spheroids from patient samples on our optimized platform and to assess reproducibility of the drug test on-chip. Accordingly, ***my first hypothesis was the optimized biochip developed in the two previous study, possibly can demonstrate strong enough cell repellent properties to deter cell adhesion to the biochip surface and therefore, promote compact and homogenous spheroids from patient cells.*** To validate this hypothesis, I have used cells obtained from patient biopsy samples from bone metastasis secondary to lung to assess their spheroid formation on-chip.

In the two previous studies, I successfully produced spheroids from established cell lines and co-culture models. In the third study of this dissertation, I intended to compare drug resistance in the three different types of spheroids: 1. Spheroids from established tumor cells (lung cancer cell lines A549), 2. Spheroids from co-culture of tumor and stromal cells (lung cell lines A549 and osteoblasts cells Qth212) and 3.Spheroids from patient cells (patient derived spine metastasis secondary to lung (BML) ***My second hypothesis in this work was that spheroids from patient cells and co-culture models may better represent the complexity of the tumor microenvironment and demonstrate drug resistance more closely to the natural tumors when compared with spheroids from single tumor cell type***. Here, I have used Doxorubicin as an anticancer agent. Cellular metabolic activity after drug exposure has been compared in the three different types of spheroids developed on our optimal platform. In this work, I was interested in comparing drug responses in 3D spheroids with 2D models. Therefore, 2D culture models from the same cells used in spheroids production have been developed on 24 wells, and analysis has been performed after drug exposure to both models (2D and 3D). As the uniformity of spheroids in terms of size, shape and level of cellular compactness play the crucial role in spheroid responses to drug compounds, ***my third hypothesis in this work was that observing reproducible drug responses on biochip may be a hallmark of uniformity of spheroids.***

Due to the modified surface properties of PDMS, relatively homogenous spheroids were produced in our platforms from various cell types including cells obtained from patient biopsy, which was my main goal of this dissertation. Therefore, our optimized biochip demonstrated to have the potential to be used as a reliable and reproducible drug-screening platform to accelerate cancer drug development and personalized medicine to improve clinical relevance.

The possibility of using patients own cells in physiologically relevant spheroid-on-a-chip platforms is a revolutionary approach in the field of cancer treatment, for precise and prompt decision on individualized cancer therapy for specific patient.

Our observations demonstrated that cell culture methods (2D or 3D) and the types of the cells (established cell lines, co-culture models, patient cells) are the two critical parameters to mimic tumor microenvironment and need to be considered to reproduce more physiologically relevance drug testing assays.

In summary, in the study 1, I have optimized the PDMS surface of the biochip to enhance spheroid formation. In the study 2, homogeneity of spheroid production from several cell lines has been investigated on the biochip with optimized surface and design. In the study 3, to reach to my main goal, production of uniform and homogenous spheroid from various cell types ranging from established tumor cells, co-culture of tumor-stromal cells and patient cells have assessed, followed by drug test to investigate the reproducibility of the drug testing on our platforms. I have observed that spheroids represent the complexity of native tumor tissues on an optimized biochip when compared to 2D models. As I have hypothesized, surface properties and design are the two critical players in reproducibility of uniform spheroids. This optimized platform demonstrated to have the potential to be used for drug development assays, disease modeling and personalized medicine.

7.2 Limitations of this dissertation work

The goal of this PhD dissertation was to develop a reproducible spheroid-on-a-chip platform with uniform and homogenous spheroids for reliable drug testing. This goal was achieved, as described in detail in previous chapters above. There are some limitations related with this work to be improved in the future.

One of these limitations is the design of the microfluidic chip. However, this design demonstrated to be an optimal design to produce long-term culture of the scaffold-free and uniform spheroids from various cell lines. This design can be adjusted to produce a higher number of spheroids on a single platform. This will lead to high throughput of uniform spheroids production.

Another drawback in this work, which is common in most biochip platforms, is losing the cell during the cell loading process on-chip. As during the introducing of the cells into the device's inlet, only some of the cells trap and sediment inside the microwells and the rest of the cells will rinse out and exit from the outlet during the medium exchange without taking part in the spheroid production. This problem is more prominent in the case of working with patient samples when the number of available cells is not high. Changing the design of the device probably can reduce the number of cells lost.

In our first study, we have observed that incubation time in surface treatment had a significant effect on surface wettability. Accordingly, the PDMS surface treated for 1 hour had similar surface properties to bare PDMS, while overnight treatment could significantly change the surface wettability at higher concentrations. However, this finding is very important toward surface optimization of PDMS; it can be considered as one of the limitations of this work. As decreasing this incubation time while keeping the same optimal surface wettability, can be useful when rapid spheroid production is required.

However, there are some potential limitations in this work, but also there are more exciting paths to explore in the future, which I will discuss in the final chapter.

CHAPTER 8 CONCLUSION AND RECOMMANDATIONS

8.1 Conclusion

This dissertation focuses on combining "surface optimization" with "design adaptation" of microfluidic biochip platforms to create an optimal and easy-to-use spheroid-on-a-chip device to generate uniform and homogenous scaffold-free spheroids for reproducible drug testing. This PhD work made a concrete advance in terms of spheroids on-chip platforms by highlighting the influence of surface wettability and morphology on spheroid production on biochips. Here, for generating uniform spheroids, I have proposed to consider surface modification as an efficient, simple, cost-effective and reproducible method. The results presented in this work demonstrated that this optimized spheroid-on-a-chip platform could be used to produce homogenous, spherical shape and compact spheroids, which allow researchers to recreate the tumor microenvironment *in vitro* in a controlled manner, enabling investigation in cancer cell behaviour and drug safety and efficacy testing. This platform incorporates cell-cell interactions and cell-extra cellular matrix interactions leading to creating tumor microenvironments much closer to *in vivo*, allowing a more physiologically relevant and clinically translatable assessment of therapeutic safety and efficacy. On this platform, uniform spheroids produced by cancer cells derived from patients could be tested against commercially available anticancer drugs to define personalized patient-specific testing.

8.2 Recommendations for the future work

Although beyond the scope of this dissertation, the following suggestions are worth considering for future research:

- In this dissertation, I have used two surface coating materials with well-known anti-fouling properties for surface modification of PDMS: BSA and Pluronic F-68. However, there are various surface coating materials (e.g. other PEO-terminated triblock polymers, PVA, poly (hydroxyethyl methacrylate) etc. which are worth investigating their effect on modifying PDMS surface properties and consequently on spheroid formation on PDMS biochips.
- One of the limitations of this dissertation is the duration of PDMS surface treatment for optimal modification of PDMS surface. To have an optimal PDMS surface wettability and

morphology for uniformly spheroid production, I needed to treat the PDMS biochip overnight with BSA or Pluronic F-68. Another interesting suggestion for future work is to assess the possibility of decreasing the duration of treatment while maintaining the optimal surface properties for PDMS. In this regard, the effect of different variables including concentration, temperature and other parameters can be investigated in the future.

- Other types of patient cells can be used to generate uniform spheroids in the same way described in this dissertation for further investigations.
- Other types of chemotherapeutics can be screened on this platform developed in this dissertation. Moreover, the effect of combinational therapy (e.g. chemotherapy, radiotherapy etc.) is worth investigating on this optimized biochip.
- The gene expression profile of tumor cells worth to investigate in spheroids produced over biochip with different surface wettability. This can prove valuable information on the role of cell's substrate characteristics at the molecular level that needs to be carefully considered when designing an optimal platform.
- Another improvement can be implemented in future studies by applying this surface optimization developed in this dissertation to other microfluidic designs. In this dissertation we highlight the effect of surface properties and design on uniformity of spheroids in our platform, however, this optimized surface can be investigated on spheroid production in different microfluidic designs.
- Integrations of this microfluidic biochip with sensors to create an automated platform for online measurements and in situ recording of data would be an interesting pathway for future work.
- In this dissertation, I have successfully demonstrated an optimized spheroid-on-a-chip platform to produce uniform and homogenous spheroids for drug screening. However, the design of this platform allowed for having one type of spheroids per single channel. In the future, unique design approaches allow for the fabrication of multiple microfluidic components on the same platform, which can include several types of spheroids interacting with each other to capture multi-organ/or body-on-a-chip platform.

REFERENCES

[1] D. R. Brenner *et al.*, "Projected estimates of cancer in Canada in 2020," *Cmaj,* vol. 192, no. 9, pp. E199-E205, 2020.

[2] C. Mattiuzzi and G. Lippi, "Current cancer epidemiology," *Journal of epidemiology and global health,* vol. 9, no. 4, p. 217, 2019.

[3] S. N. Bhatia and D. E. Ingber, "Microfluidic organs-on-chips," *Nature biotechnology,* vol. 32, no. 8, pp. 760-772, 2014.

[4] K. Gomez and R. Rabadan, "A persistent look at how tumours evade therapy," ed: Nature Publishing Group, 2021.

[5] F. Bray, J. Ferlay, I. Soerjomataram, R. L. Siegel, L. A. Torre, and A. Jemal, "Global cancer statistics 2018: GLOBOCAN estimates of incidence and mortality worldwide for 36 cancers in 185 countries," *CA: a cancer journal for clinicians,* vol. 68, no. 6, pp. 394-424, 2018.

[6] S. Ahadian *et al.*, "Organ-on-a-chip platforms: a convergence of advanced materials, cells, and microscale technologies," *Advanced healthcare materials,* vol. 7, no. 2, p. 1700506, 2018.

[7] C. Moraes, G. Mehta, S. C. Lesher-Perez, and S. Takayama, "Organs-on-a-chip: a focus on compartmentalized microdevices," *Annals of biomedical engineering,* vol. 40, no. 6, pp. 1211-1227, 2012.

[8] H. Savoji *et al.*, "Cardiovascular disease models: a game changing paradigm in drug discovery and screening," *Biomaterials,* vol. 198, pp. 3-26, 2019.

[9] M. Al-Masri *et al.*, "Architectural control of metabolic plasticity in epithelial cancer cells," *Communications biology,* vol. 4, no. 1, pp. 1-16, 2021.

[10] R. M. Sutherland, H. R. MacDonald, and R. L. Howell, "Multicellular spheroids: a new model target for in vitro studies of immunity to solid tumor allografts: brief communication," *Journal of the National Cancer Institute,* vol. 58, no. 6, pp. 1849-1853, 1977.

[11] G. Lazzari, P. Couvreur, and S. Mura, "Multicellular tumor spheroids: a relevant 3D model for the in vitro preclinical investigation of polymer nanomedicines," *Polymer Chemistry,* vol. 8, no. 34, pp. 4947-4969, 2017.

[12] A. A. Fitzgerald, E. Li, and L. M. Weiner, "3D culture systems for exploring cancer immunology," *Cancers,* vol. 13, no. 1, p. 56, 2021.

[13] J. Friedrich, C. Seidel, R. Ebner, and L. A. Kunz-Schughart, "Spheroid-based drug screen: considerations and practical approach," *Nature protocols,* vol. 4, no. 3, pp. 309-324, 2009.

[14] B. Patra *et al.*, "On-chip combined radiotherapy and chemotherapy testing on soft-tissue sarcoma spheroids to study cell death using flow cytometry and clonogenic assay," *Scientific reports,* vol. 9, no. 1, pp. 1-9, 2019.

[15] T. Collins, E. Pyne, M. Christensen, A. Iles, N. Pamme, and I. M. Pires, "Spheroid-on-chip microfluidic technology for the evaluation of the impact of continuous flow on

metastatic potential in cancer models in vitro," *Biomicrofluidics,* vol. 15, no. 4, p. 044103, 2021.

[16] J. Ruppen *et al.,* "A microfluidic platform for chemoresistive testing of multicellular pleural cancer spheroids," *Lab on a Chip,* vol. 14, no. 6, pp. 1198-1205, 2014.

[17] E. Prince *et al.,* "Microfluidic Arrays of Breast Tumor Spheroids for Drug Screening and Personalized Cancer Therapies," *Advanced Healthcare Materials,* vol. 11, no. 1, p. 2101085, 2022.

[18] W. Lim *et al.,* "Formation of size-controllable tumour spheroids using a microfluidic pillar array (μFPA) device," *Analyst,* vol. 143, no. 23, pp. 5841-5848, 2018.

[19] E. Kang, Y. Y. Choi, Y. Jun, B. G. Chung, and S.-H. Lee, "Development of a multi-layer microfluidic array chip to culture and replate uniform-sized embryoid bodies without manual cell retrieval," *Lab on a Chip,* vol. 10, no. 20, pp. 2651-2654, 2010.

[20] C. Eilenberger *et al.,* "A microfluidic multisize spheroid array for multiparametric screening of anticancer drugs and blood–brain barrier transport properties," *Advanced Science,* p. 2004856, 2021.

[21] H. Ota and N. Miki, "Microfluidic experimental platform for producing size-controlled three-dimensional spheroids," *Sensors and Actuators A: Physical,* vol. 169, no. 2, pp. 266-273, 2011.

[22] F. Akther, S. B. Yakob, N.-T. Nguyen, and H. T. Ta, "Surface modification techniques for endothelial cell seeding in PDMS microfluidic devices," *Biosensors,* vol. 10, no. 11, p. 182, 2020.

[23] M. Ferrari, F. Cirisano, and M. C. Morán, "Mammalian cell behavior on hydrophobic substrates: influence of surface properties," *Colloids and Interfaces,* vol. 3, no. 2, p. 48, 2019.

[24] K. Chen *et al.,* "Rapid formation of size-controllable multicellular spheroids via 3D acoustic tweezers," *Lab on a Chip,* vol. 16, no. 14, pp. 2636-2643, 2016.

[25] D. Bodas and C. Khan-Malek, "Formation of more stable hydrophilic surfaces of PDMS by plasma and chemical treatments," *Microelectronic engineering,* vol. 83, no. 4-9, pp. 1277-1279, 2006.

[26] A. Gokaltun, M. L. Yarmush, A. Asatekin, and O. B. Usta, "Recent advances in nonbiofouling PDMS surface modification strategies applicable to microfluidic technology," *Technology,* vol. 5, no. 01, pp. 1-12, 2017.

[27] W. Schrott *et al.,* "Study on surface properties of PDMS microfluidic chips treated with albumin," *Biomicrofluidics,* vol. 3, no. 4, p. 044101, 2009.

[28] W. Zhang, D. S. Choi, Y. H. Nguyen, J. Chang, and L. Qin, "Studying cancer stem cell dynamics on PDMS surfaces for microfluidics device design," *Scientific reports,* vol. 3, no. 1, pp. 1-8, 2013.

[29] A. C. R. Grayson *et al.,* "A BioMEMS review: MEMS technology for physiologically integrated devices," *Proceedings of the IEEE,* vol. 92, no. 1, pp. 6-21, 2004.

[30] E. Verpoorte and N. F. De Rooij, "Microfluidics meets MEMS," *Proceedings of the IEEE,* vol. 91, no. 6, pp. 930-953, 2003.

[31] N. Convery and N. Gadegaard, "30 years of microfluidics," *Micro and Nano Engineering,* 2019.

[32] G. M. Whitesides, "The origins and the future of microfluidics," *nature,* vol. 442, no. 7101, pp. 368-373, 2006.

[33] M. Astolfi *et al.*, "Micro-dissected tumor tissues on chip: an ex vivo method for drug testing and personalized therapy," *Lab on a Chip,* vol. 16, no. 2, pp. 312-325, 2016.

[34] D. Huh, G. A. Hamilton, and D. E. Ingber, "From 3D cell culture to organs-on-chips," *Trends in cell biology,* vol. 21, no. 12, pp. 745-754, 2011.

[35] W. Sun *et al.*, "Organ-on-a-chip for cancer and immune organs modeling," *Advanced healthcare materials,* vol. 8, no. 4, p. 1801363, 2019.

[36] N. S. Bhise *et al.*, "Organ-on-a-chip platforms for studying drug delivery systems," *Journal of Controlled Release,* vol. 190, pp. 82-93, 2014.

[37] A. Polini, L. Prodanov, N. S. Bhise, V. Manoharan, M. R. Dokmeci, and A. Khademhosseini, "Organs-on-a-chip: a new tool for drug discovery," *Expert opinion on drug discovery,* vol. 9, no. 4, pp. 335-352, 2014.

[38] D. Huh, B. D. Matthews, A. Mammoto, M. Montoya-Zavala, H. Y. Hsin, and D. E. Ingber, "Reconstituting organ-level lung functions on a chip," *Science,* vol. 328, no. 5986, pp. 1662-1668, 2010.

[39] Y. S. Zhang, Y.-N. Zhang, and W. Zhang, "Cancer-on-a-chip systems at the frontier of nanomedicine," *Drug Discov. Today,* vol. 22, no. 9, pp. 1392-1399, 2017.

[40] D. Huh *et al.*, "A human disease model of drug toxicity–induced pulmonary edema in a lung-on-a-chip microdevice," *Science translational medicine,* vol. 4, no. 159, pp. 159ra147-159ra147, 2012.

[41] W. Liu, M. Sun, B. Lu, M. Yan, K. Han, and J. Wang, "A microfluidic platform for multi-size 3D tumor culture, monitoring and drug resistance testing," *Sensors and Actuators B: Chemical,* vol. 292, pp. 111-120, 2019.

[42] D. Huh *et al.*, "Microfabrication of human organs-on-chips," *Nature protocols,* vol. 8, no. 11, pp. 2135-2157, 2013.

[43] S. N. Bhatia and C. S. Chen, "Tissue engineering at the micro-scale," *Biomedical Microdevices,* vol. 2, no. 2, pp. 131-144, 1999.

[44] C. D. Chin, V. Linder, and S. K. Sia, "Lab-on-a-chip devices for global health: Past studies and future opportunities," *Lab on a Chip,* vol. 7, no. 1, pp. 41-57, 2007.

[45] P. Abgrall and A. Gue, "Lab-on-chip technologies: making a microfluidic network and coupling it into a complete microsystem—a review," *Journal of micromechanics and microengineering,* vol. 17, no. 5, p. R15, 2007.

[46] Y. Temiz, R. D. Lovchik, G. V. Kaigala, and E. Delamarche, "Lab-on-a-chip devices: How to close and plug the lab?," *Microelectronic Engineering,* vol. 132, pp. 156-175, 2015.

[47] G. T. Kovacs, N. I. Maluf, and K. E. Petersen, "Bulk micromachining of silicon," *Proceedings of the IEEE,* vol. 86, no. 8, pp. 1536-1551, 1998.

[48] J. M. Bustillo, R. T. Howe, and R. S. Muller, "Surface micromachining for microelectromechanical systems," *Proceedings of the IEEE,* vol. 86, no. 8, pp. 1552-1574, 1998.

[49] M. A. Schmidt, "Wafer-to-wafer bonding for microstructure formation," *Proceedings of the IEEE,* vol. 86, no. 8, pp. 1575-1585, 1998.

[50] A. Manz, N. Graber, and H. á. Widmer, "Miniaturized total chemical analysis systems: a novel concept for chemical sensing," *Sensors and actuators B: Chemical,* vol. 1, no. 1-6, pp. 244-248, 1990.

[51] A. Manz *et al.*, "Planar chips technology for miniaturization and integration of separation techniques into monitoring systems: capillary electrophoresis on a chip," *Journal of Chromatography A,* vol. 593, no. 1-2, pp. 253-258, 1992.

[52] S. C. Jacobson, R. Hergenroder, L. B. Koutny, and J. M. Ramsey, "High-speed separations on a microchip," *Analytical Chemistry,* vol. 66, no. 7, pp. 1114-1118, 1994.

[53] D. J. Harrison, K. Fluri, K. Seiler, Z. Fan, C. S. Effenhauser, and A. Manz, "Micromachining a miniaturized capillary electrophoresis-based chemical analysis system on a chip," *Science,* vol. 261, no. 5123, pp. 895-897, 1993.

[54] C. M. Puleo, H.-C. Yeh, and T.-H. Wang, "Applications of MEMS technologies in tissue engineering," *Tissue engineering,* vol. 13, no. 12, pp. 2839-2854, 2007.

[55] R. Bashir, "BioMEMS: state-of-the-art in detection, opportunities and prospects," *Advanced drug delivery reviews,* vol. 56, no. 11, pp. 1565-1586, 2004.

[56] D. L. Polla *et al.*, "Microdevices in medicine," *Annual review of biomedical engineering,* vol. 2, no. 1, pp. 551-576, 2000.

[57] P. S. Dittrich and A. Manz, "Lab-on-a-chip: microfluidics in drug discovery," *Nature Reviews Drug Discovery,* vol. 5, no. 3, p. 210, 2006.

[58] S. R. Quake and A. Scherer, "From micro-to nanofabrication with soft materials," *Science,* vol. 290, no. 5496, pp. 1536-1540, 2000.

[59] B. Zhang and M. Radisic, "Organ-on-a-chip devices advance to market," *Lab on a Chip,* vol. 17, no. 14, pp. 2395-2420, 2017.

[60] C.-W. Tsao, "Polymer microfluidics: Simple, low-cost fabrication process bridging academic lab research to commercialized production," *Micromachines,* vol. 7, no. 12, p. 225, 2016.

[61] H. Becker and C. Gärtner, "Polymer microfabrication technologies for microfluidic systems," *Analytical and bioanalytical chemistry,* vol. 390, no. 1, pp. 89-111, 2008.

[62] J. Giboz, T. Copponnex, and P. Mélé, "Microinjection molding of thermoplastic polymers: a review," *Journal of micromechanics and microengineering,* vol. 17, no. 6, p. R96, 2007.

[63] B. J. Kim and E. Meng, "Review of polymer MEMS micromachining," *Journal of Micromechanics and Microengineering,* vol. 26, no. 1, p. 013001, 2015.

[64] J. Voldman, "BioMEMS: building with cells," *Nature materials,* vol. 2, no. 7, p. 433, 2003.

[65] D. Mark, S. Haeberle, G. Roth, F. Von Stetten, and R. Zengerle, "Microfluidic lab-on-a-chip platforms: requirements, characteristics and applications," in *Microfluidics based microsystems*: Springer, 2010, pp. 305-376.

[66] M. Canny, "Flow and transport in plants," *Annual Review of Fluid Mechanics,* vol. 9, no. 1, pp. 275-296, 1977.

[67] C. D. Chin, V. Linder, and S. K. Sia, "Commercialization of microfluidic point-of-care diagnostic devices," *Lab on a Chip,* vol. 12, no. 12, pp. 2118-2134, 2012.

[68] G. M. Whitesides, "What comes next?," *Lab on a Chip,* vol. 11, no. 2, pp. 191-193, 2011.

[69] H. A. Stone, A. D. Stroock, and A. Ajdari, "Engineering flows in small devices: microfluidics toward a lab-on-a-chip," *Annu. Rev. Fluid Mech.,* vol. 36, pp. 381-411, 2004.

[70] J. Saliba, A. Daou, S. Damiati, J. Saliba, M. El-Sabban, and R. Mhanna, "Development of microplatforms to mimic the in vivo architecture of CNS and PNS physiology and their diseases," *Genes,* vol. 9, no. 6, p. 285, 2018.

[71] T. M. Squires and S. R. Quake, "Microfluidics: Fluid physics at the nanoliter scale," *Reviews of modern physics,* vol. 77, no. 3, p. 977, 2005.

[72] R. Petri, "Eine kleine modification des Koch'schen plattenverfahrens," *Cntralbl. Bakteriol. Pasitenkunde,* vol. 1, pp. 279-280, 1887.

[73] A. T. Woolley and R. A. Mathies, "Ultra-high-speed DNA fragment separations using microfabricated capillary array electrophoresis chips," *proceedings of the National Academy of Sciences,* vol. 91, no. 24, pp. 11348-11352, 1994.

[74] J. P. Brody, Y. Han, R. H. Austin, and M. Bitensky, "Deformation and flow of red blood cells in a synthetic lattice: evidence for an active cytoskeleton," *Biophysical Journal,* vol. 68, no. 6, pp. 2224-2232, 1995.

[75] K. Srinivasan, C. Pohl, and N. Avdalovic, "Cross-linked polymer coatings for capillary electrophoresis and application to analysis of basic proteins, acidic proteins, and inorganic ions," *Analytical Chemistry,* vol. 69, no. 14, pp. 2798-2805, 1997.

[76] P. C. Li and D. J. Harrison, "Transport, manipulation, and reaction of biological cells on-chip using electrokinetic effects," *Analytical Chemistry,* vol. 69, no. 8, pp. 1564-1568, 1997.

[77] V. Hessel, H. Löwe, and F. Schönfeld, "Micromixers—a review on passive and active mixing principles," *Chemical Engineering Science,* vol. 60, no. 8-9, pp. 2479-2501, 2005.

[78] R. Daw and J. Finkelstein, "Insight: Lab on a chip," *Nature,* vol. 442, no. 7101, pp. 367-418, 2006.

[79] K. F. Lei, "Introduction: The Origin, Current Status, and Future of Microfluidics," *Microfluidics: Fundamental, Devices and Applications: Fundamentals and Applications,* pp. 1-18, 2018.

[80] P. V. Raje and N. C. Murmu, "A review on electrohydrodynamic-inkjet printing technology," *International Journal of Emerging Technology and Advanced Engineering,* vol. 4, no. 5, pp. 174-183, 2014.

[81] S. C. Terry, J. H. Jerman, and J. B. Angell, "A gas chromatographic air analyzer fabricated on a silicon wafer," *IEEE transactions on electron devices,* vol. 26, no. 12, pp. 1880-1886, 1979.

[82] S. Shoji, M. Esashi, and T. Matsuo, "Prototype miniature blood gas analyser fabricated on a silicon wafer," *Sensors and Actuators,* vol. 14, no. 2, pp. 101-107, 1988.

[83] R. Zengerle, J. Ulrich, S. Kluge, M. Richter, and A. Richter, "A bidirectional silicon micropump," *Sensors and Actuators A: Physical,* vol. 50, no. 1-2, pp. 81-86, 1995.

[84] R. Pacifici *et al.*, "Sweat testing of MDMA with the Drugwipe® analytical device: a controlled study with two volunteers," *Journal of analytical toxicology,* vol. 25, no. 2, pp. 144-146, 2001.

[85] J. Hicks and M. Iosefsohn, "Reliability of home pregnancy-test kits in the hands of laypersons," *The New England journal of medicine,* vol. 320, no. 5, pp. 320-321, 1989.

[86] A. H. Wu, "THEME: IMMUNOASSAY AUTOMATION AT THE MILLENNIUM-Laboratory and Near Patient Testing for Cardiac Markers," *Journal of Clinical Ligand Assay,* vol. 22, no. 1, pp. 32-37, 1999.

[87] S. Haeberle and R. Zengerle, "Microfluidic platforms for lab-on-a-chip applications," *Lab on a Chip,* vol. 7, no. 9, pp. 1094-1110, 2007.

[88] V. Srinivasan, V. K. Pamula, and R. B. Fair, "An integrated digital microfluidic lab-on-a-chip for clinical diagnostics on human physiological fluids," *Lab on a Chip,* vol. 4, no. 4, pp. 310-315, 2004.

[89] G. Nabovati, E. Ghafar-Zadeh, A. Letourneau, and M. Sawan, "Towards High Throughput Cell Growth Screening: A New CMOS 8$\times $8 Biosensor Array for Life Science Applications," *IEEE transactions on biomedical circuits and systems,* vol. 11, no. 2, pp. 380-391, 2016.

[90] J. Ozhikandathil, S. Badilescu, and M. Packirisamy, "Gold nanoisland structures integrated in a lab-on-a-chip for plasmonic detection of bovine growth hormone," *Journal of biomedical optics,* vol. 17, no. 7, p. 077001, 2012.

[91] H. Becker, T. Hansen-Hagge, and C. Gärtner, "Microfluidic devices for rapid identification and characterization of pathogens," in *Biological Identification*: Elsevier, 2014, pp. 220-249.

[92] W. Jung, J. Han, J.-W. Choi, and C. H. Ahn, "Point-of-care testing (POCT) diagnostic systems using microfluidic lab-on-a-chip technologies," *Microelectronic Engineering,* vol. 132, pp. 46-57, 2015.

[93] A. St John and C. P. Price, "Existing and emerging technologies for point-of-care testing," *The Clinical Biochemist Reviews,* vol. 35, no. 3, p. 155, 2014.

[94] T. R. Kozel and A. R. Burnham-Marusich, "Point-of-care testing for infectious diseases: past, present, and future," *Journal of clinical microbiology,* vol. 55, no. 8, pp. 2313-2320, 2017.

[95] M. L. Schito, M. Patricia D'Souza, S. Michele Owen, and M. P. Busch, "Challenges for rapid molecular HIV diagnostics," *Journal of Infectious Diseases,* vol. 201, no. Supplement_1, pp. S1-S6, 2010.

[96] B. Weigl, G. Domingo, P. LaBarre, and J. Gerlach, "Towards non-and minimally instrumented, microfluidics-based diagnostic devices," *Lab on a Chip,* vol. 8, no. 12, pp. 1999-2014, 2008.

[97] A. Heller and B. Feldman, "Electrochemical glucose sensors and their applications in diabetes management," *Chemical reviews,* vol. 108, no. 7, pp. 2482-2505, 2008.

[98] L. Liu, C. Peng, Z. Jin, and C. Xu, "Development and evaluation of a rapid lateral flow immunochromatographic strip assay for screening 19-nortestosterone," *Biomedical chromatography,* vol. 21, no. 8, pp. 861-866, 2007.

[99] S. A. Leavitt, "" A private little revolution": The home pregnancy test in American culture," *Bulletin of the History of Medicine,* vol. 80, no. 2, pp. 317-345, 2006.

[100] G. A. Posthuma-Trumpie, J. Korf, and A. van Amerongen, "Lateral flow (immuno) assay: its strengths, weaknesses, opportunities and threats. A literature survey," *Analytical and bioanalytical chemistry,* vol. 393, no. 2, pp. 569-582, 2009.

[101] J. Wang, "Electrochemical glucose biosensors," *Chemical reviews,* vol. 108, no. 2, pp. 814-825, 2008.

[102] L. S. Kuhn, "Biosensors: blockbuster or bomb?," *The Electrochemical Society Interface,* vol. 7, no. 4, pp. 26-31, 1998.

[103] E. W. Young, "Cells, tissues, and organs on chips: challenges and opportunities for the cancer tumor microenvironment," *Integrative Biology,* vol. 5, no. 9, pp. 1096-1109, 2013.

[104] P. Ahangar, M. E. Cooke, M. H. Weber, and D. H. Rosenzweig, "Current biomedical applications of 3D printing and additive manufacturing," *Applied sciences,* vol. 9, no. 8, p. 1713, 2019.

[105] D. Huh, Y.-s. Torisawa, G. A. Hamilton, H. J. Kim, and D. E. Ingber, "Microengineered physiological biomimicry: organs-on-chips," *Lab on a Chip,* vol. 12, no. 12, pp. 2156-2164, 2012.

[106] S. Han *et al.*, "A versatile assay for monitoring in vivo-like transendothelial migration of neutrophils," *Lab on a chip,* vol. 12, no. 20, pp. 3861-3865, 2012.

[107] J. Sosa-Hernández *et al.*, "Organs-on-a-chip module: a review from the development and applications perspective," *Micromachines,* vol. 9, no. 10, p. 536, 2018.

[108] N. J. Douville *et al.*, "Combination of fluid and solid mechanical stresses contribute to cell death and detachment in a microfluidic alveolar model," *Lab on a Chip,* vol. 11, no. 4, pp. 609-619, 2011.

[109] A. O. Stucki *et al.*, "A lung-on-a-chip array with an integrated bio-inspired respiration mechanism," *Lab on a Chip,* vol. 15, no. 5, pp. 1302-1310, 2015.

[110] A. Jain *et al.*, "Primary human lung alveolus-on-a-chip model of intravascular thrombosis for assessment of therapeutics," *Clinical pharmacology & therapeutics,* vol. 103, no. 2, pp. 332-340, 2018.

[111] T. Nguyen, D. Duong Bang, and A. Wolff, "2019 novel coronavirus disease (COVID-19): paving the road for rapid detection and point-of-care diagnostics," *Micromachines,* vol. 11, no. 3, p. 306, 2020.

[112] L. Si *et al.*, "Human organs-on-chips as tools for repurposing approved drugs as potential influenza and COVID19 therapeutics in viral pandemics," *bioRxiv,* 2020.

[113] J. Shao *et al.*, "Integrated microfluidic chip for endothelial cells culture and analysis exposed to a pulsatile and oscillatory shear stress," *Lab on a Chip,* vol. 9, no. 21, pp. 3118-3125, 2009.

[114] J. W. Song, W. Gu, N. Futai, K. A. Warner, J. E. Nor, and S. Takayama, "Computer-controlled microcirculatory support system for endothelial cell culture and shearing," *Analytical chemistry,* vol. 77, no. 13, pp. 3993-3999, 2005.

[115] T. Eschenhagen *et al.*, "Cardiovascular side effects of cancer therapies: a position statement from the Heart Failure Association of the European Society of Cardiology," *European journal of heart failure,* vol. 13, no. 1, pp. 1-10, 2011.

[116] P. Pacher and V. Kecskemeti, "Cardiovascular side effects of new antidepressants and antipsychotics: new drugs, old concerns?," *Current pharmaceutical design,* vol. 10, no. 20, pp. 2463-2475, 2004.

[117] H. T. H. Au, B. Cui, Z. E. Chu, T. Veres, and M. Radisic, "Cell culture chips for simultaneous application of topographical and electrical cues enhance phenotype of cardiomyocytes," *Lab on a chip,* vol. 9, no. 4, pp. 564-575, 2009.

[118] A. Marsano *et al.*, "Beating heart on a chip: a novel microfluidic platform to generate functional 3D cardiac microtissues," *Lab on a Chip,* vol. 16, no. 3, pp. 599-610, 2016.

[119] S. Ahn *et al.*, "Mussel-inspired 3D fiber scaffolds for heart-on-a-chip toxicity studies of engineered nanomaterials," *Analytical and bioanalytical chemistry,* vol. 410, no. 24, pp. 6141-6154, 2018.

[120] J. U. Lind *et al.*, "Instrumented cardiac microphysiological devices via multimaterial three-dimensional printing," *Nature materials,* vol. 16, no. 3, p. 303, 2017.

[121] Y. Xiao *et al.*, "Microfabricated perfusable cardiac biowire: a platform that mimics native cardiac bundle," *Lab on a Chip,* vol. 14, no. 5, pp. 869-882, 2014.

[122] L. Ren *et al.*, "Investigation of hypoxia-induced myocardial injury dynamics in a tissue interface mimicking microfluidic device," *Analytical chemistry,* vol. 85, no. 1, pp. 235-244, 2012.

[123] A. Günther *et al.*, "A microfluidic platform for probing small artery structure and function," *Lab on a Chip,* vol. 10, no. 18, pp. 2341-2349, 2010.

[124] Y. Xiong, A. Mahmood, and M. Chopp, "Animal models of traumatic brain injury," *Nature Reviews Neuroscience,* vol. 14, no. 2, p. 128, 2013.

[125] J. D. Caplin, N. G. Granados, M. R. James, R. Montazami, and N. Hashemi, "Microfluidic organ-on-a-chip technology for advancement of drug development and toxicology," *Advanced healthcare materials,* vol. 4, no. 10, pp. 1426-1450, 2015.

[126] A. M. Taylor, M. Blurton-Jones, S. W. Rhee, D. H. Cribbs, C. W. Cotman, and N. L. Jeon, "A microfluidic culture platform for CNS axonal injury, regeneration and transport," *Nature methods,* vol. 2, no. 8, p. 599, 2005.

[127] J. Park, S. Kim, S. I. Park, Y. Choe, J. Li, and A. Han, "A microchip for quantitative analysis of CNS axon growth under localized biomolecular treatments," *Journal of neuroscience methods,* vol. 221, pp. 166-174, 2014.

[128] J. Park, B. K. Lee, G. S. Jeong, J. K. Hyun, C. J. Lee, and S.-H. Lee, "Three-dimensional brain-on-a-chip with an interstitial level of flow and its application as an in vitro model of Alzheimer's disease," *Lab on a Chip,* vol. 15, no. 1, pp. 141-150, 2015.

[129] A. Kunze, M. Giugliano, A. Valero, and P. Renaud, "Micropatterning neural cell cultures in 3D with a multi-layered scaffold," *Biomaterials,* vol. 32, no. 8, pp. 2088-2098, 2011.

[130] O. Kilic *et al.,* "Brain-on-a-chip model enables analysis of human neuronal differentiation and chemotaxis," *Lab on a Chip,* vol. 16, no. 21, pp. 4152-4162, 2016.

[131] S. Dauth *et al.*, "Neurons derived from different brain regions are inherently different in vitro: a novel multiregional brain-on-a-chip," *Journal of neurophysiology,* vol. 117, no. 3, pp. 1320-1341, 2016.

[132] J. B. Mamani *et al.,* "Magnetic hyperthermia therapy in glioblastoma tumor on-a-Chip model," *Einstein (São Paulo),* vol. 18, 2020.

[133] L. A. Vernetti *et al.*, "A human liver microphysiology platform for investigating physiology, drug safety, and disease models," *Experimental biology and medicine,* vol. 241, no. 1, pp. 101-114, 2016.

[134] J. M. Prot *et al.,* "Improvement of HepG2/C3a cell functions in a microfluidic biochip," *Biotechnology and bioengineering,* vol. 108, no. 7, pp. 1704-1715, 2011.

[135] M. J. Powers *et al.*, "A microfabricated array bioreactor for perfused 3D liver culture," *Biotechnology and bioengineering,* vol. 78, no. 3, pp. 257-269, 2002.

[136] S.-A. Lee, E. Kang, J. Ju, D.-S. Kim, and S.-H. Lee, "Spheroid-based three-dimensional liver-on-a-chip to investigate hepatocyte–hepatic stellate cell interactions and flow effects," *Lab on a Chip,* vol. 13, no. 18, pp. 3529-3537, 2013.

[137] P. J. Lee, P. J. Hung, and L. P. Lee, "An artificial liver sinusoid with a microfluidic endothelial-like barrier for primary hepatocyte culture," *Biotechnology and bioengineering,* vol. 97, no. 5, pp. 1340-1346, 2007.

[138] D. Bavli *et al.*, "Real-time monitoring of metabolic function in liver-on-chip microdevices tracks the dynamics of mitochondrial dysfunction," *Proceedings of the National Academy of Sciences,* vol. 113, no. 16, pp. E2231-E2240, 2016.

[139] S. R. Khetani and S. N. Bhatia, "Microscale culture of human liver cells for drug development," *Nature biotechnology,* vol. 26, no. 1, p. 120, 2008.

[140] C. H. Cho, J. Park, A. W. Tilles, F. Berthiaume, M. Toner, and M. L. Yarmush, "Layered patterning of hepatocytes in co-culture systems using microfabricated stencils," *Biotechniques,* vol. 48, no. 1, pp. 47-52, 2010.

[141] B. Delalat *et al.*, "Microengineered bioartificial liver chip for drug toxicity screening," *Advanced Functional Materials,* vol. 28, no. 28, p. 1801825, 2018.

[142] Y. B. Kang *et al.*, "Liver sinusoid on a chip: Long-term layered co-culture of primary rat hepatocytes and endothelial cells in microfluidic platforms," *Biotechnology and bioengineering,* vol. 112, no. 12, pp. 2571-2582, 2015.

[143] Q. Zhou *et al.*, "Liver injury-on-a-chip: microfluidic co-cultures with integrated biosensors for monitoring liver cell signaling during injury," *Lab on a Chip,* vol. 15, no. 23, pp. 4467-4478, 2015.

[144] K.-i. Kamei, M. Yoshioka, S. Terada, Y. Tokunaga, and Y. Chen, "Three-dimensional cultured Liver-on-a-Chip with mature hepatocyte-like cells derived from human pluripotent stem cells," *Biomedical microdevices,* vol. 21, no. 3, p. 73, 2019.

[145] K.-J. Jang *et al.*, "Human kidney proximal tubule-on-a-chip for drug transport and nephrotoxicity assessment," *Integrative Biology,* vol. 5, no. 9, pp. 1119-1129, 2013.

[146] S. Musah *et al.*, "Mature induced-pluripotent-stem-cell-derived human podocytes reconstitute kidney glomerular-capillary-wall function on a chip," *Nature biomedical engineering,* vol. 1, no. 5, p. 0069, 2017.

[147] M. Zhou *et al.*, "Development of a functional glomerulus at the organ level on a chip to mimic hypertensive nephropathy," *Scientific reports,* vol. 6, p. 31771, 2016.

[148] J. Wang, C. Wang, N. Xu, Z.-F. Liu, D.-W. Pang, and Z.-L. Zhang, "A virus-induced kidney disease model based on organ-on-a-chip: Pathogenesis exploration of virus-related renal dysfunctions," *Biomaterials,* p. 119367, 2019.

[149] M. J. Wilmer, C. P. Ng, H. L. Lanz, P. Vulto, L. Suter-Dick, and R. Masereeuw, "Kidney-on-a-chip technology for drug-induced nephrotoxicity screening," *Trends in biotechnology,* vol. 34, no. 2, pp. 156-170, 2016.

[150] H. Kimura, T. Yamamoto, H. Sakai, Y. Sakai, and T. Fujii, "An integrated microfluidic system for long-term perfusion culture and on-line monitoring of intestinal tissue models," *Lab on a Chip,* vol. 8, no. 5, pp. 741-746, 2008.

[151] H. J. Kim and D. E. Ingber, "Gut-on-a-Chip microenvironment induces human intestinal cells to undergo villus differentiation," *Integrative Biology,* vol. 5, no. 9, pp. 1130-1140, 2013.

[152] H. J. Kim, H. Li, J. J. Collins, and D. E. Ingber, "Contributions of microbiome and mechanical deformation to intestinal bacterial overgrowth and inflammation in a human gut-on-a-chip," *Proceedings of the National Academy of Sciences,* vol. 113, no. 1, pp. E7-E15, 2016.

[153] W. Shin, C. D. Hinojosa, D. E. Ingber, and H. J. Kim, "Human Intestinal Morphogenesis Controlled by Transepithelial Morphogen Gradient and Flow-Dependent Physical Cues in a Microengineered Gut-on-a-Chip," *iScience,* vol. 15, pp. 391-406, 2019.

[154] M. Jahanshahi *et al.*, "An Engineered Infected Epidermis Model for In Vitro Study of the Skin's Pro-Inflammatory Response," *Micromachines,* vol. 11, no. 2, p. 227, 2020.

[155] M. H. Mohammadi *et al.*, "Skin diseases modeling using combined tissue engineering and microfluidic technologies," *Advanced healthcare materials,* vol. 5, no. 19, pp. 2459-2480, 2016.

[156] I. Wagner *et al.*, "A dynamic multi-organ-chip for long-term cultivation and substance testing proven by 3D human liver and skin tissue co-culture," *Lab on a Chip,* vol. 13, no. 18, pp. 3538-3547, 2013.

[157] H. E. Abaci, K. Gledhill, Z. Guo, A. M. Christiano, and M. L. Shuler, "Pumpless microfluidic platform for drug testing on human skin equivalents," *Lab on a Chip,* vol. 15, no. 3, pp. 882-888, 2015.

[158] F. A. Alexander, S. Eggert, and J. Wiest, "Skin-on-a-chip: transepithelial electrical resistance and extracellular acidification measurements through an automated air-liquid interface," *Genes,* vol. 9, no. 2, p. 114, 2018.

[159] B. S. Kwak, S. P. Jin, S. J. Kim, E. J. Kim, J. H. Chung, and J. H. Sung, "Microfluidic skin chip with vasculature for recapitulating the immune response of the skin tissue," *Biotechnology and Bioengineering,* 2020.

[160] M. Wufuer *et al.*, "Skin-on-a-chip model simulating inflammation, edema and drug-based treatment," *Scientific reports,* vol. 6, p. 37471, 2016.

[161] S. Lee, S.-P. Jin, Y. K. Kim, G. Y. Sung, J. H. Chung, and J. H. Sung, "Construction of 3D multicellular microfluidic chip for an in vitro skin model," *Biomedical microdevices,* vol. 19, no. 2, p. 22, 2017.

[162] N. Jusoh, J. Ko, and N. L. Jeon, "Microfluidics-based skin irritation test using in vitro 3D angiogenesis platform," *APL bioengineering,* vol. 3, no. 3, p. 036101, 2019.

[163] A. Rezaei Kolahchi *et al.*, "Microfluidic-based multi-organ platforms for drug discovery," *Micromachines,* vol. 7, no. 9, p. 162, 2016.

[164] H. E. Abaci and M. L. Shuler, "Human-on-a-chip design strategies and principles for physiologically based pharmacokinetics/pharmacodynamics modeling," *Integrative Biology,* vol. 7, no. 4, pp. 383-391, 2015.

[165] L. Shintu *et al.*, "Metabolomics-on-a-chip and predictive systems toxicology in microfluidic bioartificial organs," *Analytical chemistry,* vol. 84, no. 4, pp. 1840-1848, 2012.

[166] G. Vunjak-Novakovic, S. Bhatia, C. Chen, and K. Hirschi, "HeLiVa platform: integrated heart-liver-vascular systems for drug testing in human health and disease," *Stem cell research & therapy,* vol. 4, no. 1, p. S8, 2013.

[167] I. Maschmeyer *et al.*, "Chip-based human liver–intestine and liver–skin co-cultures–A first step toward systemic repeated dose substance testing in vitro," *European journal of pharmaceutics and biopharmaceutics,* vol. 95, pp. 77-87, 2015.

[168] T. Bricks *et al.*, "Development of a new microfluidic platform integrating co-cultures of intestinal and liver cell lines," *Toxicology in Vitro,* vol. 28, no. 5, pp. 885-895, 2014.

[169] I. Maschmeyer *et al.*, "A four-organ-chip for interconnected long-term co-culture of human intestine, liver, skin and kidney equivalents," *Lab on a Chip,* vol. 15, no. 12, pp. 2688-2699, 2015.

[170] J. H. Sung and M. L. Shuler, "A micro cell culture analog (μCCA) with 3-D hydrogel culture of multiple cell lines to assess metabolism-dependent cytotoxicity of anti-cancer drugs," *Lab on a Chip,* vol. 9, no. 10, pp. 1385-1394, 2009.

[171] K. Viravaidya and M. L. Shuler, "Incorporation of 3T3-L1 cells to mimic bioaccumulation in a microscale cell culture analog device for toxicity studies," *Biotechnology progress,* vol. 20, no. 2, pp. 590-597, 2004.

[172] C. Zhang, Z. Zhao, N. A. A. Rahim, D. van Noort, and H. Yu, "Towards a human-on-chip: culturing multiple cell types on a chip with compartmentalized microenvironments," *Lab on a Chip,* vol. 9, no. 22, pp. 3185-3192, 2009.

[173] E. Iori, B. Vinci, E. Murphy, M. C. Marescotti, A. Avogaro, and A. Ahluwalia, "Glucose and fatty acid metabolism in a 3 tissue in-vitro model challenged with normo-and hyperglycaemia," *PloS one,* vol. 7, no. 4, p. e34704, 2012.

[174] N. Ucciferri, T. Sbrana, and A. Ahluwalia, "Allometric scaling and cell ratios in multi-organ in vitro models of human metabolism," *Frontiers in bioengineering and biotechnology,* vol. 2, p. 74, 2014.

[175] Y. S. Zhang *et al.*, "Multisensor-integrated organs-on-chips platform for automated and continual in situ monitoring of organoid behaviors," *Proceedings of the National Academy of Sciences,* p. 201612906, 2017.

[176] D. A. Roberts, H. M. Kantarjian, and D. P. Steensma, "Contract research organizations in oncology clinical research: Challenges and opportunities," *Cancer,* vol. 122, no. 10, pp. 1476-1482, 2016.

[177] A. Valente, "MEMS Devices in Agriculture," in *Advanced Mechatronics and MEMS Devices II*: Springer, 2017, pp. 367-385.

[178] Y. Kim *et al.*, "Integrated Microfluidic Preconcentration and Nucleic Amplification System for Detection of Influenza A Virus H1N1 in Saliva," *Micromachines,* vol. 11, no. 2, p. 203, 2020.

[179] L. Li, B. Miao, Z. Li, Z. Sun, and N. Peng, "Sample-to-Answer Hepatitis B Virus DNA Detection from Whole Blood on a Centrifugal Microfluidic Platform with Double Rotation Axes," *ACS sensors,* vol. 4, no. 10, pp. 2738-2745, 2019.

[180] J. R. Mejía-Salazar, K. Rodrigues Cruz, and E. M. Materón Vásques, "Microfluidic Point-of-Care Devices: New Trends and Future Prospects for eHealth Diagnostics," *Sensors,* vol. 20, no. 7, p. 1951, 2020.

[181] J. Lu *et al.*, "Application of microfluidic chips in separation and analysis of extracellular vesicles in liquid biopsy for cancer," *Micromachines,* vol. 10, no. 6, p. 390, 2019.

[182] S. Sharma, V. Kumar, A. Chawla, and A. Logani, "Rapid detection of SARS-CoV-2 in saliva: Can an endodontist take the lead in point-of-care COVID-19 testing?," *International Endodontic Journal,* 2020.

[183] T. Yang, Y.-C. Wang, C.-F. Shen, and C.-M. Cheng, "Point-of-care RNA-based diagnostic device for COVID-19," ed: Multidisciplinary Digital Publishing Institute, 2020.

[184] B. Udugama *et al.*, "Diagnosing COVID-19: the disease and tools for detection," *ACS nano*, vol. 14, no. 4, pp. 3822-3835, 2020.

[185] R. Riahi, A. Tamayol, S. A. M. Shaegh, A. M. Ghaemmaghami, M. R. Dokmeci, and A. Khademhosseini, "Microfluidics for advanced drug delivery systems," *Current opinion in chemical engineering*, vol. 7, pp. 101-112, 2015.

[186] R. B. Mokhtari *et al.*, "Combination therapy in combating cancer," *Oncotarget*, vol. 8, no. 23, p. 38022, 2017.

[187] M. Zhao and D.-Q. Wei, "Rare diseases: Drug discovery and informatics resource," *Interdisciplinary Sciences: Computational Life Sciences*, vol. 10, no. 1, pp. 195-204, 2018.

[188] C. P. P. de Mello, J. Rumsey, V. Slaughter, and J. J. Hickman, "A human-on-a-chip approach to tackling rare diseases," *Drug Discov. Today*, 2019.

[189] R. Siegle, D. Naishadham, and A. Jemal, "Cancer statistics, 2012," *CA Cancer J. Clin*, vol. 62, no. 1, pp. 10-29, 2012.

[190] K. A. Cronin *et al.*, "Annual Report to the Nation on the Status of Cancer, part I: National cancer statistics," *Cancer*, vol. 124, no. 13, pp. 2785-2800, 2018.

[191] D. Hanahan and R. A. Weinberg, "Hallmarks of cancer: the next generation," *cell*, vol. 144, no. 5, pp. 646-674, 2011.

[192] L. Bejarano, M. J. Jordão, and J. A. Joyce, "Therapeutic targeting of the tumor microenvironment," *Cancer discovery*, vol. 11, no. 4, pp. 933-959, 2021.

[193] B. Arneth, "Tumor microenvironment," *Medicina*, vol. 56, no. 1, p. 15, 2020.

[194] G. Kaur and J. M. Dufour, "Cell lines: Valuable tools or useless artifacts," vol. 2, ed: Taylor & Francis, 2012, pp. 1-5.

[195] E. Boedtkjer and S. F. Pedersen, "The acidic tumor microenvironment as a driver of cancer," *Annual review of physiology*, vol. 82, pp. 103-126, 2020.

[196] A. C. Luca *et al.*, "Impact of the 3D microenvironment on phenotype, gene expression, and EGFR inhibition of colorectal cancer cell lines," *PloS one*, vol. 8, no. 3, p. e59689, 2013.

[197] X. Cui, Y. Hartanto, and H. Zhang, "Advances in multicellular spheroids formation," *Journal of the Royal Society Interface*, vol. 14, no. 127, p. 20160877, 2017.

[198] E. Fennema, N. Rivron, J. Rouwkema, C. van Blitterswijk, and J. De Boer, "Spheroid culture as a tool for creating 3D complex tissues," *Trends in biotechnology*, vol. 31, no. 2, pp. 108-115, 2013.

[199] G. Lazzari, V. Nicolas, M. Matsusaki, M. Akashi, P. Couvreur, and S. Mura, "Multicellular spheroid based on a triple co-culture: A novel 3D model to mimic pancreatic tumor complexity," *Acta biomaterialia*, vol. 78, pp. 296-307, 2018.

[200] R. M. Sutherland, J. A. McCredie, and W. R. Inch, "Growth of multicell spheroids in tissue culture as a model of nodular carcinomas," *Journal of the National Cancer Institute*, vol. 46, no. 1, pp. 113-120, 1971.

[201] A. S. Nunes, A. S. Barros, E. C. Costa, A. F. Moreira, and I. J. Correia, "3D tumor spheroids as in vitro models to mimic in vivo human solid tumors resistance to therapeutic drugs," *Biotechnology and bioengineering*, vol. 116, no. 1, pp. 206-226, 2019.

[202] B. Patra, C. Peng, W. Liao, C. Lee, and Y. Tung, "Drug testing and flow cytometry analysis on a large number of uniform sized tumor spheroids using a microfluidic device. Sci Rep," ed: Nature Publishing Group, 2016.

[203] R. M. Sutherland, W. R. Inch, J. A. McCredie, and J. Kruuv, "A multi-component radiation survival curve using an in vitro tumour model," *International Journal of Radiation Biology and Related Studies in Physics, Chemistry and Medicine,* vol. 18, no. 5, pp. 491-495, 1970.

[204] A. Y. Hsiao *et al.*, "Microfluidic system for formation of PC-3 prostate cancer co-culture spheroids," *Biomaterials,* vol. 30, no. 16, pp. 3020-3027, 2009.

[205] J. Ruppen *et al.*, "Towards personalized medicine: chemosensitivity assays of patient lung cancer cell spheroids in a perfused microfluidic platform," *Lab on a Chip,* vol. 15, no. 14, pp. 3076-3085, 2015.

[206] V. Dangles-Marie *et al.*, "A three-dimensional tumor cell defect in activating autologous CTLs is associated with inefficient antigen presentation correlated with heat shock protein-70 down-regulation," *Cancer research,* vol. 63, no. 13, pp. 3682-3687, 2003.

[207] S.-A. Kim, E. K. Lee, and H.-J. Kuh, "Co-culture of 3D tumor spheroids with fibroblasts as a model for epithelial–mesenchymal transition in vitro," *Experimental cell research,* vol. 335, no. 2, pp. 187-196, 2015.

[208] N. Timmins, S. Dietmair, and L. Nielsen, "Hanging-drop multicellular spheroids as a model of tumour angiogenesis," *Angiogenesis,* vol. 7, no. 2, pp. 97-103, 2004.

[209] L.-B. Weiswald, D. Bellet, and V. Dangles-Marie, "Spherical cancer models in tumor biology," *Neoplasia,* vol. 17, no. 1, pp. 1-15, 2015.

[210] N. E. Timmins and L. K. Nielsen, "Generation of multicellular tumor spheroids by the hanging-drop method," in *Tissue engineering*: Springer, 2007, pp. 141-151.

[211] J. M. Yuhas, A. P. Li, A. O. Martinez, and A. J. Ladman, "A simplified method for production and growth of multicellular tumor spheroids," *Cancer research,* vol. 37, no. 10, pp. 3639-3643, 1977.

[212] V. Dangles-Marie *et al.*, "Establishment of human colon cancer cell lines from fresh tumors versus xenografts: comparison of success rate and cell line features," *Cancer research,* vol. 67, no. 1, pp. 398-407, 2007.

[213] M. Vinci *et al.*, "Advances in establishment and analysis of three-dimensional tumor spheroid-based functional assays for target validation and drug evaluation," *BMC biology,* vol. 10, no. 1, pp. 1-21, 2012.

[214] S. L. Nyberg, J. Hardin, B. Amiot, U. A. Argikar, R. P. Remmel, and P. Rinaldo, "Rapid, large-scale formation of porcine hepatocyte spheroids in a novel spheroid reservoir bioartificial liver," *Liver transplantation,* vol. 11, no. 8, pp. 901-910, 2005.

[215] V. E. Santo *et al.*, "Adaptable stirred-tank culture strategies for large scale production of multicellular spheroid-based tumor cell models," *Journal of biotechnology*, vol. 221, pp. 118-129, 2016.

[216] N. Azizipour, R. Avazpour, D. H. Rosenzweig, M. Sawan, and A. Ajji, "Evolution of biochip technology: A review from lab-on-a-chip to organ-on-a-chip," *Micromachines*, vol. 11, no. 6, p. 599, 2020.

[217] B. Patra *et al.*, "Carboplatin sensitivity in epithelial ovarian cancer cell lines: The impact of model systems," *Plos one*, vol. 15, no. 12, p. e0244549, 2020.

[218] Y. Y. Choi, J. Kim, S.-H. Lee, and D.-S. Kim, "Lab on a chip-based hepatic sinusoidal system simulator for optimal primary hepatocyte culture," *Biomedical microdevices*, vol. 18, no. 4, pp. 1-9, 2016.

[219] A. Munaz, R. K. Vadivelu, J. A. St John, and N.-T. Nguyen, "A lab-on-a-chip device for investigating the fusion process of olfactory ensheathing cell spheroids," *Lab on a Chip*, vol. 16, no. 15, pp. 2946-2954, 2016.

[220] H. F. Chan, Y. Zhang, Y.-P. Ho, Y.-L. Chiu, Y. Jung, and K. W. Leong, "Rapid formation of multicellular spheroids in double-emulsion droplets with controllable microenvironment," *Scientific reports*, vol. 3, no. 1, pp. 1-8, 2013.

[221] C. Kim *et al.*, "Generation of core-shell microcapsules with three-dimensional focusing device for efficient formation of cell spheroid," *Lab on a Chip*, vol. 11, no. 2, pp. 246-252, 2011.

[222] B. Patra, C.-C. Peng, W.-H. Liao, C.-H. Lee, and Y.-C. Tung, "Drug testing and flow cytometry analysis on a large number of uniform sized tumor spheroids using a microfluidic device," *Scientific reports*, vol. 6, no. 1, pp. 1-12, 2016.

[223] Y.-s. Torisawa *et al.*, "Efficient formation of uniform-sized embryoid bodies using a compartmentalized microchannel device," *Lab on a Chip*, vol. 7, no. 6, pp. 770-776, 2007.

[224] K. Lee *et al.*, "Gravity-oriented microfluidic device for uniform and massive cell spheroid formation," *Biomicrofluidics*, vol. 6, no. 1, p. 014114, 2012.

[225] Z. Chen *et al.*, "Microfluidic arrays of dermal spheroids: a screening platform for active ingredients of skincare products," *Lab on a Chip*, vol. 21, no. 20, pp. 3952-3962, 2021.

[226] N. Rousset, F. Monet, and T. Gervais, "Simulation-assisted design of microfluidic sample traps for optimal trapping and culture of non-adherent single cells, tissues, and spheroids," *Scientific reports*, vol. 7, no. 1, pp. 1-12, 2017.

[227] M. Marimuthu *et al.*, "Multi-size spheroid formation using microfluidic funnels," *Lab on a Chip*, vol. 18, no. 2, pp. 304-314, 2018.

[228] J. Schakenraad and H. Busscher, "Cell—polymer interactions: The influence of protein adsorption," *Colloids and surfaces*, vol. 42, no. 3-4, pp. 331-343, 1989.

[229] A. Baszkin and W. Norde, *Physical chemistry of biological interfaces*. CRC Press, 1999.

[230] S. F. Badylak, *Host response to biomaterials: the impact of host response on biomaterial selection*. Academic Press, 2015.

[231] S. Prauzner-Bechcicki *et al.*, "PDMS substrate stiffness affects the morphology and growth profiles of cancerous prostate and melanoma cells," *Journal of the mechanical behavior of biomedical materials*, vol. 41, pp. 13-22, 2015.

[232] J. Raczkowska *et al.*, "Physico-chemical properties of PDMS surfaces suitable as substrates for cell cultures," *Applied Surface Science*, vol. 389, pp. 247-254, 2016.

[233] S. Kim, A. E. English, and K. D. Kihm, "Surface elasticity and charge concentration-dependent endothelial cell attachment to copolymer polyelectrolyte hydrogel," *Acta biomaterialia*, vol. 5, no. 1, pp. 144-151, 2009.

[234] S. Gonçalves, F. Dourado, and L. R. Rodrigues, "Overview on cell-biomaterial interactions," in *Advanced Polymers in Medicine*: Springer, 2015, pp. 91-128.

[235] M. Donoso, A. Méndez-Vilas, J. Bruque, and M. González-Martin, "On the relationship between common amplitude surface roughness parameters and surface area: Implications for the study of cell–material interactions," *International Biodeterioration & Biodegradation*, vol. 59, no. 3, pp. 245-251, 2007.

[236] T.-W. Chung, D.-Z. Liu, S.-Y. Wang, and S.-S. Wang, "Enhancement of the growth of human endothelial cells by surface roughness at nanometer scale," *Biomaterials*, vol. 24, no. 25, pp. 4655-4661, 2003.

[237] A. Ranella, M. Barberoglou, S. Bakogianni, C. Fotakis, and E. Stratakis, "Tuning cell adhesion by controlling the roughness and wettability of 3D micro/nano silicon structures," *Acta biomaterialia*, vol. 6, no. 7, pp. 2711-2720, 2010.

[238] N. Azizipour, R. Avazpour, M. Sawan, D. Rosenzweig, and A. Ajji, "Uniformity of spheroid-on-chip by surface treatment of PDMS microfluidic platforms," *bioRxiv*, 2022.

[239] M. Ferrari and F. Ravera, "Surfactants and wetting at superhydrophobic surfaces: Water solutions and non aqueous liquids," *Advances in colloid and interface science*, vol. 161, no. 1-2, pp. 22-28, 2010.

[240] M. C. Morán, G. Ruano, F. Cirisano, and M. Ferrari, "Mammalian cell viability on hydrophobic and superhydrophobic fabrics," *Materials Science and Engineering: C*, vol. 99, pp. 241-247, 2019.

[241] K. Ren, J. Zhou, and H. Wu, "Materials for microfluidic chip fabrication," *Accounts of chemical research*, vol. 46, no. 11, pp. 2396-2406, 2013.

[242] J. N. Lee, X. Jiang, D. Ryan, and G. M. Whitesides, "Compatibility of mammalian cells on surfaces of poly (dimethylsiloxane)," *Langmuir*, vol. 20, no. 26, pp. 11684-11691, 2004.

[243] M. Morra, E. Occhiello, R. Marola, F. Garbassi, P. Humphrey, and D. Johnson, "On the aging of oxygen plasma-treated polydimethylsiloxane surfaces," *Journal of Colloid and Interface Science*, vol. 137, no. 1, pp. 11-24, 1990.

[244] Z. Wang, A. A. Volinsky, and N. D. Gallant, "Crosslinking effect on polydimethylsiloxane elastic modulus measured by custom-built compression instrument," *Journal of Applied Polymer Science*, vol. 131, no. 22, 2014.

[245] J. Gu, J. Wang, Y. Li, X. Xu, C. Chen, and L. Winnubst, "Engineering durable hydrophobic surfaces on porous alumina ceramics using in-situ formed inorganic-organic

hybrid nanoparticles," *Journal of the European Ceramic Society,* vol. 37, no. 15, pp. 4843-4848, 2017.

[246] B. Van Meer *et al.*, "Small molecule absorption by PDMS in the context of drug response bioassays," *Biochemical and biophysical research communications,* vol. 482, no. 2, pp. 323-328, 2017.

[247] K. Y. Chumbimuni-Torres *et al.*, "Adsorption of proteins to thin-films of PDMS and its effect on the adhesion of human endothelial cells," *RSC advances,* vol. 1, no. 4, pp. 706-714, 2011.

[248] W. Liu, K. Han, M. Sun, and J. Wang, "Enhancement and control of neuron adhesion on polydimethylsiloxane for cell microengineering using a functionalized triblock polymer," *Lab on a Chip,* vol. 19, no. 19, pp. 3162-3167, 2019.

[249] M. H. Wu, "Simple poly (dimethylsiloxane) surface modification to control cell adhesion," *Surface and Interface Analysis: An International Journal devoted to the development and application of techniques for the analysis of surfaces, interfaces and thin films,* vol. 41, no. 1, pp. 11-16, 2009.

[250] D. Bodas and C. Khan-Malek, "Hydrophilization and hydrophobic recovery of PDMS by oxygen plasma and chemical treatment—An SEM investigation," *Sensors and actuators B: chemical,* vol. 123, no. 1, pp. 368-373, 2007.

[251] D. P. Dowling, I. S. Miller, M. Ardhaoui, and W. M. Gallagher, "Effect of surface wettability and topography on the adhesion of osteosarcoma cells on plasma-modified polystyrene," *Journal of biomaterials applications,* vol. 26, no. 3, pp. 327-347, 2011.

[252] I. Wong and C.-M. Ho, "Surface molecular property modifications for poly (dimethylsiloxane)(PDMS) based microfluidic devices," *Microfluidics and nanofluidics,* vol. 7, no. 3, pp. 291-306, 2009.

[253] A. Shakeri, S. Khan, and T. F. Didar, "Conventional and emerging strategies for the fabrication and functionalization of PDMS-based microfluidic devices," *Lab on a Chip,* vol. 21, no. 16, pp. 3053-3075, 2021.

[254] H. Zhang and M. Chiao, "Anti-fouling coatings of poly (dimethylsiloxane) devices for biological and biomedical applications," *Journal of medical and biological engineering,* vol. 35, no. 2, pp. 143-155, 2015.

[255] C. Kim, J. H. Bang, Y. E. Kim, S. H. Lee, and J. Y. Kang, "On-chip anticancer drug test of regular tumor spheroids formed in microwells by a distributive microchannel network," *Lab on a chip,* vol. 12, no. 20, pp. 4135-4142, 2012.

[256] N. Dadgar *et al.*, "A microfluidic platform for cultivating ovarian cancer spheroids and testing their responses to chemotherapies," *Microsystems & Nanoengineering,* vol. 6, no. 1, pp. 1-12, 2020.

[257] D. Dorrigiv *et al.*, "Microdissected Tissue vs Tissue Slices—A Comparative Study of Tumor Explant Models Cultured On-Chip and Off-Chip," *Cancers,* vol. 13, no. 16, p. 4208, 2021.

[258] K. Ziółkowska, A. Stelmachowska, R. Kwapiszewski, M. Chudy, A. Dybko, and Z. Brzózka, "Long-term three-dimensional cell culture and anticancer drug activity

evaluation in a microfluidic chip," *Biosensors and Bioelectronics,* vol. 40, no. 1, pp. 68-74, 2013.

[259] Y.-C. Chen, X. Lou, Z. Zhang, P. Ingram, and E. Yoon, "High-throughput cancer cell sphere formation for characterizing the efficacy of photo dynamic therapy in 3D cell cultures," *Scientific reports,* vol. 5, no. 1, pp. 1-12, 2015.

[260] F. Re *et al.,* "Inhibition of anchorage-dependent cell spreading triggers apoptosis in cultured human endothelial cells," *The Journal of cell biology,* vol. 127, no. 2, pp. 537-546, 1994.

[261] J. Zhou, D. A. Khodakov, A. V. Ellis, and N. H. Voelcker, "Surface modification for PDMS-based microfluidic devices," *Electrophoresis,* vol. 33, no. 1, pp. 89-104, 2012.

[262] J. Zhou, A. V. Ellis, and N. H. Voelcker, "Recent developments in PDMS surface modification for microfluidic devices," *Electrophoresis,* vol. 31, no. 1, pp. 2-16, 2010.

[263] G. K. Toworfe, R. J. Composto, C. S. Adams, I. M. Shapiro, and P. Ducheyne, "Fibronectin adsorption on surface-activated poly (dimethylsiloxane) and its effect on cellular function," *Journal of Biomedical Materials Research Part A: An Official Journal of The Society for Biomaterials, The Japanese Society for Biomaterials, and The Australian Society for Biomaterials and the Korean Society for Biomaterials,* vol. 71, no. 3, pp. 449-461, 2004.

[264] T. A. Wani, A. H. Bakheit, M. Abounassif, and S. Zargar, "Study of interactions of an anticancer drug neratinib with bovine serum albumin: spectroscopic and molecular docking approach," *Frontiers in chemistry,* vol. 6, p. 47, 2018.

[265] D. Kim and A. E. Herr, "Protein immobilization techniques for microfluidic assays," *Biomicrofluidics,* vol. 7, no. 4, p. 041501, 2013.

[266] D. A. Belinskaia *et al.,* "The Universal Soldier: Enzymatic and Non-Enzymatic Antioxidant Functions of Serum Albumin," *Antioxidants,* vol. 9, no. 10, p. 966, 2020.

[267] Q. Tan, J. Ji, F. Zhao, D.-Z. Fan, F.-Y. Sun, and J.-C. Shen, "Fabrication of thromboresistant multilayer thin film on plasma treated poly (vinyl chloride) surface," *Journal of Materials Science: Materials in Medicine,* vol. 16, no. 7, pp. 687-692, 2005.

[268] T. Windvoel, M. Mbanjwa, N. Mokone, A. Mogale, and K. Land, "Surface analysis of polydimethylsiloxane fouled with bovine serum albumin," 2010.

[269] K. Boxshall, M. H. Wu, Z. Cui, Z. Cui, J. F. Watts, and M. A. Baker, "Simple surface treatments to modify protein adsorption and cell attachment properties within a poly (dimethylsiloxane) micro-bioreactor," *Surface and Interface Analysis: An International Journal devoted to the development and application of techniques for the analysis of surfaces, interfaces and thin films,* vol. 38, no. 4, pp. 198-201, 2006.

[270] V. A. Liu, W. E. Jastromb, and S. N. Bhatia, "Engineering protein and cell adhesivity using PEO-terminated triblock polymers," *Journal of biomedical materials research,* vol. 60, no. 1, pp. 126-134, 2002.

[271] T. Tharmalingam, H. Ghebeh, T. Wuerz, and M. Butler, "Pluronic enhances the robustness and reduces the cell attachment of mammalian cells," *Molecular biotechnology,* vol. 39, no. 2, pp. 167-177, 2008.

[272] C. Freij-Larsson, T. Nylander, P. Jannasch, and B. Wesslén, "Adsorption behaviour of amphiphilic polymers at hydrophobic surfaces: effects on protein adsorption," *Biomaterials,* vol. 17, no. 22, pp. 2199-2207, 1996.

[273] S. Pinto *et al.*, "Poly (dimethyl siloxane) surface modification by low pressure plasma to improve its characteristics towards biomedical applications," *Colloids and Surfaces B: Biointerfaces,* vol. 81, no. 1, pp. 20-26, 2010.

[274] Z. Wu and K. Hjort, "Surface modification of PDMS by gradient-induced migration of embedded Pluronic," *Lab on a Chip,* vol. 9, no. 11, pp. 1500-1503, 2009.

[275] M. H. Wu, J. P. Urban, Z. Cui, and Z. F. Cui, "Development of PDMS microbioreactor with well-defined and homogenous culture environment for chondrocyte 3-D culture," *Biomedical microdevices,* vol. 8, no. 4, pp. 331-340, 2006.

[276] C. Calitz, N. Pavlović, J. Rosenquist, C. Zagami, A. Samanta, and F. Heindryckx, "A biomimetic model for liver Cancer to study Tumor-Stroma interactions in a 3D environment with tunable Bio-Physical properties," *JoVE (Journal of Visualized Experiments),* no. 162, p. e61606, 2020.

[277] J. Fukuda *et al.*, "Micromolding of photocrosslinkable chitosan hydrogel for spheroid microarray and co-cultures," *Biomaterials,* vol. 27, no. 30, pp. 5259-5267, 2006.

[278] G. Mehta, A. Y. Hsiao, M. Ingram, G. D. Luker, and S. Takayama, "Opportunities and challenges for use of tumor spheroids as models to test drug delivery and efficacy," *Journal of controlled release,* vol. 164, no. 2, pp. 192-204, 2012.

[279] J. N. Lee, C. Park, and G. M. Whitesides, "Solvent compatibility of poly (dimethylsiloxane)-based microfluidic devices," *Analytical chemistry,* vol. 75, no. 23, pp. 6544-6554, 2003.

[280] A. Gökaltun, Y. B. A. Kang, M. L. Yarmush, O. B. Usta, and A. Asatekin, "Simple surface modification of poly (dimethylsiloxane) via surface segregating smart polymers for biomicrofluidics," *Scientific reports,* vol. 9, no. 1, pp. 1-14, 2019.

[281] J. A. Vickers, M. M. Caulum, and C. S. Henry, "Generation of hydrophilic poly (dimethylsiloxane) for high-performance microchip electrophoresis," *Analytical chemistry,* vol. 78, no. 21, pp. 7446-7452, 2006.

[282] X. Zhang, L. Li, and Y. Zhang, "Study on the surface structure and properties of PDMS/PMMA antifouling coatings," *Physics Procedia,* vol. 50, pp. 328-336, 2013.

[283] Q. Tu *et al.*, "Surface modification of poly (dimethylsiloxane) and its applications in microfluidics-based biological analysis," *Reviews in Analytical Chemistry,* vol. 31, no. 3-4, pp. 177-192, 2012.

[284] M. Zhang, J. Wu, L. Wang, K. Xiao, and W. Wen, "A simple method for fabricating multi-layer PDMS structures for 3D microfluidic chips," *Lab on a Chip,* vol. 10, no. 9, pp. 1199-1203, 2010.

[285] Z. Cai, W. Qiu, G. Shao, and W. Wang, "A new fabrication method for all-PDMS waveguides," *Sensors and Actuators A: Physical,* vol. 204, pp. 44-47, 2013.

[286] G. Comina, A. Suska, and D. Filippini, "PDMS lab-on-a-chip fabrication using 3D printed templates," *Lab on a Chip,* vol. 14, no. 2, pp. 424-430, 2014.

[287] T. J. Hinton, A. Hudson, K. Pusch, A. Lee, and A. W. Feinberg, "3D printing PDMS elastomer in a hydrophilic support bath via freeform reversible embedding," *ACS biomaterials science & engineering,* vol. 2, no. 10, pp. 1781-1786, 2016.

[288] J. M. Kelm, N. E. Timmins, C. J. Brown, M. Fussenegger, and L. K. Nielsen, "Method for generation of homogeneous multicellular tumor spheroids applicable to a wide variety of cell types," *Biotechnology and bioengineering,* vol. 83, no. 2, pp. 173-180, 2003.

[289] R. Fraioli, J. M. Manero Planella, F. J. Gil Mur, and C. Mas-Moruno, "Blocking methods to prevent non-specific adhesion of mesenchymal stem cells to titanium and evaluate the efficiency of surface functionalization: albumin vs poly (ethylene glycol) coating," *Premio SIBB 2014,* 2014.

[290] P. Van Wachem *et al.*, "Adhesion of cultured human endothelial cells onto methacrylate polymers with varying surface wettability and charge," *Biomaterials,* vol. 8, no. 5, pp. 323-328, 1987.

[291] Y.-W. Huang and V. K. Gupta, "A SPR and AFM study of the effect of surface heterogeneity on adsorption of proteins," *The Journal of chemical physics,* vol. 121, no. 5, pp. 2264-2271, 2004.

[292] R. Tzoneva, N. Faucheux, and T. Groth, "Wettability of substrata controls cell–substrate and cell–cell adhesions," *Biochimica et Biophysica Acta (BBA)-General Subjects,* vol. 1770, no. 11, pp. 1538-1547, 2007.

[293] S. Canada, "Leading causes of death, total population, by age group," ed: Statistics Canada Ottawa, ON, 2019.

[294] Y. Belotti and C. T. Lim, "Microfluidics for liquid biopsies: Recent advances, current challenges, and future directions," *Analytical Chemistry,* vol. 93, no. 11, pp. 4727-4738, 2021.

[295] A. Grimmer, X. Chen, M. Hamidović, W. Haselmayr, C. L. Ren, and R. Wille, "Simulation before fabrication: a case study on the utilization of simulators for the design of droplet microfluidic networks," *RSC advances,* vol. 8, no. 60, pp. 34733-34742, 2018.

[296] M. Razavi and A. S. Thakor, "An oxygen plasma treated poly (dimethylsiloxane) bioscaffold coated with polydopamine for stem cell therapy," *Journal of Materials Science: Materials in Medicine,* vol. 29, no. 5, pp. 1-14, 2018.

[297] K. S. Masters and K. S. Anseth, "Cell–material interactions," *Advances in Chemical Engineering,* vol. 29, pp. 7-46, 2004.

[298] J. A. Hubbell, "Biomaterials in tissue engineering," *Bio/technology,* vol. 13, no. 6, pp. 565-576, 1995.

[299] S. Cai, C. Wu, W. Yang, W. Liang, H. Yu, and L. Liu, "Recent advance in surface modification for regulating cell adhesion and behaviors," *Nanotechnology Reviews,* vol. 9, no. 1, pp. 971-989, 2020.

[300] M. Astolfi, "Tumeurs micro-disséquées sur puce microfluidique," École Polytechnique de Montréal, 2015.

[301] H. Hashemzadeh, S. Shojaeilangari, A. Allahverdi, M. Rothbauer, P. Ertl, and H. Naderi-Manesh, "A combined microfluidic deep learning approach for lung cancer cell high

throughput screening toward automatic cancer screening applications," *Scientific Reports,* vol. 11, no. 1, pp. 1-10, 2021.

[302] L. A. Torre, R. L. Siegel, and A. Jemal, "Lung cancer statistics," *Lung cancer and personalized medicine,* pp. 1-19, 2016.

[303] Z. Zhang *et al.*, "Establishment of patient-derived tumor spheroids for non-small cell lung cancer," *PLoS One,* vol. 13, no. 3, p. e0194016, 2018.

[304] L. G. Collins, C. Haines, R. Perkel, and R. E. Enck, "Lung cancer: diagnosis and management," *American family physician,* vol. 75, no. 1, pp. 56-63, 2007.

[305] A. Villasante and G. Vunjak-Novakovic, "Tissue-engineered models of human tumors for cancer research," *Expert opinion on drug discovery,* vol. 10, no. 3, pp. 257-268, 2015.

[306] S. Wu, Y. Pan, Y. Mao, Y. Chen, and Y. He, "Current progress and mechanisms of bone metastasis in lung cancer: a narrative review," *Translational Lung Cancer Research,* vol. 10, no. 1, p. 439, 2021.

[307] H. Shen, S. Cai, C. Wu, W. Yang, H. Yu, and L. Liu, "Recent advances in three-dimensional multicellular spheroid culture and future development," *Micromachines,* vol. 12, no. 1, p. 96, 2021.

[308] H. Zou *et al.*, "Microfluidic platform for studying chemotaxis of adhesive cells revealed a gradient-dependent migration and acceleration of cancer stem cells," *Analytical chemistry,* vol. 87, no. 14, pp. 7098-7108, 2015.

[309] L. Businaro *et al.*, "Cross talk between cancer and immune cells: exploring complex dynamics in a microfluidic environment," *Lab on a Chip,* vol. 13, no. 2, pp. 229-239, 2013.

[310] J. Rodrigues, M. A. Heinrich, L. M. Teixeira, and J. Prakash, "3D in vitro model (R) evolution: unveiling tumor–stroma interactions," *Trends in cancer,* vol. 7, no. 3, pp. 249-264, 2021.

[311] O. Chaudhuri, J. Cooper-White, P. A. Janmey, D. J. Mooney, and V. B. Shenoy, "Effects of extracellular matrix viscoelasticity on cellular behaviour," *Nature,* vol. 584, no. 7822, pp. 535-546, 2020.

[312] A. D. Rhim *et al.*, "Stromal elements act to restrain, rather than support, pancreatic ductal adenocarcinoma," *Cancer cell,* vol. 25, no. 6, pp. 735-747, 2014.

[313] D. Huang, X. Zhang, X. Fu, Y. Zu, W. Sun, and Y. Zhao, "Liver Spheroids on Chips as Emerging Platforms for Drug Screening," *Engineered Regeneration,* 2022.

[314] J. Dornhof, J. Kieninger, H. Muralidharan, J. Maurer, G. A. Urban, and A. Weltin, "Microfluidic organ-on-chip system for multi-analyte monitoring of metabolites in 3D cell cultures," *Lab on a Chip,* 2022.

[315] E. C. Costa, A. F. Moreira, D. de Melo-Diogo, V. M. Gaspar, M. P. Carvalho, and I. J. Correia, "3D tumor spheroids: an overview on the tools and techniques used for their analysis," *Biotechnology advances,* vol. 34, no. 8, pp. 1427-1441, 2016.

[316] A. Essaouiba *et al.*, "Analysis of the behavior of 2D monolayers and 3D spheroid human pancreatic beta cells derived from induced pluripotent stem cells in a microfluidic environment," *Journal of Biotechnology,* vol. 330, pp. 45-56, 2021.

[317] Y. L. Huang, Y. Ma, C. Wu, C. Shiau, J. E. Segall, and M. Wu, "Tumor spheroids under perfusion within a 3D microfluidic platform reveal critical roles of cell-cell adhesion in tumor invasion," *Scientific reports,* vol. 10, no. 1, pp. 1-11, 2020.

[318] Y. Song *et al.*, "Patient-derived multicellular tumor spheroids towards optimized treatment for patients with hepatocellular carcinoma," *Journal of Experimental & Clinical Cancer Research,* vol. 37, no. 1, pp. 1-13, 2018.

[319] N. Baek, O. W. Seo, M. Kim, J. Hulme, and S. S. A. An, "Monitoring the effects of doxorubicin on 3D-spheroid tumor cells in real-time," *OncoTargets and therapy,* vol. 9, p. 7207, 2016.

[320] P. Ahangar, E. Akoury, A. S. Ramirez Garcia Luna, A. Nour, M. H. Weber, and D. H. Rosenzweig, "Nanoporous 3D-printed scaffolds for local doxorubicin delivery in bone metastases secondary to prostate cancer," *Materials,* vol. 11, no. 9, p. 1485, 2018.

[321] E. M. Czekanska, "Assessment of cell proliferation with resazurin-based fluorescent dye," in *Mammalian cell viability*: Springer, 2011, pp. 27-32.

[322] K. Pietras and A. Östman, "Hallmarks of cancer: interactions with the tumor stroma," *Experimental cell research,* vol. 316, no. 8, pp. 1324-1331, 2010.

[323] I. B. Fridman, G. S. Ugolini, V. VanDelinder, S. Cohen, and T. Konry, "High throughput microfluidic system with multiple oxygen levels for the study of hypoxia in tumor spheroids," *Biofabrication,* vol. 13, no. 3, p. 035037, 2021.

[324] N. Rohwer and T. Cramer, "Hypoxia-mediated drug resistance: novel insights on the functional interaction of HIFs and cell death pathways," *Drug Resistance Updates,* vol. 14, no. 3, pp. 191-201, 2011.

[325] F. Ansarizadeh, M. Singh, and D. Richards, "Modelling of tumor cells regression in response to chemotherapeutic treatment," *Applied Mathematical Modelling,* vol. 48, pp. 96-112, 2017.

[326] N. Rousset, "Simulation numérique de l'opération de pièges microfluidiques à échantillons," École Polytechnique de Montréal, 2016.

[327] R. Guay-Lord, "Conception d'un dispositif microfluidique permettant l'analyse histopathologique à haut rendement de la réponse thérapeutique des tumeurs solides," École Polytechnique de Montréal, 2018.

APPENDIX A SIMULATE AND DESIGN OF THE MICROFLUIDIC BIOCHIP

This appendix presents the preliminary work on design of the first microfluidic platform used in this PhD dissertation. To design the biochip platform for spheroid formation and culture on-chip, I have used analytical modeling and simulation to understand the physical principals behind the phenomena and to predict experimental results to accordingly reduce the time and costs of experiments [305]. Several parameters could be determined by simulation to design a microfluidic platform for long-term culture of spheroids. Channel dimensions, cellular glucose uptake rate and oxygen consumption rate are the principal parameters to simulate and determine the required time to replenishment the culture media for keeping the spheroids viable for duration of the study. The 3D geometry of the microfluidic device has drawn and influences of different physical parameters solved numerically with COMSOL Multiphysics®. COMSOL Multiphysics (version 5.4, COMSOL) software generously has provided by Prof.Thomas Gervais to perform finite element analysis.

The first design of the microfluidic devices used in this dissertation were adapted from the design developed by Astolfi et al. [1]. The parameters of each channel and wells were broadly similar to the device described by Astolfi et al, except the height of the wells have been changed to 540 μm instead of 500 μm to optimize device operation according to the results have been done by Rousset et al [306]. Rousset et al. demonstrated that if d is the tissue diameter, the optimal dimensions of a well are a square base of 2d × 2d (W=D=2d) with a height slightly lower than 2d. (h≈0.9 W) [306]. The geometric properties of the channel (H, W, L) determine the volume of accessible culture media for each sphere and have influence on the time required to completely change the culture media in the system and also on the nature of the flow in the system to minimize the flow velocity and Reynolds number as much as possible [307]. Each channel with the length of 78 mm, consists of five micro-wells, which are distributed all along the channel. This provides the maximum amount of available nutrients for spheroids in non-infusion conditions [1]. Square section of the channel is 600 μm by 600 μm and square bottom of wells have 600 μm wide by 540 μm deep. The total volume of each channel is 29 μL. This dimensions can provide enough space for spheroids around 300 μm diameter [1].

To guarantee that a consistent number of cells will be trapped into each well, an appropriate flow rate to form spheroids on-chip by sedimentation had been calculated. We had considered sedimentation for a cell with about 30 μm diameter in our calculations when the sedimentation distance is the radius of the cell to trap the cell in the well. Sedimentation will happen if:

$$t_{sed} < t_{cross\ the\ well}$$

With considering the Stokes' law for settling velocity of a sphere falling in a fluid:

$$v = \frac{2}{9}\frac{(\rho_p - \rho_f)}{\mu} g R^2$$

We had calculated the velocity of sedimentation and flow rate with above equations. When cell suspension is loaded into the channel, a portion of the cells will be settled down into the micro-well by sedimentation. According to the results of calculations, to guarantee that a consistent number of the cells will be trapped into each well, we need to apply flow rate less than 0.16 μl/s during cell loading process. Also, there is a chance that cells agglomerate before reach to the wells and increase the sedimentation mass. This will increase the velocity of the sedimentation into the wells.

To determine appropriate flow rate in the system when perfuse the media, I refer to the work presented by Astolfi et al. [1]. As long as Reynolds number is low and the system is in laminar regime, spheroids stay stable at the bottom of wells (Re <0.1) and there is laminar regime and dominate viscous forces, if the flow rate is approximately 2 to 3.6 μL / min. But Re> 10 when the flow rate exceeds about 200 to 360 μL / min while the system is still in laminar regime, but the inertial forces are dominate [1]. Astolfi et al. observed that at flow rates above 800 μL / min samples could release from their wells [1]. Since the maximum flow induced in the channels with a micropipette are 300 μL / min, even if the inertial forces are dominate the samples remain in the wells. Therefore with this geometry design of the channels and wells, they are not released at normal operating rates [1].

Refill the culture media regularly in specific time periodic in a non-perfused system is the key factor to sustain and maintain high viability of cells. In this model, I have focused on characterizing oxygen and glucose which are the two essential nutrients for cell growth found in

culture media. According to the equation of diffusion time for a molecule (bellow), since the total distance to the bottom of each well is very small in our design (540 μm), diffusion transport of glucose and oxygen is easy within a reasonable time.

$$t \approx \frac{x^2}{2D}$$

x^2: Total distance to the bottom of the well

$2D$: Diffusion constant of a molecule

To determine the replenishment time of culture media in the non-perfused system and to access if cells have enough oxygen and nutrients to survive for at least first 24 hours, oxygen consumption rate and glucose uptake rate by spheroids have simulated by COMSOL Multiphysics® software. The critical review has been down for the parameters of diffusion, solubility and consumption of glucose and oxygen through literature. For simulations, parameters referred by Astolfi et al. [1] have been chosen (Table B.1). The diffusion-reaction with a time-dependent solver and a threshold on the minimum tissue concentration at the Michaelis-Menten constant (KM) have been used to solve the numerical simulations in COMSOL Multiphysics® software to find the exchange times of the medium. I used a simple diffusion model for theoretical calculation of the oxygen distribution inside the spheroids.

In steady state (∂C / ∂t = 0), the equation is simplified and can solved with these equations:

$$\frac{\partial c}{\partial t} = D\nabla^2 c - q(c)$$

Cells in spheroids consume metabolites with Michaelis-Menten kinetics:

$$q(c) = q_{\max}\frac{c}{c + k_M}$$

$q_{\max}$: Maximum consumption rate

k_M: Michaelis-Menten constant

Oxygen diffusion in a PDMS microfluidic device

We need to consider that in the spheroids, there is diffusion and consumption of oxygen. However, in the surrounding environment, oxygen only diffuses. To solve this problem we consider that all domains (spheroids, media and PDMS) are saturated with oxygen. When there is no perfusion in the system, we can simplify the convection-diffusion equation to its diffusion terms. This is obvious that there is continuous consumption of oxygen by the cells in spheroids. In this model, all walls are set with no-flux (Neumann) boundary conditions. The interface boundary of PDMS/Medium is set with a continuity condition on metabolite concentration normalized by the saturation concentration in the material, and on diffusive flow through these interfaces (Figure A.1).

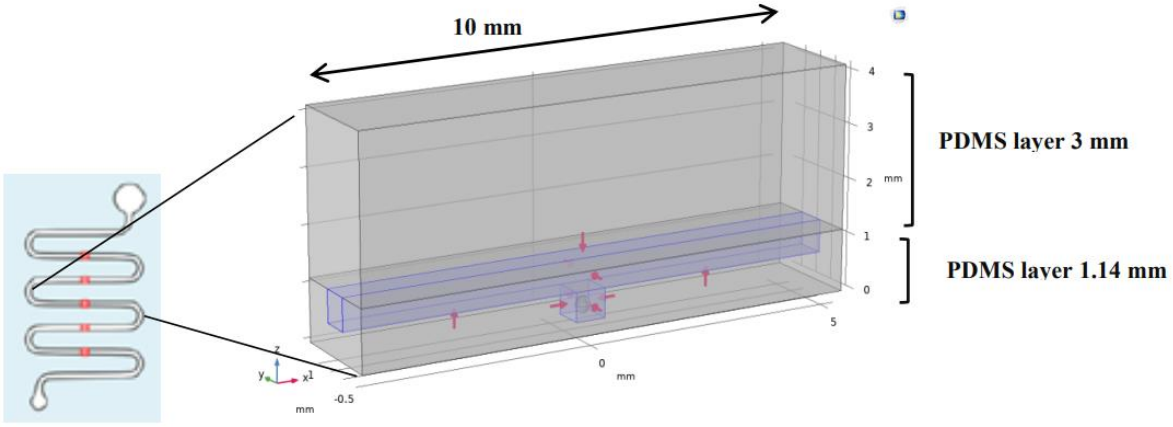

Figure A.1 Schema of the front view of each micro-well

We put symmetry condition in COMSOL to solve the problem, since each block will repeat five times. Red flashes are to show the patrician coefficient between PDMS and media. I have considered no-flux condition for the system to be able to measure oxygen consumption in simulations.

Results of the simulations showed that we would have enough oxygen for at least first 24 hours before replenishment of media (Figure A.2).

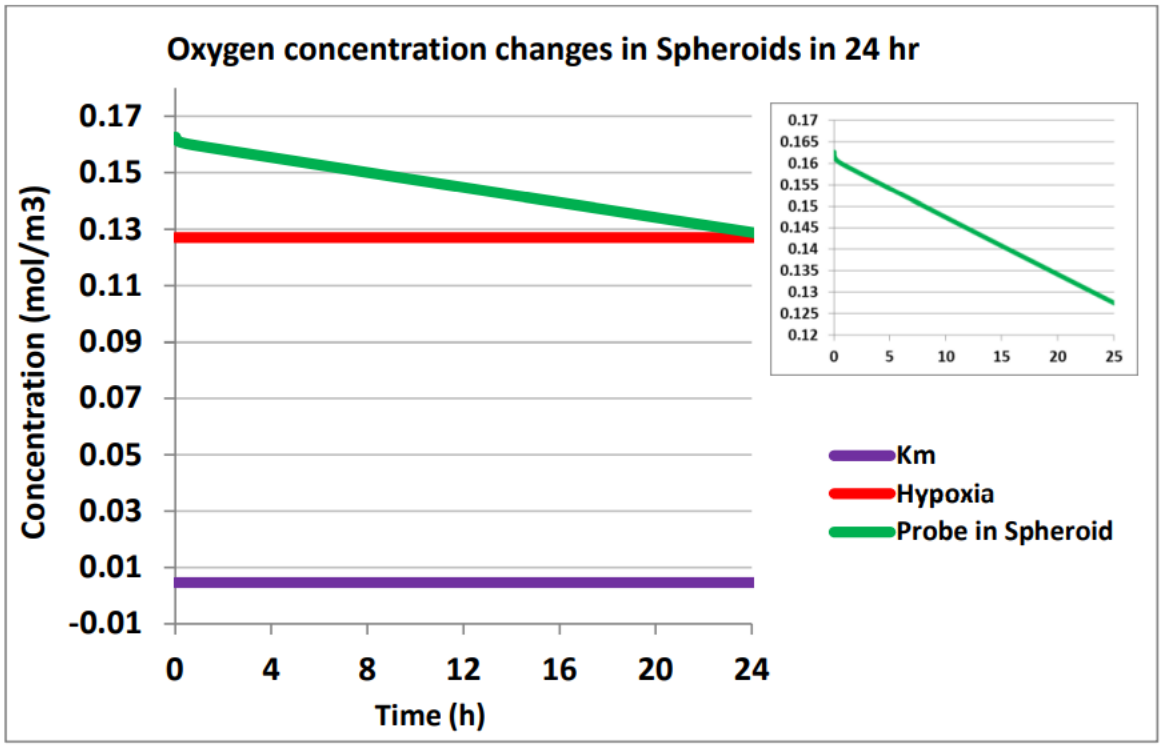

Figure A.2 Oxygen consumption in the spheroid

Oxygen consumption in a spheroid during the first 24 hours after refreshing the media has been simulated with COMSOL. We have put the no-flux condition on all walls to measure the consumption rate

Diffusion of glucose from media to spheroid

Glucose will be consumed by cells and will decrease in the medium. Therefore, to refill glucose, medium needs to be change. A time-dependent solver on the spheroids domain applied and initially available nutrients in the medium consumed. When the minimum concentration of nutrients in sphere reaches the Michaelis-Menten constant (k_M), the threshold commonly accepted under which concentration limits uptake kinetics. In this level of concentration, the uptake rate of cells is reduced to half of that of cells with an abundance of nutrient ($q$max with a zero order kinetic). Figure A.3 shows the results of simulation by COMSOL for glucose uptake by spheroid.

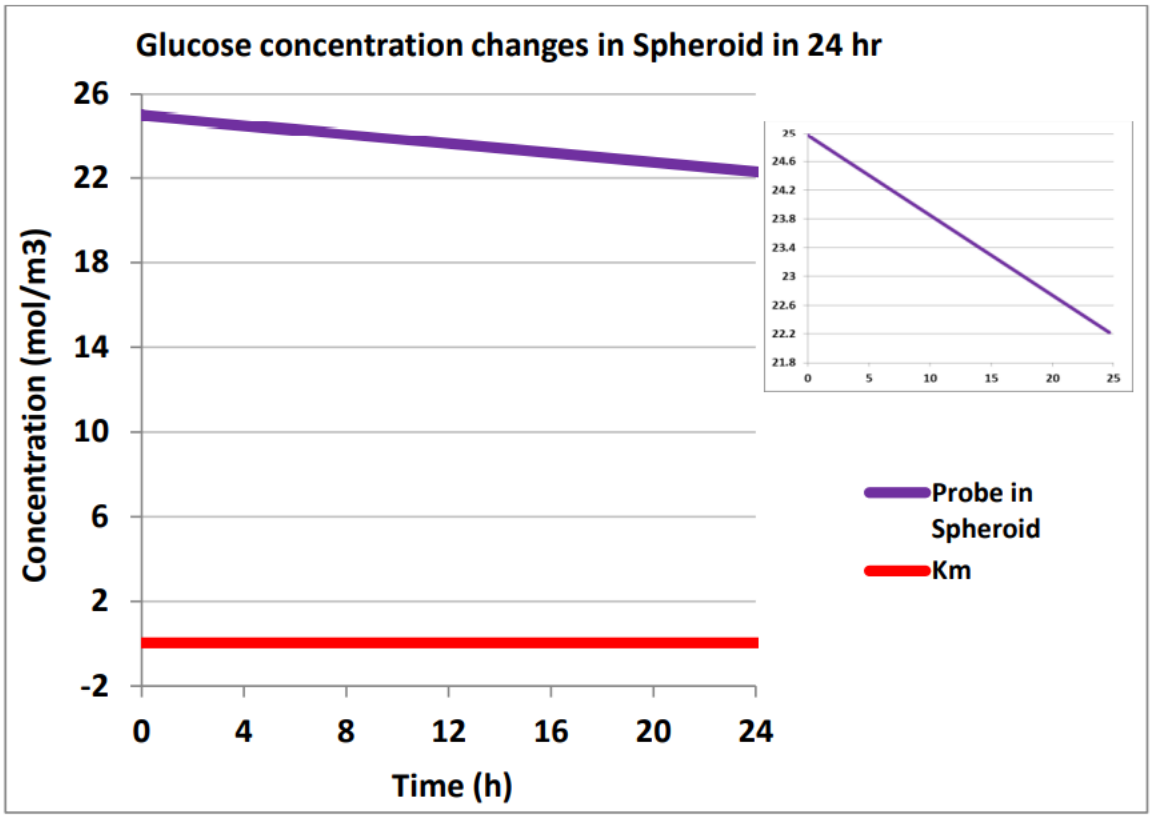

Figure A.3 Glucose uptake in the spheroid

Glucose uptake profile during the first 24 hours after refreshing the media has been simulated by COMSOL. This simulation demonstrates that there is enough glucose for the first 23-24 hours. We use high glucose concentration media (25mM) for cells and after 24 hours, cells consumed approximately %12 of the available glucose in media.

These presented results above, are for the first design of microfluidic biochip, which I have fabricated and employed in the first study of this dissertation presented as article 1, in Chapter 4. For the study 2 and 3, I have modified the design as explained in details in Chapters 5 and 6. Since the new design is enlarged compared to this initial design presented above, while the initial numbers of cells to make spheroids did not change, we assured that the new design provide enough oxygen and glucose for spheroids by replenishment of media every 22-24 hours.

APPENDIX B DESCRIPTION OF THE PARAMETERS USED IN COMSOL

Table B.1 represent parameters defined for simulations in COMSOL in terms of oxygen consumption and glucose uptake by spheroids inside the chambers.

Table B.1 Parameters defined for COMSOl simulations

Description of the parameters to characterize the microfluidic system in term of the operation of the device and cellular uptake parameters

Description of parameter	Value	References
	Geometry	
Thickness of PDMS layer (bottom)	3 mm	[1]
Well height	540 μm	N/A
Well width (square-bottom)	600 μm	[1]
Channel width (square section)	600 μm	[1]
Channel length	1 cm	[1]
Distance between wells	1.5 mm	[1]
Spheroid diameter	400 μm	N/A
	Diffusion parameters	
Diffusion of oxygen through PDMS	3.4×10^{-5} cm^2/s	[1]
Diffusion of oxygen through water	2.6×10^{-5} cm^2/s	[1]

Diffusion of oxygen through human cancerous spheroid	1.83×10^{-5} cm²/s	[1]
Diffusion of glucose through water	9.27×10^{-6} cm²/s	[1]
Diffusion of glucose through cancer tissue	2.70×10^{-6} cm²/s	[1]
	Solubility parameters	
Solubility of oxygen in PDMS vs water	6.8	[1]
Solubility of oxygen in tissue vs water	4.81	[1]
Concentration of glucose in DMEM medium	25×10^{-3} mol/L	Wisent Inc. website
Concentration of oxygen in medium	0.2×10^{-3} mol/L	[1]
	Michaelis-Menten uptake parameters	
Maximum uptake rate of glucose by cancerous cells	0.39×10^{-16} mol/cell/s	[1]
Maximum uptake rate of oxygen by cancerous cells	7.37×10^{-17} mol/cell/s	[1]
Uptake saturation constant of glucose by cancerous cells	4.00×10^{-5} mol/L	[1]
Uptake saturation constant of oxygen by cancerous cells	4.63×10^{-6} mol/L	[1]

APPENDIX C SPHEROID FORMATION ON BIOCHIPS

This appendix presents the materials I have presented as the appendix of article 1. Article 1 is presented in chapter 4. The first part of the appendix of article 1 is already reviewed in chapter 2 (critical review) of this dissertation. Therefore, in Appendix C I only present the rest of the materials which is already published as the appendix article 1. Figure C.1 shows the schematic of the 2D view of a spheroid which have been used for calculations of the average mean diameter, spheroid size and the circularity of each spheroid. The average mean diameter is calculated as Dm= (Dmax+Dmin)/2 m [281]. The spheroid's sizes were presented as mean diameter ± standard deviation. The circularity of the spheroids has been reported by the Circularity=Dmin/Dmax.

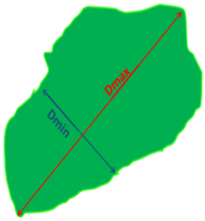

Figure C.1 Schematic of the 2D view of the spheroid
Maximum diameter (Dmax) and minimum diameter (Dmin) which have been used in image J calculations to access the growth pattern and spheroid size over the 7 days periods

Figure C.2 demonstrates the microscopic image of the microfluidic channels and chambers, a picture of the resin mold which is fabricated by stereolithography technic and a picture of the PDMS biochip which is used in this study.

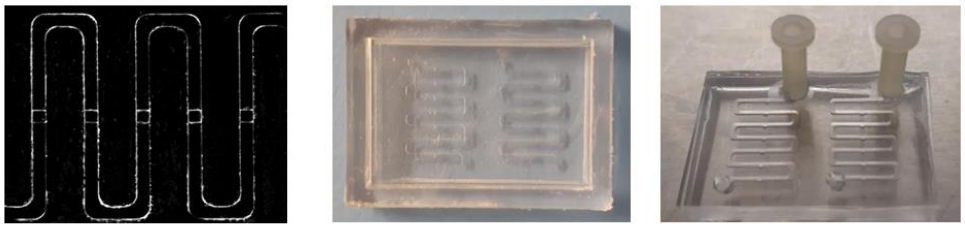

Figure C.2 Microfluidic biochip platform
(a) Microscopic image of channels and chambers, (b) Picture of the 3D printed resin mold, (c) Picture of the PDMS microfluidic device with inlets

Figure C.3 demonstrate the initial cell seeding process on biochip. Cell mixture is introduce to the inlet and some of the cells will trapped inside each well and the rest of the cells will exit through the outlet of the channel. As the inner surface of the PDMS biochip is treated with chemical coatings and render cell repellent properties, cells which are trapped inside the wells through sedimentation and containment will agglomerate together and proliferate to make 3D tumour spheroids on the day after cell seeding.

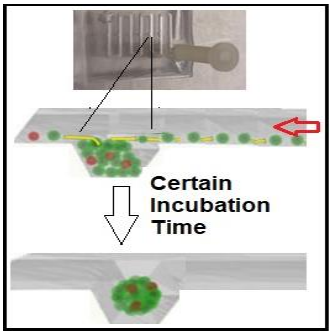

Figure C.3 Schematic illustrations of the cell seeding process and spheroid formation through sedimentation and containment

Figure C.4 shows a comparison between the different treated PDMS surfaces in terms of the chance of the numbers of the spheroids formed on biochip. As discussed above, between 6 studied surfaces in this work, BSA 10% show the best cell repellent properties by increasing the number of possible spheroid formed on biochip. BSA 3% showed the least cell repellent properties and the less number of spheroid formed on-chip.

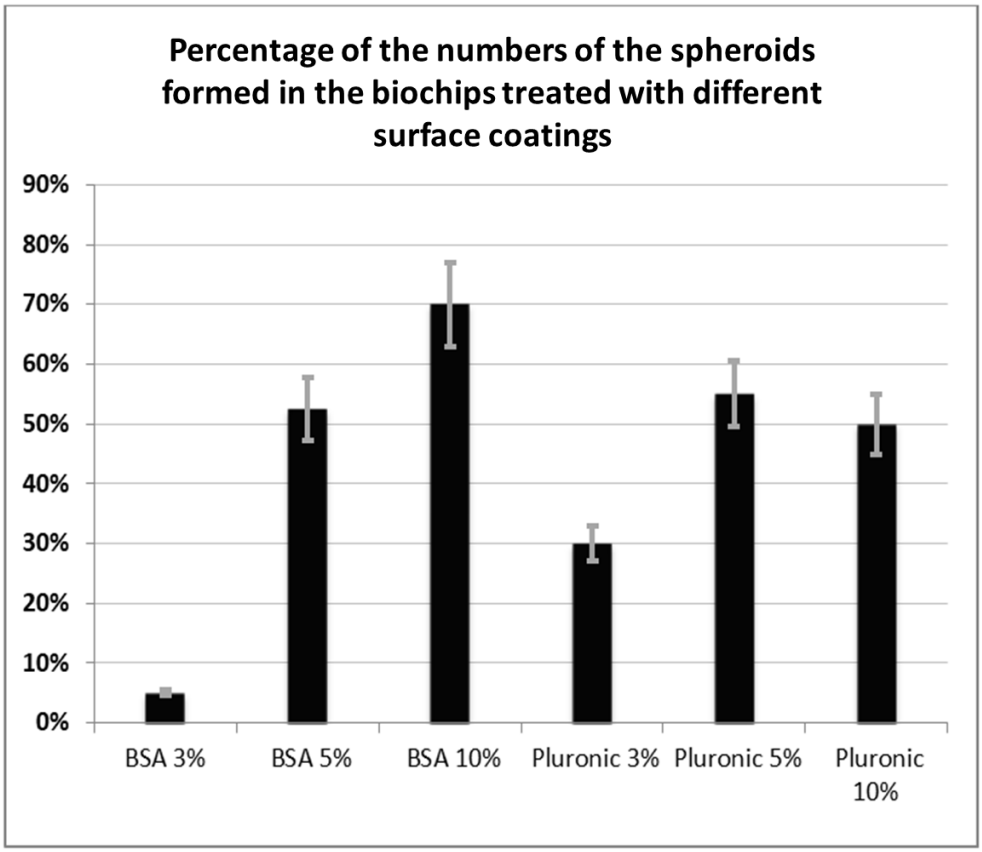

Figure C.4 The chance of spheroid formation on-chip with different surface treatments Error bars represent ± SE, n=3

APPENDIX D CELL ADHESION TO THE CORNERS OF THE CHAMBERS

In this appendix, I present the materials which are presented in appendix article 2. Article 2 is presented in chapter 5. Here, I show that cells have more chance to stick to the corners of the cube shape cell trapping micro-wells design of our microfluidic device, therefore in the study 2, the shape of the cell trapping micro wells have modified to cylindrical shapes to decrease this phenomenon.

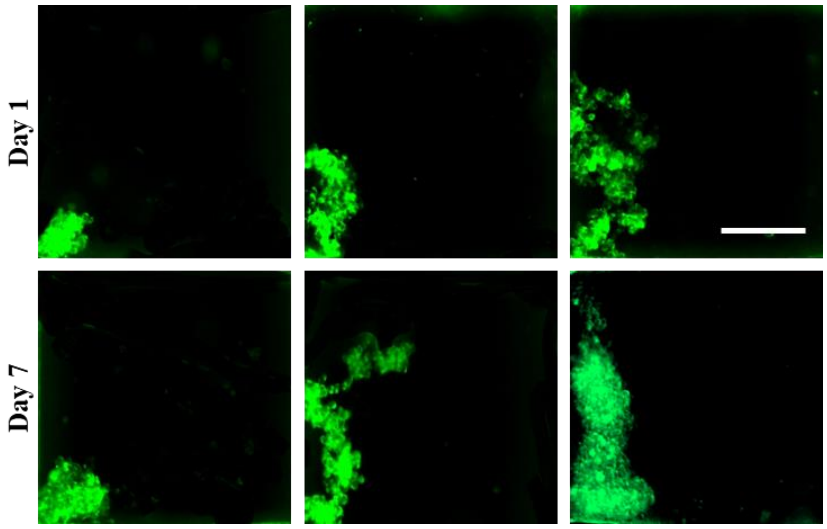

Figure D.1 Cell attachment to the corners of the cube shapes micro-wells

Cells sometimes tend to attach to the corners of the cube form cell trapping microwells even though the surfaces were pre-coated with 10% BSA. This could lead to decrease the chance of spheroid formation on chip by increasing the possibility of forming the lobular or any non-spherical cell agglomerations. Figures a, b and c are representing different forms of cell aggregations which produced in different cube shape cell trapping chambers in our old design. MDA-MB-231-GFP cells are pictured in this image. The green color is due to green-fluorescent protein (GFP) in MDA-MB-231 cells. Scale bars: 200 μm.